DOKUZ EYLÜL UNIVERSITY
GRADUATE SCHOOL OF NATURAL AND APPLIED SCIENCES

INVESTIGATING THE COOLING AFFECT OF GREEN SPACES IN URBAN AREAS WITHIN THE SMART CITIES FRAMEWORK

Yasemin ŞENTÜRK

February, 2024

İZMİR

INVESTIGATING THE COOLING AFFECT OF GREEN SPACES IN URBAN AREAS WITHIN THE SMART CITIES FRAMEWORK

A Thesis Submitted to the
Graduate School of Natural and Applied Sciences of Dokuz Eylül University
In Partial Fulfillment of the Requirements for the Degree of Doctor of Philosophy in Department of City and Regional Planning, City and Regional Planning Doctorate Program

by

Yasemin ŞENTÜRK

February, 2024

İZMİR

Ph.D. THESIS EXAMINATION RESULT FORM

We have read the thesis entitled **"INVESTIGATING THE COOLING AFFECT OF GREEN SPACES IN URBAN AREAS WITHIN THE SMART CITIES FRAMEWORK "** completed by **YASEMİN ŞENTÜRK** under supervision of **PROF.DR. K. MERT ÇUBUKÇU** and we certify that in our opinion it is fully adequate, in scope and in quality, as a thesis for the degree of Doctor of Philosophy.

Prof.Dr. Kemal Mert ÇUBUKÇU

Supervisor

Prof. Dr. Çiğdem COŞKUN HEPCAN

Thesis Committee Member

Prof. Dr. Mediha Burcu SILAYDIN

Thesis Committee Member

Doç. Dr. Nurdan ERDOĞAN

Examining Committee Member

Doç. Dr. Birsen KESGİN ATAK

Examining Committee Member

Prof. Dr. Okan FISTIKOĞLU

Director

Graduate School of Natural and Applied Sciences

ACKNOWLEDGMENT

I would like to express my gratitude to my thesis advisor Prof. Dr. K. Mert Çubukçu, whom I took as an example as an academician, for his understanding and generosity in sharing his knowledge during my doctoral education. I would like to express my thanks to the member of the thesis committee members, Prof. Dr. Mediha Burcu Sılaydın and Prof. Dr. Çiğdem Coşkun Hepcan who did not spare his contributions for development of the research approach of the thesis.

I offer my eternal love to my dear father Ahmet Şentürk, my dear sister Ayşegül Şentürk and my mother Sabriye Şentürk, who have supported me in my development throughout my life. I would like to express my love to my colleagues Özlem Şenyol, Nur Gülerdoğan and Uğur Bayrak, who have an important place in my professional and private life due to their moral support in the process, and to my dear friends Atakan Ekiz and Pelin Tatlı, who provide their academic support. I extend my sincere thanks to Sevda Arslan Poyraz and Savaş Kaplan. Lastly, I would like to thank Halil Burak Yılmaz for his contribution to my thesis on software.

Yasemin ŞENTÜRK

INVESTIGATING THE COOLING AFFECT OF GREEN SPACES IN URBAN AREAS WITHIN THE SMART CITIES FRAMEWORK

ABSTRACT

Urban heat island (UHI) plays a crucial role in determining local climate conditions. In urban area, green-blue infrastructure plays an important role in regulating local temperatures against the heating effect of areas without vegetation. These areas, which shape the spatial distribution of temperature in urban space, are called urban cold islands (UCIs). In this study, cooling intensity of UCIs, their extents and temperature of the extents of UCIs were taken as main components to increase cooling capacity of the urban environments. The study first aims to develop an innovative spatial statistics approach to detect patches of UCIs. Results of the study showed that UCIs in İzmir were observed on seaside, urban green areas, low-density campus areas, and some residential districts. Secondly, the study measured the contribution of important parameters in explaining the cooling intensity of UCIs with developing multiscale geographically weighted regression models of LST_{min} and LST_{mean}. According to results, the significant categories in terms of contribution rate in explaining the cooling intensity, land cover configuration, outer thermal effect, UCI characteristics and composition and configuration of green area. Thirdly, the significant categories in terms of contribution rate in explaining the cooling extents are UCIs configuration, green configuration, and urban morphology, respectively. Lastly, the increased cooling intensity of UCIs played a strong role in reducing the temperature of the adjacent urban environment while it had less effective in increasing the cooling extent. Accordingly, the thermal interaction between the built environment and the UCIs can create a multi-cooling effect, which is very important for enhancing urban thermal comfort in the urban environment. As a result, the research approach and the findings will insight for mitigation of urban heat island effect in the context of sustainable urban planning and management.

Keywords: Climate change, urban heat island, urban cool island, cooling capacity, climatic planning, spatial statistics, remote sensing, geographic information system

YEŞİL ALANLARIN KENTSEL ALANLARDA SOĞUTMA ETKİSİNİN AKILLI KENTLER ÇERÇEVESİNDE İNCELENMESİ

ÖZ

Kentsel ısı adası (KIA), yerel iklim koşullarının belirlenmesinde önemli bir rol oynamaktadır. Kentsel alanda yeşil-mavi altyapı, bitki örtüsü olmayan alanların ısınma etkisine karşı yerel sıcaklıkların düzenlenmesinde önemli bir rol oynamaktadır. Kentsel mekânda sıcaklığın mekânsal dağılımını şekillendiren bu alanlara kentsel soğuk adalar (KSA) denir. Bu çalışmada, kentsel ortamların soğutma kapasitesini artırmak için KSA'ların soğutma şiddeti, yayılımları ve KSA yayılım alanı sıcaklığı ana bileşenler olarak alınmıştır. Öncelikle, çalışma KSA sınırlarının tespit etmek için yenilikçi bir mekânsal istatistik yaklaşımı geliştirmeyi amaçlamaktadır. Çalışmanın sonuçları, İzmir'deki KSA'ların deniz kenarı, kentsel yeşil alanlar, düşük yoğunluklu kampüs alanları ve bazı yerleşim bölgelerinde gözlemlendiğini göstermiştir. Çalışma, çok ölçekli coğrafi ağırlıklı regresyon modelleri geliştirerek kentsel ısı adası etkisini hafifletmek için alternatif çözümleri tartışırken, önemli parametrelerin KSA'ların soğutma kapasitesi üzerindeki etkisini ölçmüştür. Elde edilen sonuçlara göre soğutma şiddetinin açıklanmasında anlamlı kategoriler arazi örtüsü düzeni, dış termal etki, KSA özellikleri ve yeşil alanın biçim ve düzeni olmuştur. Üçüncü olarak, soğutma yayılımının açıklanmasında katkı oranı açısından anlamlı kategoriler KSA düzeni, yeşil alan düzeni ve kentsel morfoloji olmuştur. Son olarak, KSA'ların artan soğutma şiddeti, bitiğindeki kentsel yapılı çevrenin sıcaklığının azaltımında güçlü bir rol oynarken soğutma yayılımının artmasında daha az etkili olmuştur. Buna göre, bitişiğindeki yapılı çevre ve KSA arasındaki termal etkileşim, kentsel termal konforun artması için önemli etkiye sahiptir. Sonuç olarak, araştırma yaklaşımı ve bulgular, sürdürülebilir kentsel planlama bağlamında KIA etkisinin azaltılmasına yönelik öngörüler sağlayacaktır.

Anahtar kelimeler: İklim değişikliği, kentsel ısı adası, kentsel soğuk ada, soğutma kapasitesi, iklimsel planlama, mekansal istatistik, uzaktan algılama, coğrafi bilgi sistemleri

CONTENTS

Page

Ph.D. THESIS EXAMINATION RESULT FORM ii
ACKNOWLEDGMENT iii
ABSTRACT iv
ÖZ v
CONTENTS vi
LIST OF FIGURES viii
LIST OF TABLES x

CHAPTER ONE - INTRODUCTION 1

1.1 Problem Definition 1
1.2 Aim and Scope of The Study 3
1.3 Research Method 5

CHAPTER TWO LITERATURE REVIEW 7

2.1 Cooling Effect of Blue and Green Infrastructure 8
2.2 Measuring the Cooling Intensity of Urban Cool Island 9
2.2.1 UCI characteristics 11
2.2.2 Abundance of the green 12
2.2.3 Land cover 14
2.2.4 Outer effect 15
2.3 Measuring the Cooling Extents 15
2.4 Measuring the Cumulative Cooling Effect of UCIs 17
2.5 Measuring Urban Morphological Character of Cooler Areas 19
2.6 Research Approaches in Measuring the Cooling Capacity 22

CHAPTER THREE DATA AND METHOD 26

3.1 Research Approach and Hypothesis 26
3.2 Study Area 27
3.3 Pre-processing of The Data 28

3.3.1 Land surface temperature 29
3.3.2 Land covers mapping 30
3.4 Spatial Statistics for Analysis of LST Distribution 32
3.5 Statistical Analysis 36
3.6 Analyzing Thermal Conditions of Urban Environments 36
3.7 Measuring The Cooling Intensity of Urban Cool Islands 37
3.8 Measuring The Cooling Extents of Urban Cool Islands 41

CHAPTER FOUR - RESULT 44

4.1 LST Distribution In İzmir 44
4.2 The Characteristics of UCIs Within The İzmir Urban Area 47
4.3 Relationship Between the Components of Thermal Environment 51
4.4 Relationship Between the Cooling Capacity and Important Parameters . 52
4.4.1. Results of Multiple Linear Regression Models 53
4.4.2. MGWR Model Results 58
4.5 Predictions of The Regression Models Measuring The Cooling Capacity ……..68

CHAPTER FIVE - DISCUSSION AND CONCLUSION 71

5.1 Evaluation of The Results 71
5.2 Limitations of The Study 79
5.3 Contribution of The Study and Suggestions for the Future Studies 80

REFERENCES 83

LIST OF FIGURES

Page

Figure 1. Schema of Urban Heat Island Profile 1

Figure 2. Steps of Research Method 5

Figure 3. Context of the thesis 6

Figure 4. The Relationships Between the Cooling Capacity of Urban Environment 26

Figure 5. Schematic Representation of An Urban Relatively Cooler Area 27

Figure 6. Location of Study Area 29

Figure 7. LST Distribution Map of The Study Area 30

Figure 8. Land Cover Map of İzmir 31

Figure 9. The Spatial Analysis Flowchart of This Study in Geographical Information System 33

Figure 10. Map of Relatively Cooler Areas (RCAs) and Urban Cool Islands (UCIs) 35

Figure 11. The Components Related Urban Thermal Conditions 37

Figure 12. Anselin Local Moran I Low and High-Temperature Clusters in İzmir 46

Figure 13. K means clusters of LL polygons for İzmir 47

Figure 14. Histograms of LST_{mean} and LST_{min} 48

Figure 15. LST distribution of LL and UCIs polygons for İzmir 49

Figure 16. Examples of UCIs of Izmir and their adjacent urban area 50

Figure 17. Scatter plots of the cooling capacity components 52

Figure 18. Scatter diagram of residual versus fit plot of LST_{min} model 53

Figure 19. Scatter diagram of residual versus fit plot of LST_{mean} model 55

Figure 20. Scatter diagram of residual versus fit plot of $Extent_1$ model 56

Figure 21. Scatter diagram of residual versus fit plot of $Extent_2$ model 56

Figure 22. Scatter diagram of residual versus fit plot of LST_{min} MGWR model 59

Figure 23. Scatter diagram of residual versus fit plot of LST_{mean} MGWR model 59

Figure 24. Proportion of negative and positive effect of the local variables of LSTmin MWGR model 65

Figure 25. Proportion of negative and positive effect of the local variables of LSTmean MWGR model 66

Figure 26. The contribution of the independent variables in the LST_{mean} and LST_{min} model according to category 66

Figure 27. Scatter diagram of residual versus fit plot of $Extent_1$ MGWR model 68

Figure 28. Scatter diagram of residual versus fit plot of $Extent_2$ MGWR model 68

Figure 29. Proportion of negative and positive effect of the local variables of $Extent_1$ MWGR model 66

Figure 30. Proportion of negative and positive effect of the local variables of $Extent_2$ MWGR model 67

Figure 31. Contribution of categories of independent variables to the Cooling Extent Models 67

Figure 32. Examples for a comparison of UCI and legal park boundary 73

Figure 33. Relationships between important components and parameters related to the cooling capacity according to findings of the regression models 79

LIST OF TABLES

Page

Table 1.Parameters Affecting the Cooling Intensity in the Literature 10

Table 2. Parameters Related to UHI Concerning Urban Morphology 20

Table 3. Research Approaches in Analyzing the Cooling Capacity in the Literature 24

Table 4. The Description of Dependent and Independent Variables in The Cooling Intensity (LST_{mean} and LST_{min}) Regression Model 39

Table 5. Descriptive Statistics of The Description of Dependent and Independent Variables in The Cooling Intensity Regression Model 40

Table 6. The Description of Dependent and Independent Variables in The Cooling Extent Regression Model 41

Table 7. Descriptive Statistics of Variables of The Cooling Extent Model (n=292) . 43

Table 8. The statistics for LST distribution according to Moran Cluster Types* 44

Table 9. Descriptive statistics of LST of k-means clusters 45

Table 10. The Statistics for LST Distribution of RCAs and UHIs 46

Table 11. Descriptive Statistics for Land Cover Surfaces within UCIs (n=862) 49

Table 12. Pearson correlation analysis results of the components affecting the thermal environment 51

Table 13. The LST_{min} Model Estimates (n=862) 1

Table 14. The LST_{mean} Model Estimates (n=862) 1

Table 15. The Cooling Extent $Model_1$ Estimates (n=292) 58

Table 16. The Cooling Extent $Model_2$ Estimates (n=292) 58

Table 17. Spatial Autocorrelation results of the multi linear regression models 58

Table 18. Statistical description of LSTmin MGWR model coefficient 60

Table 19. Statistical description of LSTmean MGWR model coefficient 60

Table 20. Statistical description of $Extent_1$ MGWR model coefficient 65

Table 21. Statistical description of $Extent_2$ MGWR model coefficient 65

Table 22. Results of The Predictions Measuring the Cooling Intensity 69

Table 23. Results of The Predictions Measuring the Cooling Extent Models 70

CHAPTER ONE
INTRODUCTION

1.1 Problem Definition

Nowadays increasing urbanization, industrialization and consumption attitudes with environmental and atmosphere pollution brought about global climate change, one of the most crucial environmental problems. In addition to tendency of global warming, changes of atmosphere temperatures resulted in alteration of urban microclimate and zonal heating in urban areas because of reasons such as densely built-up areas, decreasing natural areas, increasing impermeable surfaces, changing urban land topography. Changing land cover and atmospheric modifications, coming with rapid urbanization, determined local climate in the urbanized areas, especially warmer city center than rural area at night. This event, affecting urban comfort of habitants, represented as urban heat island (UHI) (Leconte et al., 2015; Liu et al., 2017; Voogt & Oke, 2003; Wong & Yu, 2005) (Figure 1). The urban heat island (UHI) phenomenon played a critical role in shaping the comfort levels of urban residents, particularly considering the escalating duration of extremely hot days driven by global warming. Extented periods of intense heat could lead to various health issues, particularly among vulnerable social groups, and could also inflict damage upon urban infrastructure (İzmir Metropolitan Municipality, 2020).

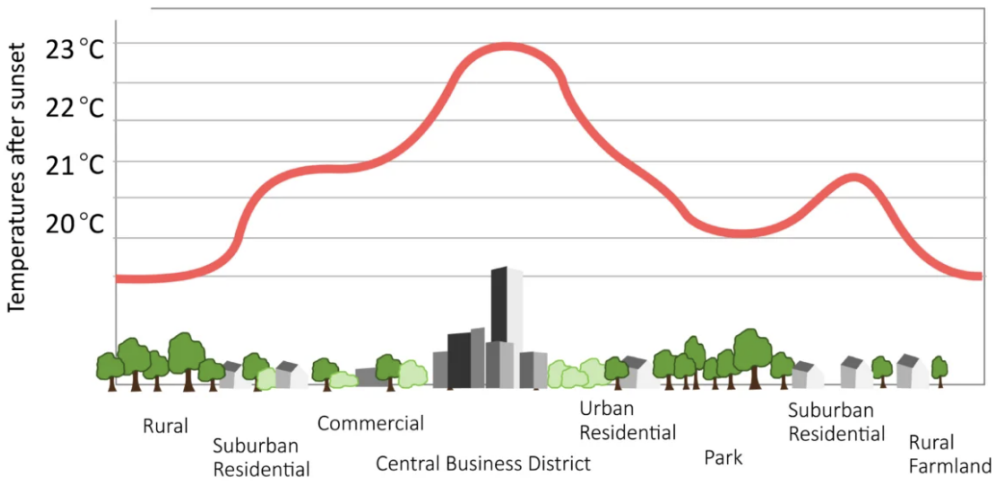


Figure 1. Schema of Urban Heat Island Profile (MetLink, Royal Meteorological Society, 2023)

Increased temperatures, extreme cool and heat, and heat islands were occurring in urban centers because large proportion of the world population, economic activity, and physical infrastructure in the cities (Romero-Lankao et al., 2012). This aggregation of population and urban activities resulted in the creation of local climate conditions in the urban areas. Heat stress was a natural disaster because the reason for reported thousands of deaths is related to heat illnesses in a year (Mirzaei and Haghighat, 2010). In this regard, reducing urban heat island effects has been one goal of the climate change adaptation issues due to improving urban comfort, protecting human health, and reducing energy use (Wheeler et al., 2019).

High dense urban or construction sites, especially high-density commercial areas, accounted for the highest mean LST which is followed by urban lands and open vegetation (Liu et al., 2017; Leconte et al., 2015; Wong and Yu, 2005). Zhang et al. (2016) and Kong et al. (2014) also measured, approximately, 3.0 C higher air temperatures on impervious surfaces than average surface temperature of the cities in China due to solar radiation emission all daytime. Higher air temperature and lower wind speed caused reduced urban comfort in the city center (Liu et al., 2017). This provided evidence that urbanization and removal of vegetation cover contributed to increase land surface temperature.

Urbanization reduces the microclimate regulation function of vegetation and water bodies (Kong et al. 2014). Urban wetlands and rivers play a role to role to control the microclimate in all seasons (Zhang etc., 2016). Like wetlands, lower temperature measurements on vegetation cover proved the importance of the greenery to mitigate the UHI effect in cities, especially large green areas (Wong and Yu, 2005). In additionally, urban thermo-physical and geometrical characteristics affect the microclimate of an urban area (Dimoudi et al., 2013). Many causes are creating this environmental problem- heat stress- which comes with rapid urbanization. Rapid land cover alteration with the loss of greenery and water surfaces, increasing impervious surfaces, air pollution and increasing energy consumption mainly are some of the reasons for UHI.

Creating “Cool Cities” has been seen as a solution to deal with extreme heat stress (C40 Cities, 2020). The concept of “Cool city” was one of the sustainable urban solutions targeting promoting cooling in the urban environment in this concept, some decision occurred for Stuttgart like creating green corridors, improving green and blue infrastructure, enlarging urban parks, increasing vegetation, cool buildings with cool roofs and changing material with cooler ones (Rehan, 2016). Therefore, it is necessary to develop solution-based approaches for design and practice to reduce the temperature in urban environments (C40 Cities, 2020). Analyzing the urban micro-climate at the local level and integrating the local-level cooling interventions into the planned developments were necessary to investigate.

1.2 Aim and Scope of The Study

This study mainly aims to investigate spatial interventions for increasing the cooling capacity of urban areas at a patch scale, which is more applicable to sustainable urban planning practice (Guo et al., 2019; Li et al., 2017; Maimaitiyiming et al., 2014; Peng et al., 2017; Rakoto et al., 2021; Zhou et al., 2017; Shih, 2017). The main questions of this study are;

1. How can LST distribution be analyzed in terms of understating the cooling effect in urban area?
2. What are the characteristics of UCIs in İzmir?
3. How can the cooling intensity of UCIs be measured?
4. How can the cooling extent of UCIs be measured?
5. How can components of the cooling capacity affect the thermal conditions of the urban environment?

This study aims to develop an innovative spatial statistical method based on the distribution of LST, consisting of three successive steps to extract patches of UCIs and provide a new definition for UCIs. In the study, UCIs are defined as the coolest areas corcerning their surrounding environment. The utilization of spatial analysis approach will provide an opportunity to examine spatial characteristics of the spaces with cooling capacity. This approach will enable a comprehensive discussion of the

extent to which urban parks contribute to the spatial pattern of UCIs, which was limited in the literature (Peng et al., 2022).

This study target to reach outcomes for the urban planning process that will impact urban climate planning. The objectives can be listed:

1. Understanding the cooling capacity creation in urban areas
2. Discussing the cumulative cooling effect
3. Reaching quantifiable results for increasing cooling capacity
4. Analyzed the cooling capacity with both of regarding two- and three-dimensional urban environment
5. Discussing limitation of the study in term of dataset, methodology and approach
6. Developed innovative spatial statistical method based on the distribution of LST to investigate the cooling
7. Comparing and discussing the findings of the pilot case with the previous ones

For measuring the cooling intensity of UCIs, this study is conducted to: (1) extract UCIs within the İzmir urban area, (2) quantify the contributions of landcover composition of UCIs, green configuration within UCIs, UCI characteristics, and other effects on the cooling capacity of UCIs. For measuring the cooling extent of UCIs, this study is conducted to (1) identify the extent area, (2) quantify the contributions of the cooling intensity of UCIs, (2) UCI composition and configuration, (3) Green composition and configuration of the extent area and (4) urban morphology of the extents. Lastly, the relation between these components of the cooling capacity and thermal climate conditions is investigated. All the proposed models discuss regarding alternative solutions for spatial planning decisions to mitigate the UHI effect. The results will provide insight to find global and local alternative solution for cities with high urban comfort.

1.3 Research Method

While developing the research method of the thesis, firstly, previous studies were investigated in term of how to analyze the cooling effect in the urban environment. The literature review conducted in the second chapter of the thesis. The studies were mainly explained under four headings for analyzing how the literature undertook the cooling effect (1) measuring the cooling intensity of urban cool islands (UCIs), (2) measuring cooling extent, (3) measuring the cumulative cooling effect of UCIs measuring and (4) urban morphological character of cooler areas. Research approaches of the studies in measuring the cooling capacity were additionally explained (Figure 2, Figure 3).

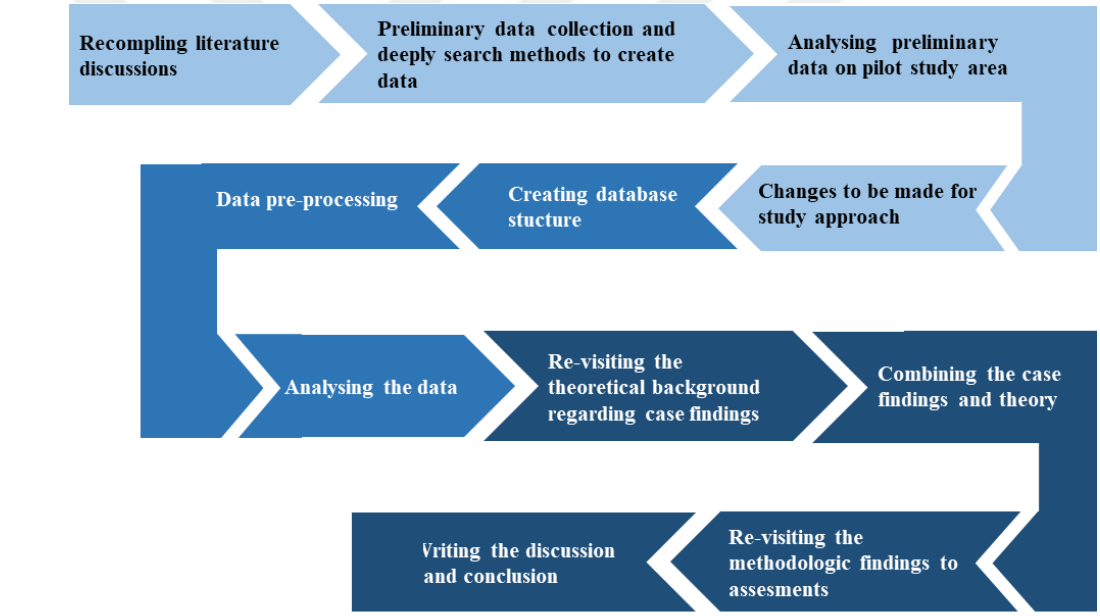


Figure 2. Steps of Research Method

After recompiling the literature discussions, primary data was collected and deeply methods to create data and preliminary data of pilot study area were analyzed. Together with literature discussions and primary findings, the study approach was developed. The cooling capacity was measured by two parameters in the thesis which were the cooling intensity and the cooling extent. The main issues related to these parameters and the interactions between these parameters and conditions of thermal

environment were schematized for the hypothesis of the thesis. To measure the cooling intensity of UCIs and cooling extents, two database structures were developed. Before creating the spatial database in ArcGIS Pro, the data was pre-processed using remote sensing techniques and spatial analysis occurred. In the chapter 3, data and method were explained. The chapter consisted of the research approach and hypothesis, preprocessing of the data, and spatial statistics for analysis of LST distribution, statistical analysis. Additionally, the regression models were explained to measure the cooling intensity of UCIs and the cooling extent and to understand the thermal conditions of urban environments (Figure 2, Figure 3).

After creating databases and the analyses approach, analyses were conducted using SPSS. Initial findings were developed by re-visiting the theoretical background. The final findings were about the results of the spatial analysis, the regression models and policy analysis. The findings were explained in Chapter 4. The findings were compared with the previous studies. According to these, the hypotheses were discussed for the case and other findings. This part was explained in the chapter 5, discussion, and conclusion (Figure 2, Figure 3).

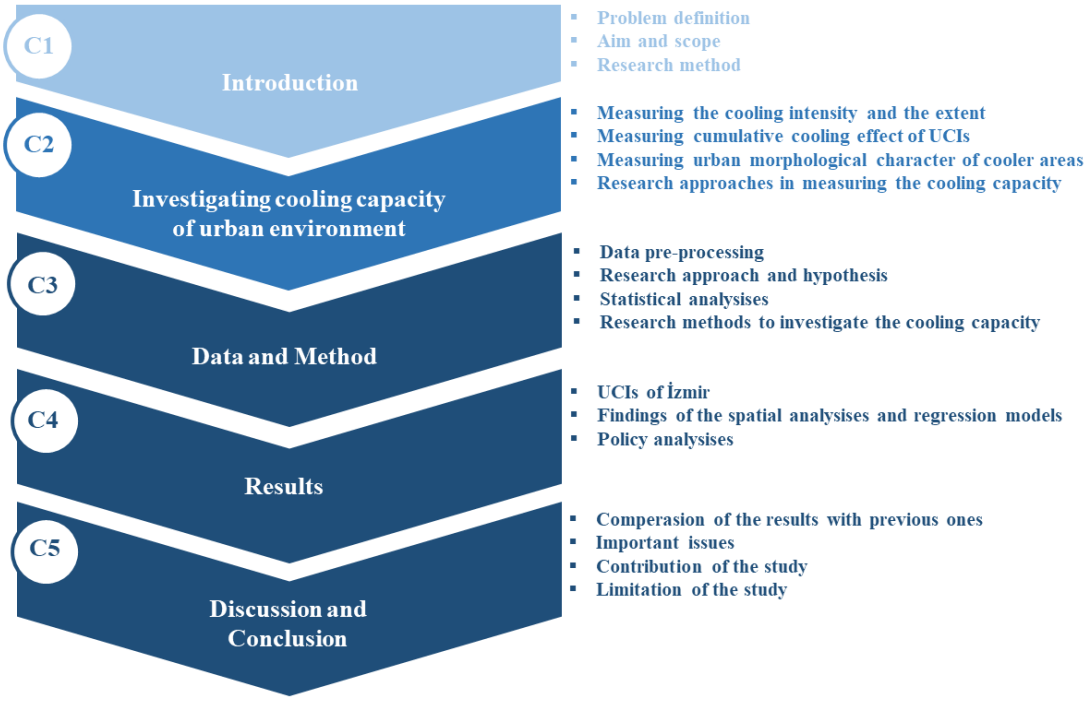


Figure 3. Context of the thesis

CHAPTER TWO
LITERATURE REVIEW

The spatial pattern of LST does not distribute homogeneously in urban areas. Densely urban areas generally produce UHI are defined as heat source (Li et al., 2017), urban heat island (Li et al., 2009), local heat island (Chang & Li, 2014) or hot spots (Walawender et al., 2014) which results in contributing heat to the adjacent environment. When the average size of these homogeneous patches, dominated by the urbanization density, is increased, the extent and magnitude of UHIs also increase (Li et al., 2009). Regularly lower LST values, beside adjacent built-up areas, are also observed (Chen et al., 2012; Dousset & Gourmelon, 2003; Kong et al. 2014) on some parts of the city that these areas were termed as the heat sink (Li et al., 2017), cool island (Kong et al., 2014), local cool island (Chang and Li, 2014), cool spot (Walawender et al., 2014), or park cool island (Cao et al., 2010) because of exerting cooling effects on the adjacent environment like urban heat island, effectively regulating neighborhood cooling (Sppronken-Smith & Oke, 1998). A cool island was the aggregated result of the surrounding cooler areas. Thus, this cumulative cooling effects of the surrounding cool islands generated UCI intensities (Kong et al., 2014). Zhang et al. (2016), described the cooling effect as a benefit when one neighborhood was exposed to one more cooling effect of green spaces where there was a multiple effect.

Microscale UHIs were observed in the heterogeneous urban fabric areas (Leconte et al., 2015) like industrial areas and, densely urbanized commercial and residential areas of the city (Liu et al., 2017; Zang et al.; 2018; Walawender et al., 2014) with airport and large railway (Walawender et al., 2014). UCIs were generally located on in forests, waters, meadows, permanent crops, and green urban areas (Kong et al., 2014; Walawender et al., 2014). Lower temperatures were measured near urban green areas while higher ones were measured in dense building clusters (Ng et al., 2012; Liu et al., 2017). Walawender et al. (2014) results also showed that 92% of continuous urban fabric areas had higher LST than the mean value without any cold spot level. When the development density of the built-up area increased, the

necessity of the cooling service increased due to higher thermal stress and population to reduce vulnerability (Peng et al., 2020).

2.1 Cooling Effect of Blue and Green Infrastructure

Urban green spaces consist of an urban environment covered by vegetation, and additionally blue areas like streams, and lakes with adjacent green areas. Urban green spaces, can also be identified as urban ecosystems, comprised of various natural areas even if managed by man, from parks to wetlands, and urban forests. Green spaces have various services in ecosystems such as carbon storage, water drainage, flooding control, and enhancing biological diversity (Bolund & Hunhammar, 1999).

Local climate condition was shaped by the mutual effect of global and local circulation pattern (Groot et al., 2002) according to natural and unnatural structure. Urban blue and green infrastructure regulate local temperatures (Hardin & Jensen, 2007) against the heating effect of non-vegetated areas. Waterbody acts as a cool heat in summer and release absorbed heat in winter. The reflection function of natural ecosystems especially affects the climate at various scales (Groot et al., 2002). In urban areas, vegetation plays an important role in regulating the climate due to evapotranspiration and shading (Bolund and Hunhammar, 1999). Evapotranspiration is the process of extracting water from the soil via the roots of plant species and moving it to their leaves, which is called transpiration. Evapotranspiration is very important especially in low-humidity environments, which is altering the species (Chaparro and Terradas, 2009). In addition, trees absorb solar radiation and prevent the surfaces from exposing the radiation directly thanks to shading (Santamouris et al., 2001). Leafy species, such as silver birch, oak, or beech, generally show higher cooling capacity due to effectively releasing water vapor (Chaparro and Terradas, 2009) and supplying shading. Similarly, fine-textured vegetation had a structure with frequent and larger leaves so that, course textured vegetation showed less cooling capacity than fine textured one (Du et al., 2016).

2.2 Measuring the Cooling Intensity of Urban Cool Island

Previous studies measured lower air or surface temperatures on vegetated areas like tree-covered street, urban parks, and forestry (Li et al., 2009; Ng et al., 2012). Wong and Yu (2005) observed a maximum difference of 4.01 ˚C between well planted area and the CBD area in Singapore and Ng et al. (2012) documented a significant reduction in air temperature of 0.8 ˚C and 1.3 ˚C in the park area compared with nearby built-up urban areas. Kong et al. (2014) measured UCI mean temperature reduction for different parks, minimum −0.6 ˚C and maximum −6.9 ˚C by analyzing 116 urban green areas. Geng et al. (2022) measured the cooling effect for 207 urban parks the average cooling intensity was 2.31 ˚C with a minimum 0.60 and maximum 5.13 ˚C. Most of the parks, 58%, was between 0 and 2 C values within different local climate conditions. Peng et al. (2020) measured the cooling intensity of 200 different waterbody patches, changing from 0 and - 5.54 ˚C with an average of 1.1 ˚C. Oliveira et al. (2011) found that the garden was cooler than the surrounding areas, either in the sun or in the shade.

Some of the previous studies investigated parameters affected by the cooling intensity of UCIs. Rizwan et al. (2008) observed a cooling effect of nearly 1 ˚C - 1.5 ˚C for various applications like greening and lighter cooler pavement. For this research, parameters affecting the cooling capacity of UCIs were defined on 6 categories, waterbody abundance, green abundance, green configuration, UCI characteristics, land cover and outer effect (Table 1).

Table 1.Parameters Affecting the Cooling Intensity in the Literature

Focus	Parameters	References
Waterbody abundance	Percentage of water surfaces /water proportion	Geng et al 2022, Zhang et al. (2016); Yin et al. (2018)
Green abundance	Percentage of green area/ tree-covered area/ grass area/ NDVI	Ng et al. (2012), Mackey et al. (2012) Maimaitiyiming et al. (2014), Peng et al. (2018), Peng et al. (2020), Gemg et al. 2022, Shih (2017), Peng et al. (2020), Shahidan et al. (2012), Cheng et al. (2015), Chang and Li (2014), Estequo et al. (2017), Yin et al. (2018)
	Canopy effect	Shashua-Bar and Hoffman (2000), Shahidan et al. (2012)
Green configuration	Mean patch size of tree-covered area/green area	Kong et al. (2014); Maimaitiyiming et al. (2014, Du et al. (2016), Zhou et al. (2017), Shih, 2020, Peng et al. 2018, Estequo et al. (2017)
	Fragmentation of green area	Myint et al (2015)
	Standard deviation of patch area	Du et al. (2016),
	Mean patch shape index	Zhou et al. (2017), Peng et al (2018), Peng et al (2020)
	Edge density	Zhou et al. (2017); Geng et al. 2022
	Largest patch index	Zhou et al. (2017)
	Coherence, nearest distance	Shih, 2020, Asgarian et al. (2015)
	The fractal dimension of waterbody patch	Peng et al. (2020)
	Fractal shape of a park area	Geng et al. (2022)
	Shannon diversity index	Peng et al (2018)
	Shape complexity	Estequo et al. (2017)
	Aggregation	Estequo et al. (2017)
	Core area index	Asgarian et al. (2015)
UCI characteristics	UCI size/ Park area	Lin et al. (2015), Ren et al. (2013), Kong et al. (2014), Cao et al. (2014), Geng et al 2022, Peng et al. (2020); Shih (2017), Yang et al. (2023)
	Shape index	Cao et al. (2010), Geng et al., (2022), Asgarian et al. (2015), Shih (2017); Peng et al. (2020)
	Perimeter to area	Asgarian et al. (2015)
Land cover	Percentage of built-up area/construction land	Peng et al. 2018, Estequo et al. (2017), Chang and Li (2014),
	NDBI	Peng et al. 2018
Outer effect	Distance to UHI	Kong et al. (2014)
	Proximity to mountain Proximity to river	Shih (2017)
	Buffer water area percentage	Geng et al 2022
	Buffer green rate	Geng et al 2022, Yan et al. 2014
	Road density of buffer area	Geng et al 2022
	Building density of buffer area	Geng et al 2022,
	Population density	Peng et al. (2020)

2.2.1 UCI characteristics

There were some studies analyzing the relationship between the mean temperature reduction and the size of each UCIs. The results showed that the size was most important parameter to explain the intensity. When the urban park size increased, the intensity also increased (Cao et al., 2010; Cheung and Jim, 2019; Kong et al., 2014; Lin et al., 2015; Peng et al., 2020; Shashau-Bar and Hoffman, 2010). Kong et al. (2014) measured that the intensity strongly correlated with UCI area (R= 0,87, p<0,01) by analyzing 92 urban parks with different sizes changing between 0.1 ha and 41.9 ha. The correlation showed non–linearity (Kong et al., 2014; Peng et al., 2017; Ren et al., 2013; Shashua-Bar and Hoffman, 2000; Sun et al., 2020). Ren et al., (2013), concluded that urban park area and perimeter as independent variables could explain 54.66%–56.22% of the intensity variance respectively in summer where size was the most important parameter by analyzing 33 park areas. Similarly, Cao et al. (2010) supposed that park size, could explain only 60% of the intensity variances. Thus, the complex relationship between the intensity and park characteristics could not be represented only by park size. Geng et al. (2020), measured that the relative contribution to the cooling effect variation for park size was 50%.

Moreover, Cao et al. (2010) supposed that only parks larger than 2 ha showed a significant cooling effect greater than 1.5 ˚C. Lin et al. (2015) focused on the cooling effect and showed extraordinary importance when the park size was larger than 640 ha in terms of regulation of the climate. Cheng et al. (2015) classified the parks according to their size, and then the average LST values were calculated for each group by analyzing 39 parks. According to the results, there was not a dramatic temperature difference between parks, between 0.1 ha and 10 ha, and adjacent built-up areas, but parks, bigger than 10 ha, were coolest than those under 3 ha with 1.8 ˚C. In contrast to these acceptances, Oliveira et al. (2011) measured 6.9 ˚C air temperature reduction in a small-scale urban park, 0.24 ha in size, between the inner and outdoors of that park. This result emphasized that small parks could have a cooling capacity. However, Shih (2017) argued that greenspace size may have a limited effect on mitigating UHI by analyzing urban green areas in a basin.

In addition, Peng et al. (2020) underlined that increasing the patch size of UCIs would be more important to increase the intensity especially for densely built environment due to having lower LST inside of the UCIs. However, this increasing trend reached an optimal limit. (Fan et al., 2019). Geng et al. (2022) measured threshold park size for different local climate conditions. The findings showed that the cooling effect related to the size could alter climate conditions. For example, the cooling effect of smaller parks may be more effective when closer to equator (Geng et al., 2022).

Results of the previous studies showed that there was a negative relation between the intensity and compactness of the shape. Thus, more compact parks had a higher cooling effect (Cao et al., 2010). Thus, the simplicity of the geometry increased the cooling effect like circle and square shapes (Du et al. 2016). This result was also observed for the landscape shape index, used to measure the shape complexity such as the fractal shape of the park (Geng et al. 2022), and perimeter to area ratio (Asgarian et al., 2015). Geng et al. (2022) observed that park shape played very crucial role determining the cooling effect. with explaining relatively 50% of the cooling effect variation. The proportion for determination of the cooling effect of the fractal shape of the park was 18% with negative correlation.

In contrast to this finding, Yang et al. (2023) argued that the complexity of the shape decreased the LST values when the park size was larger than a threshold, altering according to local climate conditions. Shih (2017) also supposed that greenspace shape may have limited effect.

2.2.2 Abundance of the green

Previous studies generally measured lower temperatures in the urban areas in well-vegetated areas (Cao et al., 2010; Cheung and Jim, 2019; Maimaitiyiming et al., 2014; Ng et al., 2012), so abundance of greenery is crucial to understanding the cooling capacity of UCIs. For example, Kong et al. (2014) indicated that UCIs are located in areas, which cover percent of forest vegetation larger than 60%. Some of the studies measured a strong negative correlation relationship between LST and Normalization Vegetation Index (NDVI), and remote sensing data measured

abundance of the vegetation (Amiri et al, 2009, Carlson & Arthur, 2000, Hung et al, 2006; Mackey et al, 2012; Marando et al, 2019, Yuan and Bauer, 2007; Tiangco et al, 2008; Weng and Lu, 2008). In this way, the higher abundance of the green area resulted in higher temperature reduction. Amir & AbdElfattah (2017) measured a 3-4 ˚C temperature difference during daytime and nighttime between two open spaces, planted with trees and lawn and a non-vegetated one. Peng et al. (2018), observed that the green abundance factor, NDVI, forest ratio and grass ratio, explained LST with 76.4% in summer. Mackey et al. (2012) investigated the cooling effect of the vegetation by analyzing NDVI and vegetated area change within 15 years in the city of Chicago. He exerted that vegetated area averagely increased from 31.1% in 1995 to 33,0% in 2010. This decrease resulted in an average temperature change of +1.9 ˚C.

Some previous studies suggested that vegetation type was also important in that trees had a higher cooling effect (Cao et al., 2012; Ng et al., 2012) because of especially having canopy effect. Results of the studies showed that there were extreme temperature differences between the shaded and the sunny sides of the streets (Fintikakis et al., 2011; Oliveira et al., 2011). Fintikakis et al. (2011) analyzed the canopy effect of the trees that high size ones offered coolness evapotranspiration wad almost 0.2 ˚C lower than medium trees or just use of grass. The canopy effect was very crucial to define cooling effect in summer times, it was 80% of the cooling supplied by tree shading (Shashua-Bar and Hoffman (2000). Similarly, Shahidan et al. (2012) measured the impact of the shading 60%. As a result, canopy density had a significant relationship with LST (Cao et al., 2012; Ng et al., 2012; Ren at al., 2013) because number of the trees affects both indoor and outdoor temperatures (Shahidan et al., 2012).

Some previous studies created various simulations for a specific site to measure the cooling effect of the green abundance. Shahidan et al. (2012) simulated using ENVI-met, there could be supply 1 ˚C the reduction when the number of trees increased by 33% in the densely urban area. Similarly, Cheng et al. (2015) measured a 1 ºC reduction when the ratio of green area raised from 0% to 28,5% whereas a 0,4 ºC, reduction was observed when the ratio was raised to 59,94% from 28,9%. Ng et

al. (2012) studied on a case area, high-density built-up area. The results of simulations indicated that grass coverage is considerably less effective on urban cooling than tree planting, and the amount of tree planting should be approximately 30% of the urban area to mitigate UHI intensity. A similar result was measured by Chang and Li (2014), parks, covered by more than 30% tree and shrub, showed effective cooling effect in terms of regulating local climate. After all, there needs to be larger green surfaces than impervious surfaces to mitigate UHI for megacities (Estequo et al., 2017). Yet, Shih (2017) measured that NDVI values of green spaces had a weak correlation with the cooling intensity, but it was significant.

2.2.3 Land cover

Land cover of the UCIs was related to explaining intensity of UCIs (Cao et al, 2010), water and impervious surfaces like green-covered area. Kong et al. (2014) extracted UCIs that UCIs are located in areas where the percent coverage of water area <20%. Zhang et al. (2016) analyzed temperature change for a wetland and natural lake between 1990 and 2010, water body was hotter in 2010 with 8.59 C because reduction of water surfaces. Water body had a positive correlation with LST with 13.24% relative contribution. Qaid et al., (2016) emphasized that water body abundance had a priority to designing building layout than shading due to cooling effect.

Chang and Li (2014), parks with less than 50% paved cover showed cooler temperature according to nearby areas whereas parks with more than 50% paved cover was hotter. Shahidan et al. (2012) simulated using ENVI-met, when pavement material and tree species well-regulated temperature decrease can be reached to 3.5 ºC. Peng et al (2020) measured albedo effect with NDBI and perception of construction land area that it was explaining LST with 88.9% rate. Estequo et al. (2017) supposed that an abundance of impervious surfaces affects much more than green surfaces. Qaid et al., (2016) suggested that the impervious surfaces needed to be shaded to mitigate UHI intensity.

2.2.4 Outer thermal effect

Peng et al. (2020) proved that the surrounding density of the built-up environment and activities was significant in determining the intensity, which resulted in a decreased cooling effect due to traffic activity and storage of radiation. Kong et al. (2014) measured a negative relationship between the cooling intensity and distance to hot spots. In contrast to thermal heating sources, the mountain, sea and forest areas were taken as the outer cooling sources in the literature (Kong et al., 2014; Li et al., 2017; Shih, 2017). The natural environment surrounding the city centers was an important component in regulating the climatic conditions of the cities. “

2.3 Measuring the Cooling Extents

Lower LST values observed in the park gradually increased with distance from the park for all daytime (Hamada et al., 2013; Oliveira et al., 2011; Peng et al., 2017). A similar gradient observation also was on the riverside (Zhang et al., 2016). This temperature difference between urban green area and adjacent urban areas was logarithmically increased when father from their boundary (Chang and Li, 2014; Hamada et al., 2013; Lin et al. 2015; Monteiro et al., 2016). This difference could be very dramatic according to urban pattern (Chen et al, 2012; Hamada et al., 2013, Kong et al, 2014). The difference measured by Aram et al. (2019), nearly 2°C difference between 150 meters and 665 meters away from an urban large park, 125 ha in size. Additionally, Chen et al. (2012), measured a maximum temperature reduction of 2.03 °C for 400 m away from the park within investigating 10 large parks. Wang & Zhu (2011) measured LST values for a wetland and a natural lake as UCIs that the reduction of about 2.5 C at 50 m buffer, for after 300m and 450 m buffer the reduction become stable. Thus, the studies presented that there was a transition area, measured medium temperatures, between UCIs and adjacent urban area. This area could be also defined as the extent of UCI where felt cooling effect of the UCI, which help to understand the impact level of UCI’s climate regulation function (Wang & Zhu, 2011). In this way, closeness to UCI is an important indicator to of defining urban thermal comfort (Cheung & Jim, 2019).

The cooling extent quantified by Lin et al, (2015) that the median LST values were between 85 m and 284 m. The maximal cooling extents of the six urban parks, ranging from 14 ha to 1000 ha, reached as far as 840 m while the minimal cooling extent was only 35 m. The minimal cooling extents were generally under 100 m, with the median values normally under 200 m, irrespective of the size of the green park. The studies showed that there was a significant relationship between cooling extent and both UCI size and intensity (Chen et al., 2012). Chen et al. (2012) supposed that park size had a stronger correlation with cooling extent compared to cooling intensity.

Cheng et al. (2015) calculated the average maximum cooling distance as 276,7 m with a very large standard deviation for 39 parks, but the distance generally reached to 600m. Hamada et al. (2013) analyzed an urban park, sized 147 ha, and its periphery. In commercial areas, consisting of concrete buildings of various height and heavy traffic roads, at 50–250 m buffer of the park, the temperature difference was very dramatic, so that spatial distribution of the cooling effect was affected by specific land-use types. However, the study did not reach any significant results for mid- and high- rise dwelling areas and the effect of the wind on the spreading cooling effect of the park. Heatway & Sharples (2012) chose a river corridor consisting of water and green areas as UCIs. The results showed that the cooling effect of the water significantly influenced on 30 m buffer, but there was a considerable variation depending on the local urban form, provision of vegetation and surface materials, after 30 m. Similarly, Chang & Li (2014) executed the cooling effect of 60 different parks having size of 0.01 and 39,7 ha, was felt at distances ranging from 60 meters to 300 meters. Shashua-Bar & Hoffman (2000) analyzed 11 different open spaces with trees. According to the results of the study, the lowest temperatures measured mid of the case sites, besides, 2.8 K temperature reduction was felt on a limited distance from 20 m to 60m due to case areas, consisting of smaller green spaces.

2.4 Measuring the Cumulative Cooling Effect of UCIs

Previous studies indicated that spatial configuration of green areas was also important in mitigating UHI (Ren et al., 2013; Kong et al., 2014, Maimaitiyiming et al., 2014), so the configuration was more effective for UCIs intensity compared to the abundance of the greenery (Zhou et al, 2017). The parameters of the green configuration used in the literature are shown in Table 1, which were important factors in determining the cooling capacity. Results of the studies showed that not only the composition of the tree-covered area was important to mitigate UHI, but also parameters regarding the configuration were also significant. According to this, mean patch size, shape index and edge density were significant explaining LST (Zhou et al. (2017). Cheng et al. (2015) measured that patch density and the largest patch index negatively correlated with the intensity.

Estequo et al. (2017) argued the cumulative heating effect by comparing three megacities that aggregated impervious surfaces or fragmented green surfaces resulted in higher LST values. Larger green patch sizes and higher connectivity also resulted in lower LST values. When compared with mean size, mean shape index and aggregation, aggregation was the most significant parameter to determine LST. Although the total sizes of green areas were equal and had a continuous pattern, larger patches had a stronger cooling effect (Cao et al., 2010; Li et al., 2012). Similarly, Asgarian et al. (2015) emphasize larger green areas with lower distances between patches, taken as a homogeneous land cover pattern, resulted in LST decrease. As a result, vegetation fraction had a strong relationship with LST (Carlson and Arthur, 2000; Weng and Larson, 2005; Hung et al., 2006; Yuan and Bauer, 2007; Tiangco et al., 2008; Weng and Lu, 2008; Amiri et al., 2009). In addition to vegetation, fragmentation of the waterbody patch had a negative correlation with its cooling intensity (Peng et al., 2020).

The importance of the composition and configuration of trees could be different for cities (Zhou et al., 2017). Zhou et al. (2017) compared two cities in that the cooling effect of the spatial configuration of the trees could alter according to local climate. For example, greater edge density could result in much more thermal flow

between green and its adjacent area. Greater edge density could occur due to fragmented and smaller green areas which brought out decreasing evapotranspiration efficiency. Yet, it can be much more shading area resulting in lower LST in a fixed amount of green area.

Cheng et al. (2015) supposed that there was a mutual effect between the green area and adjacent green abundance which shaped the cooling intensity of UCIs. In this way, the dominant land cover, adjacent to the UCIs, played important role in defining the intensity due to creating cumulative cooling effect. According to this argument, small parks could be regulated by local climate due to the division of the large urban patches so that park size could not be dominant in determining thermal comfort. The fragmentation of urban patches can be an alternative solution for cities having limited vacant land areas in terms of optimizing the configuration of different land covers (Du et al., 2016). Similarly, Shih (2017) indicated that amplifying cooling intensity and cooling extent was very effective in mitigating UHI by greening nearby areas of UCIs and enhancing UCIs cohesion. In this way, the cumulative cooling effect can be extented by increasing the connectivity of small cool islands and other outer cool islands like natural areas, mountains, and rivers. On the other hand, Peng et al. (2020) focused that the same-size UCIs may not have cooling effect for different urban areas because the outer heat effect of the surrounding area restrict the function of climate regulation of UCIs, which increases demand for large-size UCIs. Similarly, Heatway and Sharples (2012) argued that surface materials were more dominant than water bodies in the air temperatures.

Shih (2017) also measured the cumulative effect by analyzing the relationship between the LST of the inner greenspace and buffer area. The findings showed that the greenery of the buffer area is more significant in defining the cooling intensity and temperature of the buffer. To deal with UHI, increasing the green abundance of the buffer could be more effective than increasing the greenspaces. Results from these studies can expand our understanding of the relationship between LST and street trees and vegetation and provide insights for sustainable urban planning and management in achanging climate.

2.5 Measuring Urban Morphological Character of Cooler Areas

With a two-dimensional approach, impervious surfaces generally reduce the UHI effect, but the urban form play a more effective role in controlling it. Thus, random factors also played a significant role in causing the complexity in patterns of UHI. Li et al., (2009) supposed that the structural variation accounted for approximately 50% of the total UHI variation. Higher building mass occurred higher LST values because of increasing heat storage in the daytime (Silva et al., 2018; Yan et al., 2014; Zhao et al. 2011) with increasing surfaces exposing solar radiation (Silva et al., 2018). In addition to this, interventions, enhancing air ventilation, played an important role, especially the extending the cooling effect by optimizing building shape and street layout. The parameters measuring urban morphological parameters used in the literature are shown in Table 2 with groups according to built-up density, three-dimensional built-up area, urban geometry, material, and anthropogenic indicators.

Parameters, measuring built-up density, were the most important ones to identify UHI such as building density (Li et al., 2020; Zhao 2011, Yin et al. (2018), Yan et al., 2014, Yan et al., 2014, Silva et al. 2018), building coverage ratio (Ng et al., 2012, Leconte et al. (2015), Unger 2006), floor area ratio (Silva et al. 2018) porosity (Silva et al. 2018, Park et al. 2017) or impervious surface fraction (Maimaitiyiming et al., 2014), Yin et al., 2018; Leconte et al., 2015) Middel et al., 2014, Pan (2016), Silva et al. 2018). Building density showed priority while shaping the thermal environment (Li et al., 2020; Yan et al., 2014). Because it also referred to urban activities resulting in the production of anthropogenic heat, like energy consumption for heating and cooling or traffic density (Yan et al., 2021). Supporting this argument, Unger (2006) measured that built-up area explained the UHI intensity with nearly 66% variation. Although it varied according to the aspect ratio, building coverage ratio could be more effective than vertical density (Li et al., 2020). The decisions about urban morphology should protect the impervious surfaces from solar radiation (Chun and Guldmann, 2014; Qaid et al., 2016).

Table 2. Parameters Related to UHI Concerning Urban Morphology

Focus	Parameter	Authors
Built-up density	Impervious/ pervious surface fraction/ areas of impervious surfaces	Leconte et al. (2015); Middel et al., 2014, Pan (2016); Silva et al. 2018; Maimaitiyiming et al. (2014); Yin et al. (2018)
	Building coverage ratio	Ng et al. (2012), Leconte et al. (2015), Unger 2006
	Building surface fraction	Middel et al., 2014
	Floor area ratio	Zhao 2011, Yin et al. (2018)
	Building density	Li et al., 2020; Zhao 2011, Yin et al. (2018), Yan et al., 2014, Silva et al. 2018
	Porosity	Silva et al. 2018, Park et al. 2017
Three-dimensional built-up area	Building-height/verticality	Ng et al. (2012), Leconte et al. (2015), Peng et al. (2017) Middel et al., 2014
	Building height limit	Zhao 2011, Silva et al. 2018
	Mean compactness	Unger 2006
	Weighted volumetric compactness	Unger 2006
	Surface roughness	Park et al., 2017
Urban geometry	Sky view factor	Leconte et al. (2015), Peng et al. (2017), Middel et al., 2014, Unger 2004, Unger, 2006, Yin et al. (2018), Yan et al. (2014), Park et al. 2017
	Canyon aspect ratio/ H/W aspect ratio	Lİ et al. 2020; Leconte et al. (2015), Silva et al. 2018
	Street orientation	Oliveira et al. (2011)
	Distance between buildings	Zhao 2011
	Roughness length	Silva et al. 2018
Material	Albedo	Leconte et al. (2015) Middel et al., 2014
Anthropogenic indicators	Anthropogenic heat flux	Leconte et al. (2015)

Understanding the complex mechanism of UHI intensity, there was a need to analyze the built-up area with three-dimensional parameters. Previous studies measured significant relationship between UHI intensity and building height (Ng et al., 2012; Leconte et al., 2015); Peng et al., 2017) Middel et al., 2014), but the direction of the relation was different. According to this, the some of previous studies found there was a significant negative relationship between building height and UHI (Qaid et al. 2016; Zhao et al., 2011). However, Sakar (2018) argued by simulating UHI intensity for different urban morphological types that UHI intensity became higher when building height increased for the same building footprint. In contrast to this, the intensity is reduced by about 0.20°C over 8 floors with decreasing building footprint. Similarly, Li et al. (2020) supposed that slower increase in UHI intensity could be observed for the building density with a high-rise building. Open spaces between buildings could be more important than building height because of rising the emittance of long-wave radiation Sakar (2018). urban layout with small buildings

instead of continuous blocks also reduced the infrared radiation at street level creating higher shading and reflection (Silva et al., 2018). Unger (2006) measured three-dimensional urban pattern by generating volumetric compactness which was strongly positively correlated with UHI intensity. In a multi-regression model with water surface and building density, 9.2% increase in the intensity supplied by weighted-compactness index.

To boost the airflow in the city, built-up density, three-dimensional parameters and urban geometry played an important role. In addition to building height, length of facades, permeability level of urban pattern and street wide were key determinants to reducing the magnitude of UHI (Sakar (2018). Like building density, higher porosity, representing the ratio of void space within a total volume of space boosted air flow, higher flow decreased UHI (Park et al., 2017). Continuous blocks resulted in decreasing intersection of the streets meanwhile restricting to spread cooling effect of the parks (Silva et al., 2018). Peng et al. (2017) and Qaid et al., (2016) suggested that urban centers should be mix of high and low buildings to create a fluid dynamic path in terms of ventilation. Qaid et al., (2016), recorded a 4 ºC difference between the low-rise buildings and the high-rise residential area and a 3 ºC difference between the low-rise buildings and suburban area. Qaid et al., (2016) suggested that residential area of high-rise buildings with a large distance between buildings can provide better local climate conditions than residential area of low-rise buildings with proximity, shading and wind direction should be undertaken while designing the residential areas. In contrast, Park et al. (2017) exerted that irregularity of the buildings, measured by surface roughness, restricted air flow in the city because higher buildings could function as a barrier. Heatway and Sharples, (2012) emphasized the block effect of the wall and the buildings which prevent to expansion cooling effect of the river corridor to inner sides like Qaid et al., (2016). To spreading of the cooling effect showed variations depending on the local urban form and abundance of vegetation opening the streets to riverside.

Previous studies generally analyzed the relationship between UHI, and urban geometry as measured by sky view factor (SVF). Air temperature increased as the SVF increased in the daytime (Leconte et al. (2015), Peng et al. (2017), Middel et al.,

2014, Unger 2004, Unger, 2006, Yin et al. (2018), Yan et al. (2014), Park et al. 2017). Yan et al. (2021) concluded that a 0,14 ºC temperature increase occurred by per 10% increase in SVF. Unger (2004) measured a strong negative correlation between the temperature and SVF with explaining variation by 47%. As a result, reducing sky view factor by optimizing building height and spaces between buildings, could be a crucial precaution (Sakar, 2018). Similar findings were found in another parameter to measure urban geometry, H/W aspect ratio or canyon aspect ratio. Higher values of H/W aspect ratio, high buildings with narrow streets, and increased to UHI intensity (Lİ et al. 2020; Leconte et al. (2015), Silva et al. 2018) due to changing radiation balance with less porosity (Silva et al. 2018).

Moreover, air ventilation, sun exposure and urban geometry were the potential factors that particularly explained the different local weather conditions according to findings of the previous studies (Fintikakis et al., 2011; Oliveira et al., 2011; Peng et al., 2017; Qaid et al., 2016). Qaid et al. (2016) emphasized that designing streets regarding to wind flow direction and enhancing the number of streets perpendicular to UCIs could raise urban thermal comfort in other words, the observed air temperature showed that the buildings oriented against to wind direction blocked the ventilation of the residential areas. This block effect also prevented the expansion of lake water's cooling effect, and in the Boulevard area, faster wind speed carried lake water's cooling effect to small perpendicular streets in residential areas (3). Oliveira et al. (2011) analyzed the effect of street orientation on air temperature by investigating shaded and sunny sides of the streets. According to the results, there was no significant difference between streets exposed to solar radiation during similar time in various orientations.

2.6 Research Approaches in Measuring the Cooling Capacity

Previous studies generally investigated the relationship between cooling capacity and UCI characteristics (Bacci et al. 2022; Cao et al., 2010; Chang & Li, 2014; Cheng et al., 2014; Cheung & Jim, 2019; Ren et al. 2013; Vidrih & Medved, 2013) green abundance (Cheng et al. 2014; Ng et al., 2012; Wang & Zhu, 2011), composition and configuration of UCI (Guo et al., 2019; Li et al., 2016);

Maimaitiyiming et al. 2014; Rakoto et al. 2021; Zhou et al. 2017; Shih 2017) or land cover (Myint et al. 2017) and urban morphology (Oliveira et al., 2011; Hamada et el., 2013; Heatway & Sharples, 2012). These studies analyzed the cooling capacity at micro and mezzo scales at various analytical units, patches, and pixels. It is necessary to determine an appropriate spatial scale to describe meaningful association in terms of land cover management in urban planning (Guo et al., 2015). For patch scale, urban park (Bacci et al. 2022; Cao et al. 2010; Chang & Li, 2014; Cheng et al., 2014; Cheung & Jim, 2019; Ren et al. 2013; B. Vidrih & Medved, 2013), natural area boundary (Wang and Zu, 2011), administrative district Li et al. (2012), and polygons delineated by statistical methods (Guo et al., 2015; Guo et al., 2019; Pan, 2016 ; Zhang et al., 2018) were defined in the literature (Table 3).

The studies investigating the composition and configuration of UCI were at mezzo scale (Guo et al., 2019); Maimaitiyiming et al., 2014); Rakoto et al., 2021); Zhou et al., 2017); Shih, 2017; Zhang et al., 2017; Li et al., 2012; Li et al., 2017; Myint et al. 2017) because of need of the research aim. Yet, micro-scale studies generally analyzed the inner features of the UCI, but some of the studies included buffer zone of the UCIs to take into consideration on interference with the environment (Li et al., 2016; Cheng et al., 2014). While analyzing a micro-scale case with small data, the findings helped to observe specific reasons for creating the cooling capacity of the case area. However, these studies could not generate a certain result that their findings were like observation generally due to the small dataset (Bacci et al. 2022; Cheung & Jim, 2019). To get over this problem, some studies took several sampling areas to reach general results (Cao et al., 2010); Chang & Li, 2014); Cheng et al., 2014). On the other hand, the studies using large datasets, generally pixel-based data, were not successful in explaining the relationship between the cooling capacity and spatial features of a place. The results of these studies were successful in directly explaining correlated parameters with LST without undertaking the interaction of one pixel to any other (Şimşek and Şengezer, 2012; Marando et al. ,2019). To deal with this problematic situation, (Myint et al. 2017) involved the interaction between pixels using the spatial autocorrelation method for measuring the cooling effects of the configuration of land cover.

Table 3.Research Approaches in Analyzing the Cooling Capacity in the Literature

Aim	Research area	Analytical unit	Measuring cooling capacity	Authors
Estimation of the relationship between urban park /UCI characteristics and the cooling intensity	Micro	Urban Park	PCI intensity / UCI intensity	Bacci et al. 2022; Cao et al. (2010); Chang & Li (2014); Cheng et al. (2014); Cheung & Jim (2019); Ren et al. 2013; Vidrih & Medved (2013)
			UCI intensity based on distance	Chen et al. (2012); Chang & Li (2014)
		Wetland		Wang and Zu (2011)
	Mezzo	UCI	PCI intensity / UCI intensity	Kong et al. (2014)
		Green urban infrastructure	Cooling capacity score	Zardo et al. (2017)
Analyzing of the cooling intensity of green abundance		Pixel	LST	Şimşek & Şengezer (2012); Marando et al. (2019)
Measuring the effects of the composition and configuration of greenspace		Urban green area		Guo et al. (2019); Maimaitiyiming et al. (2014); Rakoto et al. (2021); Zhou et al. (2017); Shih (2017)
			Cooling benefit	Zhang et al. (2017)
		Administrative district	LST	Li et al. (2012)
Measuring the cooling effects of the composition and configuration of heat sink and source		Patch		Li et al. (2017)
Measuring the cooling effects of the configuration of land cover		Pixel		Myint et al. 2017
Estimation of the relationship between urban park characteristics and the cooling extent	Micro	Urban Park	Average cooling distance	Lin et al. (2015)
			Maximum cooling distance	Cheng et al. (2014)
Measuring the effects of the composition and configuration of land cover and cadastral–demographic–economic variables		Case area	LST	Li et al. (2016)
Simulating the effect of greenery ratio on the cooling			Air temperature	Cheng et al. 2014; Ng et al. (2012); Wang&Zhu (2011);
Analyzing impact of urban morphology on cooling extent			Weather conditions	Oliveira et al. 2011
			LST based on distance	Hamada et el. (2013)
			UCI intensity based on distance	Heatway & Sharples (2012)
Analyzing impact of the surrounding landscape patterns on parks 'cooling effect		Urban Park	LST	Cheng et al. (2014)

As a result, analyzing cooling capacity at a patch level has supplied direct observations about the relationship with the spatial pattern of the cities. Because the scale is coherent with urban planning practice the results of the patch-level studies are more applicable to sustainable urban planning (Chen et al., 2012; Guo et al., 2019; Li et al., 2017; Maimaitiyiming et al., 2014; Peng et al., 2017; Rakoto et al., 2021; Zhou et al., 2017; Shih, 2017) In this way, enlarging the sampling size of patch scale research could result in reaching general results with understanding specific causality of a local area.

To measure cooling capacity, UCI intensity generally was used as a parameter, but LST and cooling distance were also used. Some studies executed different definitions like park cooling intensity, cooling capacity score and cooling benefit (Table 3). The studies analyzing both cooling intensity and extent were limited (Cheng et. al., 2014).

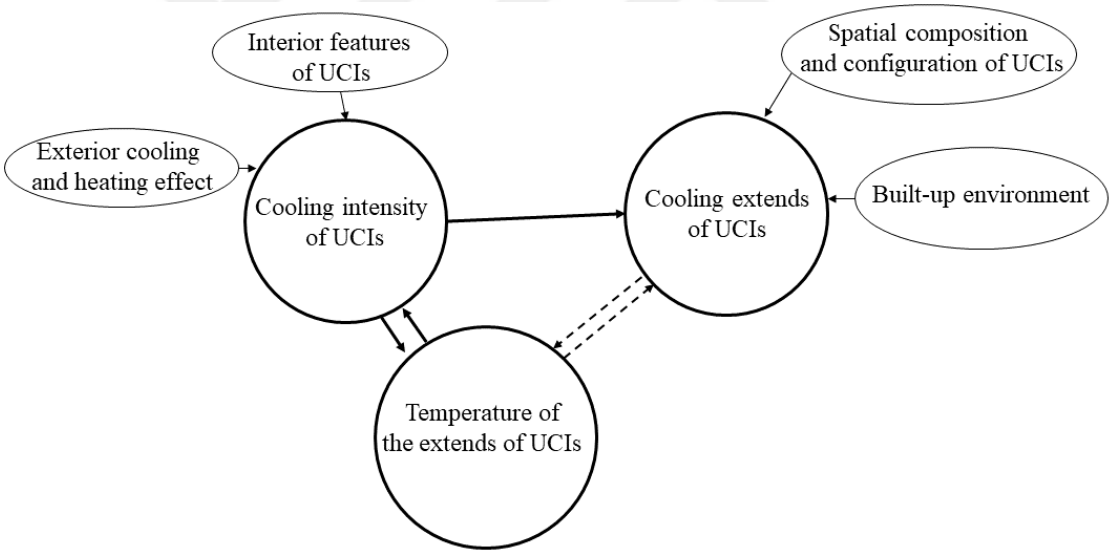
Moreover, the studies aimed to reach quantitative results or thresholds by using different statistical methods. In this way, some of them preferred to measure the relationship between the cooling capacity and related parameters using correlation and regression as a method (Cao et al.2010; Cheng et al. 2014; Kong et al., 2014; Ren et al., 2013; Shih, 2017; Vidrih & Medved, 2013). Some of them was chosen to simulate temperature change for different scenario belonging to the construction conditions or greening (Cheng et al. 2014; Ng et al.; 2012; Wang&Zhu, 2011).

CHAPTER THREE
DATA AND METHOD

3.1 Research Approach and Hypothesis

Cooling components were defined as the cooling capacity of UCIs, cooling extents of UCIs and thermal conditions of the extents. These components had a relationship with each other's. However, the direction of the relationship needed to be analyzed. Additionally, previous studies showed that there were important parameters shaping the components. In this study, the cooling capacity of UCIs was measured using two parameters which were the cooling intensity, and the cooling extents. These parameters regulated the thermal conditions of the urban areas showing relatively lower temperatures (Figure 4).

Figure 4. The Relationships Between the Cooling Capacity of Urban Environment



When observed LST distribution in urban areas, relatively lower temperatures were clustered in some part of the urban areas in İzmir. LST did not distribute homogenously within these urban areas. Within these urban areas, LST was very low and these pixels clustered, showing different spatial patterns. Based on this, this research assumed that the UCIs and the surrounding built environment defined a spreading area where the cooling effect is felt (Figure 5). With the expansion of these areas, it may be possible to prevent the risks associated with the urban heat island

effect. As a result, hypotheses were developed to investigate parameters and components regulating urban thermal comfort according to primary observations and results of the literature review.

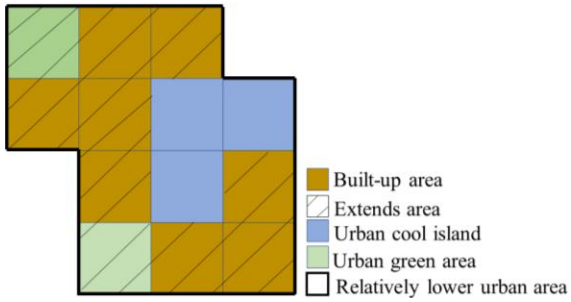


Figure 5.Schematic Representation of An Urban Relatively Cooler Area

The hypotheses could be listed:

- *Hypothesis 1:* There were urban patches having cooling capacity which were relatively the coolest areas in relation to their surrounding environment.
- *Hypothesis 2:* External and internal factors shaped the cooling intensity of UCIs.
- *Hypothesis 3:* UCIs and their extents came together to form urban relatively cooler areas compared to other parts of the urban metropolitan area.
- *Hypothesis 4:* Cooling extents of UCIs enlarge by creating a cumulative cooling effect with the surrounding built environment.
- *Hypothesis 5:* If the cooling intensity became more effective cooling extents became larger, and larger extents and the cooling intensity reduced the LST of urban environments.

3.2 Study Area

İzmir is in the Aegean region, the west of Turkey, between 37º 39’ north meridian and 26º 28’ east. With a total population of 4 486.84 as of the year 2023, İzmir is the third-biggest city in Turkey, covering an area of 11 973 sq. meters. The Gulf city of İzmir has a Mediterranean climate, where summers are dry and hot, and winters are mild and rainy. The mountains lie perpendicular to the sea, and the sea effect reaches

the inner side (Figure 6). In the period 1930 to 2022, the average highest temperature in İzmir was measured as 33 °C in August, with an average of 11.9 hours of sunshine. The highest temperature of 43 °C was observed in August 2002 (General Directorate of Meteorology, 2022). Since 1975, the city has experienced an increasing trend in the number of extremely hot days, like the other parts of Turkey (Kuba et al., 2016). In summer, temperatures drop by 1-2 °C due to the influence of the sea breeze in the coastal area. Although the mountains are usually covered with maquis shrubland and forest areas, 27% of them consist of urban areas (IMM, 2019). According to the climate projections for İzmir province and its surroundings, the average annual temperature differences between the years 1971-2000 and the period from 2050 to 2100 were expected to increase between 1°C and 3°C in the urban area of İzmir (İzmir Metropolitan Municipality (IMM) & Landscape Research Society, 2019). The heat risk is very high for İzmir because of the relatively limited green space at 8.6 m^2 per capita (İzmir Metropolitan Municipality, 2020), along with increasing solar radiation. In this study, the metropolitan urban area of the city was considered the study area, consisting of the built-up area of districts. The total size of the study area was 25,428.6 hectares, which is 2% of the total area of the city (Figure 6).

3.3 Pre-processing of The Data

Some studies used raw LST values (Guo et al., 2014; Pan, 2016; Dai et al., 2010; Zhang et al., 2018) to measure temperature, like this study. In this study, remote sensing images without any cloudiness in the study area were utilized. Landsat OLI 8 satellite images were used to map land surface temperature (LST). These images were obtained from the United States Geological Survey (USGS) and were captured on June 8, August 25, and September 10, 2020, Thermal OLI bands, known as the Thermal Infrared Sensor (TIRS), possess a spatial resolution of 30 meters. The land cover of İzmir was downloaded from the European Space Agency (EPA).



Figure 6. Location of Study Area

3.3.1 Land surface temperature

LST was retrieved from thermal images of Band 10 and Band 11 of Landsat OLI 8. The calculation process consisted of three sequential steps: (1) converting the digital numbers (DN) of the TIR bands to spectral radiance, (2) converting radiance to top-of-atmospheric (TOA) reflection, (3) performing the last step of land surface temperature inversion, transforming the LST unit from Kelvin to Celsius (Congedo & Munafo, 2014; Quin et al., 2001; Zhang et al., 2018). This process was applied to all Band 10 and Band 11 data of the hottest three months of 2020. Subsequently, the resulting LST map of İzmir was produced by averaging the values (Figure 7).

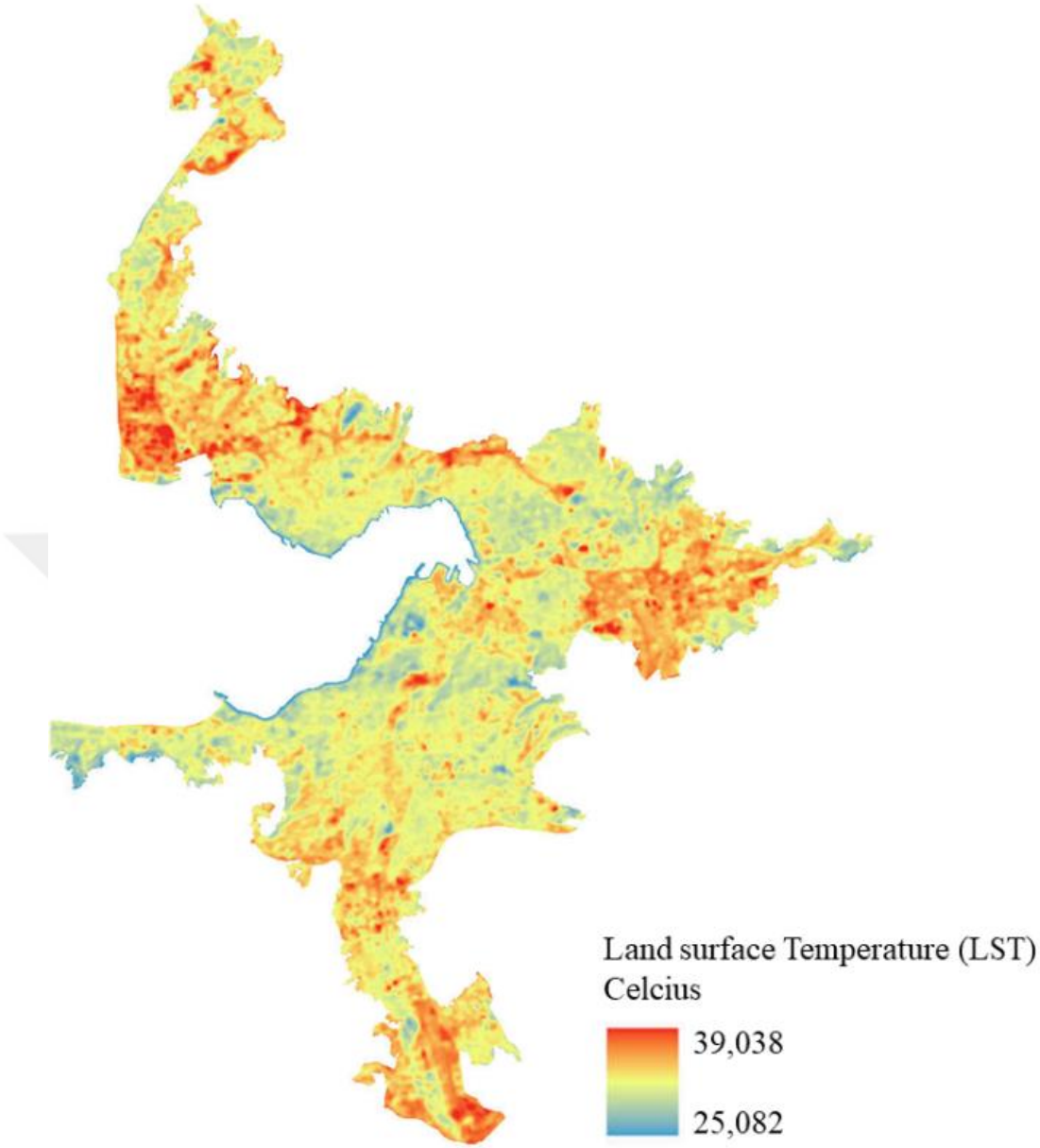


Figure 7.LST Distribution Map of The Study Area

3.3.2 Land covers mapping

To create the land cover map for the study area, Band 2 (blue), Band 3 (green), Band 4 (red), and Band 8 (Near Infrared (NIR) of Sentinel 2A) were utilized. A composite band map was produced, which was then used to extract pixels for five land cover classifications: tree, grass, bare soil, impervious and water surface. The supervised image classification method, a remote sensing technique on ArcGIS Pro,

conducted using training samples for the five classes. Finally, the pixels classified as tree-covered were aggregated for patch scale analysis (Figure 8).

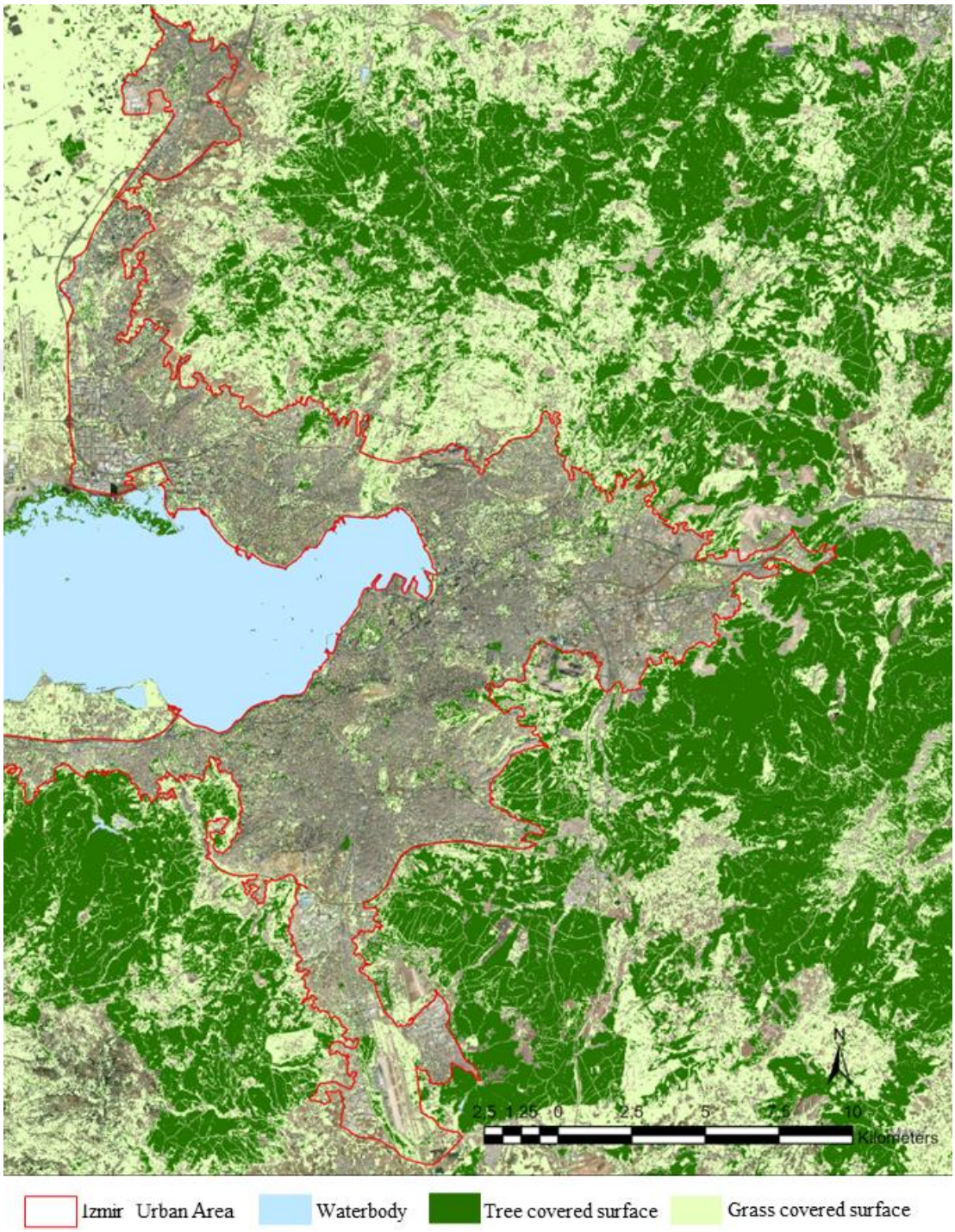


Figure 8. Land Cover Map of İzmir

3.4 Spatial Statistics for Analysis of LST Distribution

This study applied three successive spatial analysis methods to understand urban thermal dynamics, as measured by LST using ArcGIS Pro. The LST distribution in the urban area allowed for the extraction of core lowest temperature areas. However, accurate boundaries of these areas, named urban cold islands (UCIs) in the study, needed to be mapped. The UCI extraction process was developed from the mezzo scale to the micro-scale, which is shown in Figure 9. At the mezzo scale, relatively colder and hotter area in the urban area were mapped using Anselin Local Moran I as a spatial autocorrelation method (Anselin et al., 2010). The method was chosen based on successful results from previous studies in detecting clusters of LST (Çubukçu, 2015; Guo et al., 2015; Guo et al., 2019). It facilitated the identification of relatively homogeneous and geographically closed groups of LST pixel (Guo et al., 2019). The analysis output contained clusters of pixels with higher LST values (H-H), and lower ones (L-L) compared to neighboring pixels, within a specific radius. Radius values of 60 m., 180 m., and 240 m. were applied, with 60 m. ultimately being selected as the most effective radius in defining the colder areas. Increasing the radius resulted in mapping larger L-L cluster areas, indicating a higher standard deviation of LST within an L-L cluster.

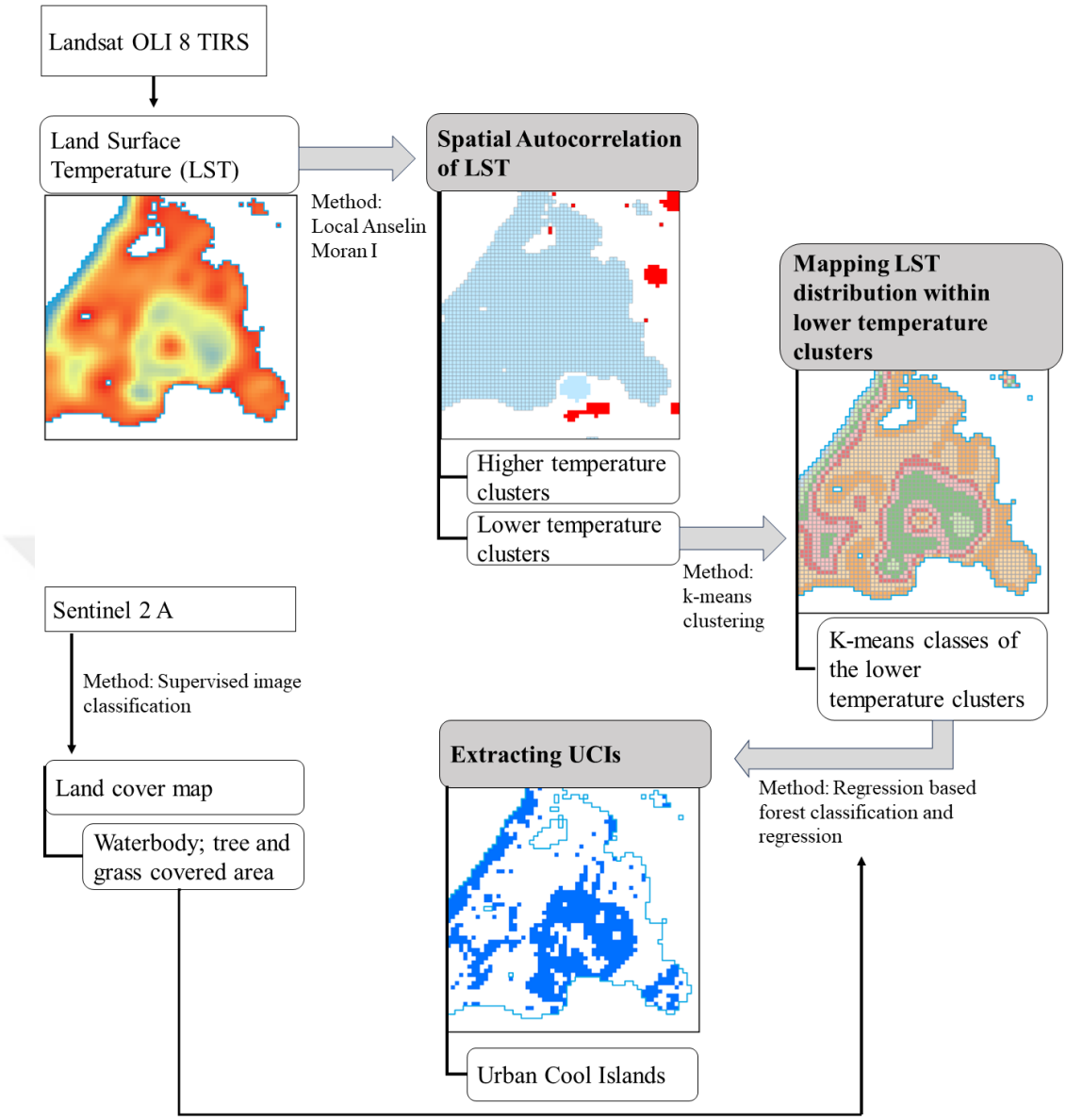


Figure 9. The Spatial Analysis Flowchart of This Study in Geographical Information System

For the second step, the L-L pixels resulting from the Anselin Local Moran I analysis were used as input for the gradient LST pattern analysis. In this analysis, the L-L clusters were further examined using the k-means clustering method. The method assigns values closest to a central point based on a specified number (k) of classes determined by the variable value. The center point of the selected class was updated, and the process was repeated to reclassify the closest value. This iteration continued until consistent results were obtained (Tan et al., 2005). This approach was widely used to describe the LST pattern as an unsupervised classification algorithm

(Esche et al., 2002; Kwak et al., 2020; Luo et al., 2010; Zhang et al., 2018). The method was applied separately within each UCI. As a result, the LST values of the center points varied different for each UCI, resulting in seven classes. Although the process was based solely on LST, previous studies highlighted a strong relationship between vegetation and LST (Chang and Li, 2014; Cheng et al., 2014; Estequo et al., 2017; Geng et al., 2022; Ng et al., 2012, Mackey et al., 2012; Maimaitiyiming et al., 2014; Peng et al., 2018; Peng et al., 2020; Shahidan et al., 2012; Shih, 2017; Yan et al. 2014; Yin et al., 2018; Zhao et al., 2011). Therefore, relying solely on LST may not be sufficient to define UCIs. To accurately delineate the boundaries of UCIs, the forest-based classification and regression method, a tool of ArcGIS, was applied instead of taking k-means clusters with lower temperatures. This method utilized a random forest algorithm, which was a supervised machine learning approach. The model produced various decision trees, and the ultimate decision tree was produced based on certain criteria (Breiman, 2001). In this study, the forest-based classification and regression method predicted 1, 2, and 3 k-means classes as UCIs, while classes 5 and 7 were classified as non-UCIs. Class 4 was out of the dataset as it was accepted as a transition area, which did not show certainty. The training variables for the method were defined as the size of the tree and grass area in sq. meters. To evaluate the model's accuracy, 10% of the dataset was used as training data for testing. The forest-based classification and regression method detected pixels belonging to UCIs and "not UCI" categories based on the relationship between vegetation and UCIs. Anselin Moran I low-low polygons and UCIs in İzmir was shown in Figure 10.

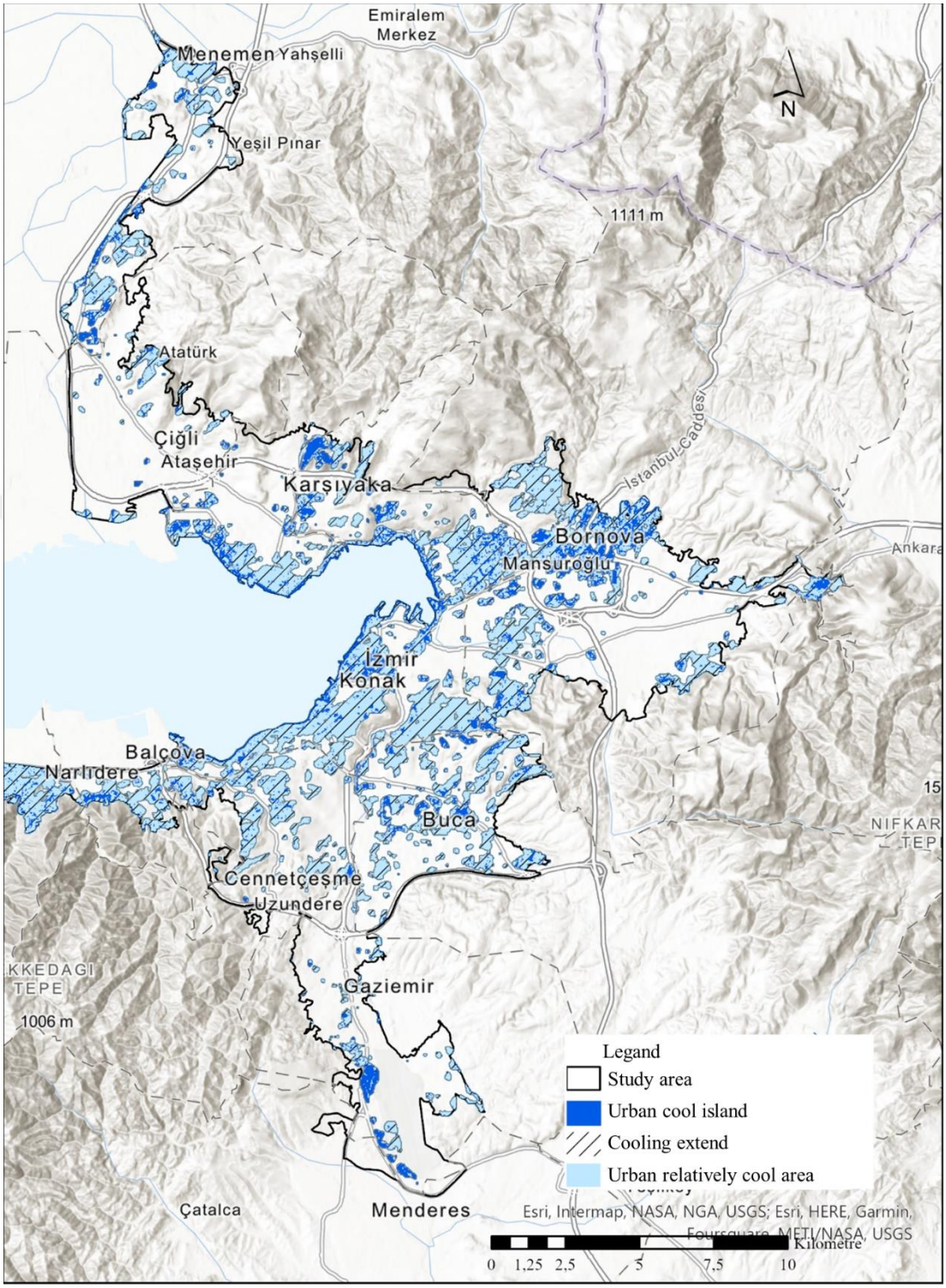


Figure 10. Map of Relatively Cooler Areas (RCAs) and Urban Cool Islands (UCIs)

3.5 Statistical Analysis

To investigate the relationship between important parameters and the cooling capacity represented by the cooling intensity of UCIs and the cooling extent of UCIs in this study, two multiple regression models were developed. The function of the cooling intensity and extents can be written as:

$$y = f(x_1, x_{2\ldots\ldots})$$

y represents the cooling intensity while measuring the cooling intensity of UCIs and y represents the cooling extent while measuring the cooling extent of UCIs. X is the vector of potential explanatory variables for the model, which are in detail explained in the subtitles of 3.6. and 3.7. The backward elimination technique was used to determine the variables included and excluded from the regression models. Maximum R^2 and lowest standard error of estimate were considered as the best combination of the variables for the models. To address the collinearity problem among the independent variables, variance inflation factor (VIF) value less than 5 were taken into consideration. The standardized regression coefficient (beta value) was used to measure the relative contribution of each independent variable to the cooling capacity (Rogerson, 2010).

3.6 Analyzing Thermal Conditions of Urban Environments

The cooling intensity of UCIs and the cooling extent of UCIs were defined as main components of the urban cooling capacity in this study. The components were dominant in shaping the LST distribution of the urban environment. The extraction of RCAs and UCIs, spatial statistical process based on LST. In this way, to measure thermal comfort condition of the urban environment, temperature (LST) of extents was used as a component. This study supposed that increasing cooling intensity of UCIs, larger cooling extents and lower LST of urban environment resulted in increasing the cooling capacity of the cities and the relationships were two ways (Figure 11). The relationship between these tree components was analyzed with using Pearson Correlation Coefficient and scatter plot of the components. The value

of the coefficient ranged between -1 and 1 and the correlative relationship becomes stronger when the value reaches 1 or -1.

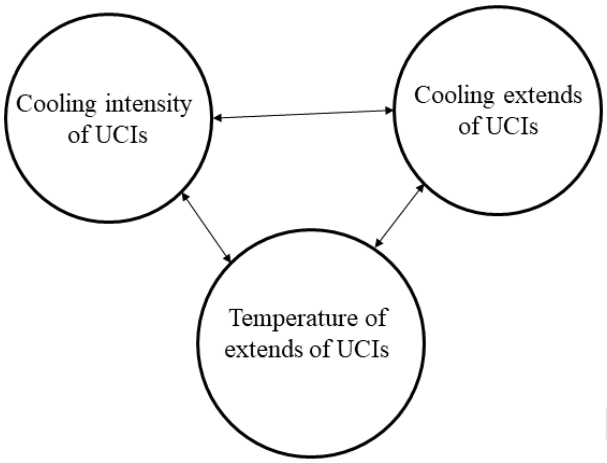


Figure 11. The Components Related Urban Thermal Conditions

3.7 Measuring The Cooling Intensity of Urban Cool Islands

Table 4 shows the variables used in the regression models in measuring the cooling intensity of UCIs. Two regression models, namely the LST_{min} model and LST_{mean} model, were developed to explain the cooling capacity. The models utilized 12 different parameters as explanatory (independent) variables, including land cover composition, green configuration, UCI characteristics, and outer thermal effects.

The proportion of grass-covered areas (P_GR), tree-covered areas (P_TR), and water bodies (P_WA) were selected as variables representing land cover composition. These variables were commonly used to investigate the potential cooling effect of vegetation and water on LST (Chang and Li, 2014; Cheng et al., 2014; Estequo et al., 2017; Geng et al., 2022; Ng et al., 2012, Mackey et al., 2012; Maimaitiyiming et al., 2014; Peng et al., 2018; Peng et al., 2020; Shahidan et al., 2012; Shih, 2017; Sun et al., 2020; Yan et al. 2014; Yin et al., 2018; Zhao et al., 2011). The mean patch size of tree-covered areas (M_TR) and patch density of tree-covered areas (PD_TR) were selected as parameters related to green configuration, representing the fragmentation of dense vegetation. Previous studies analyzing the contribution of UCI characteristics on the cooling capacity in the literature were very

common. UCI size parameter (S_UCI) was the most used parameter (Cao et al., 2014; Geng et al., 2022; Kong et al., 2014; Lin et al., 2015; Monteiro et al., 2016; Peng et al., 2020; Ren et al., 2013; Shih, 2017; Yang et al., 2023) and shape index (LSI) (Asgarian et al., 2015; Cao et al., 2010; Geng et al.,2022; Peng et al., 2020; Shih, 2017) to explain to regulate climate conditions, so the parameters were included in the models. The shape index was an effective parameter to measure the compactness of UCI patches, used in the literature (Asgarian et al., 2015; Cao et al., 2010; Geng et al., 2022; Peng et al., 2020; Shih, 2017) LSI was calculated with the equation below:

$$LSI = \frac{P}{2 * Sqrt\ (\pi * A)}$$

where *P* is the total perimeter of the UCI patch and *A* is the area of the patch (Cao et al., 2010; Shih, 2017; Sun et al., 2020). LSI value for a square-shaped patch was 1.12, representing a compact and simple shape.

The study also considered the thermal interaction between the heating and cooling sources in the city (Cheng et al., 2015), which contributes to cumulative cooling effects. While UCIs, were defined as cooling sources, previous studies identified the sea (Kong et al., 2014; Li et al., 2017; Shih, 2017) and forests as important cooling sources. On constant, UHIs acted as heating sources (Kong et al., 2014; Li et al., 2017) in the cities. The effects of the cooling and heating sources were measured by taking the distance from one UCI to the edge of the sources. Distance to nearest UCI (D_UCI) (Asgarian et al., 2015) and coherence of UCIs (C_UCI) (Shih, 2017) were used in the model to explore the role of the connectivity between UCIs to mitigate the UHI effect in terms of the spatial configuration of UCIs within L-L polygons (Table 4).

Table 4. The Description of Dependent and Independent Variables in The Cooling Intensity (LSTmean and LSTmin) Regression Model

Category	Variable	Abbreviation	Definition	Unit
Dependent variables				
Cooling the capacity of UCIs	Mean of land surface temperature	LST_{mean}	Average land surface temperature value of UCI	^oC
	Minimum land surface temperature	LST_{min}	Minimum land surface temperature value of UCI	^oC
Independent variables				
Land covers composition	The proportion of grass-covered area	P_GR	The total area of grass-covered patches/UCI area	%
	The proportion of tree-covered area	P_TR	The total area of tree-covered patches/UCI area	%
	The proportion of water bodies	P_WA	The total area of water patches/UCI area	%
Green configuration	The patch density of tree-covered area	PD_TR	(n_i/A) *100, where n_i is the total number of tree-covered patches in each UCI	%
	Mean patch size of tree-covered area	M_TR	Average area of all tree-covered patches within a UCI	ha
UCI characteristics	The size of UCIs	S_UCI	The total area of UCIs	ha
	The shape index of UCIs	LSI	$P/2\ \sqrt{\pi}*A$ where P is the total perimeter around a UCI, and A is the area of the UCI	km/ha
Outer thermal effect	Distance to the sea	D_SEA	The nearest distance from the edge of the polygon of UCI to boundary of the sea	km
	Distance to the forest	D_FR	The nearest distance from the edge of the polygon of UCI to the edge of the tree – covered areas outside the urban area	km
	Distance to the urban heat island	D_UHI	The nearest distance from the edge of the polygon of UCI to edge of the urban heat island	km
	Distance to nearest UCI	D_UCI	The nearest distance from the edge of the polygon of UCI to edge of the closest neighborhood of UCI	km
	The coherence of UCIs	CH_UCI	Average distance from the edge of the polygon of UCI to edge of the closest neighborhood of UCIs within a 500-m buffer	km

A database for the LST models was created with using the ArcGIS Pro. First, the pixels named by UCI according to the spatial analysis were aggregated and converted into polygons. The attribute table of UCIs contained values of the dependent and independent variables of LST_{min} and LST_{mean} models. Each row in the analysis dataset represented information about a specific UCI patch. The regression

model incorporated various variables, which were calculated using the spatial join technique in ArcGIS Pro. Mean, minimum, and sum values completely within the boundaries of each UCI were considered. The variables based on distance, the "Near" tool was used to measure the nearest distance from the edge of UCI to edge of UHI, other UCIs, the sea, and forest areas. After creating spatial database using geographical information system, the attribute table was exported to analysis the relationships in SPSS.

Descriptive statistics of the variables of the LST_{mean} and LST_{min} models were shown in Table 5. LST_{mean} for İzmir's UCIs ranged between 26.705 ºC and 32.450 ºC with, a mean value of 31.308 ºC. Similarly, LST_{min} values ranged from 25.705 ºC to 32.330 ºC, with a mean value of 30.924 ºC. The S_UCI variable ranged from 0.270 ha to 42.840 ha, and it exhibited higher standard deviation in the dataset, with a mean value of 1.680 ha. Some of the UCIs did not have any grass-covered areas, tree-covered areas, and waterbody, so the minimum value of P_GR, P_TR, WA, PD_TR, and M_TR were 0.000 (Table 5).

Table 5. Descriptive Statistics of The Description of Dependent and Independent Variables in The Cooling Intensity Regression Model

Variable		Unit	Minimum	Maximum	Mean	Medium	Std. deviation
Dependent variables							
LST_{mean}		ºC	26.705	32.450	31.308	31.709	0.989
LST_{min}		ºC	25.082	32.330	30.924	31.586	1.322
Explanatory (Independent) variables							
P_GR		%	0.000	1.000	0.499	0.527	0.255
P_TR		%	0.000	0.979	0.201	0,083	0.221
P_WA		%	0.000	0.638	0.049	0.000	0.119
PD_TR		%	0.000	0.296	0.085	0.111	0.062
M_TR		ha	0.000	8.270	0.092	0.100	0.367
S_UCI		ha	0.270	42.840	1.680	0.180	3.624
LSI		km/ha	1.130	5.490	1.640	0.670	0.520
D_SEA		km	0.000	15.81	3.668	2.634	3.712
D_FR		km	0.000	5.24	1.335	0.745	1.342
D_UHI		km	0.000	2.380	0.416	0.301	0.409
D_UCI		km	0.000	0.470	0.031	0.030	0.057
CH_UCI		km	0.000	0.370	0.238	0.250	0.061

3.8 Measuring The Cooling Extents of Urban Cool Islands

Table 6 shows the variables used in the regression model to measure the cooling extent of UCIs. The dependent variable was identified as the size of the cooing extents of UCIs. The regression model, namely the cooling extent model and LST models, was developed to explain the cooling capacity. The models utilized 10 different spatial parameters as independent variables, including UCI configuration, green configuration within the extents, and urban morphology.

Table 6. The Description of Dependent and Independent Variables in The Cooling Extent Regression Model

Category	Variable	Abbreviation	Definition	Unit
Dependent variables				
Cooling extents of UCIs	Size of extent area of UCIs	S_EXT	The area of relatively cooler area (RCA) minus total area of UCIs within that RCA	ha
Independent variables				
UCI configuration	Maximum patch size of UCI	MAX_UCI	Maximum area of all UCI patches within an RCA	ha
	The patch density of UCI	PD_UCI	Total number of UCI patches in each RCA/ total area of the cooling extents	%
	Core index of UCI	CORE_UCI	Total UCI area within an RCA / Total area of UCI within study area	%
	Dummy variable of UCI	DA_UCI	Abundance of UCI, 0 represented “no UCI”; 1 “yes UCI”	
Green configuration	Maximum patch size of tree covered area	MAX_TR	Maximum area of all tree-covered patches within a cooling extent	ha
	The patch density of tree covered area	PD_TR	Total number of tree covered patches in each RCA/ total area of the cooling extents	%
	Core index of tree covered area	CORE_UCI	Total tree covered area within an RCA / Total area of tree covered patches within study area	%
	Dummy variable of tree covered area	DA_TR	Abundance of tree, 0 represented “no UCI”; 1 “yes tree”	
Urban morphology	Mean building height	B_H	Average building heights within a cooling extent	m
	Elevation ratio	E_RATIO	Total area of elevation surfaces of the blocks of buildings/ total area of the cooling extents	%

The configuration of UCIs was also considered in the model to comprehend the role of the UCIs in explaining the extent area. The configuration was determined by the patch density (PD_UCI), maximum size of UCIs, core index and dami variable of UCI. In the literature the cooling extent was generally evaluated using the park size, where larger park sizes were found to correspond to a larger extent area (Cheng et al., 2015; Lin et al., 2015; Ren et al., 2013). The extent area encompassed the cumulative extent areas of multiple UCIs within a relatively cooler region, rather than individual extent of each UCI. Zhang et al. (2017) referred to the overlapping cooling extent as multiple benefit areas. CORE_UCI quantified the percentage of a patch that is comprised of core area (Asgarian et al., 2015) which helped to measure cumulative effect of the UCI. Previous studies suggest that the green areas near UCIs, along with the UCIs themselves, generated a combined cooling effect that intensified with higher vegetation density (Cheng et al., 2015; Shih, 2017). Core area index, patch density index, maximum patch index and dummy variable was calculated for both of UCI and tree covered patches. Some of the RCAs did not contain any UCI and tree covered patches, so dummy variables were added to measure effect of the abundance of them.

The literature extensively analyzed the relationship between urban morphology and UHI (Fintikakis et al., 2011; Hamada et al., 2013; Oliveira et al., 2011; Peng et al., 2017; Qaid et al. 2016). Hamada et al. (2013) proposed that densely built-up areas could create a barrier effect, limiting the penetration of the cooling effect to the inner sides. Furthermore, several studies examining local climate zones explored that open-built environment with greenspaces tended to exhibit lower temperatures (Lee & Oh, 2018; Zheng et al., 2023). The built environment characters were involved in the model both of the spatial layout of tree-covered areas and urban morphology. The relationship between urban morphology and UHI was largely analyzed in the literature (Fintikakis et al., 2011; Hamada et al., 2013; Oliveira et al., 2011; Peng et., 2017; Qaid et al. 2016). The variable chosen to analyze the heating contribution of impervious surfaces was elevation ratio (E_RATIO), which was an important parameter in identifying development density. The impervious surfaces absorbed the solar radiation throughout the entire day (Abougendia et al., 2020). Building height (B_H) was involved in the model to understand effects of three-dimensional urban

morphology. The previous results showed that a greater cooling capacity was developed by larger urban gaps in both two and three dimensions (Şentürk and Çubukçu, 2023).

Descriptive statistics of the variables of the cooling extent model were shown in Table 7. İzmir's cooling extents ranged between 0.270 ha and 761.580 ha with, a mean value of 18.115 ha. The extents exhibited the highest standard deviation in the dataset. MAX_UCI reached to 42.840 ha and its mean value was 4.029 while MAX_TR reached to 1.581 ha and its mean value was 0.069 ha. (Table 7). CORE_UCI reached to 0.181with 0.003 mean value. Similarly, CORE_TR reached to 0.172 with 0.003 mean value. Descriptive statistics of other variables showed in the Table 7.

Table 7. Descriptive Statistics of Variables of The Cooling Extent Model (n=292)

Variable	Unit	Minimum	Maximum	Mean	medium	Std. deviation
Dependent variables						
S_EXT	ha	0.270	761.580	18.115	2.340	76.284
Independent variables						
MAX_UCI	ha	0.000	42.840	4.029	1.260	3.312
PD_UCI	%	0.000	3.703	0.292	0E-13	0.610
CORE_UCI	%	0.000	0.181	0.003	0E-13	0.016
DA_UCI		0.000	1.000		0.000	0.499
PD_TR	%	0.000	11.111	1.2221	0.720	1.540
MAX_TR	ha	0.000	1.581	0.069	0.010	0.184
CORE_TR	%	0.000	0.172	0.003	0.000	0.015
DA_TR		0.000	1.000		1.00	0.030
B_H	m	0.000	17	4,47	3.990	2.762
E_RATIO	%	0.000	79.785	4.799	4.143	8.915

CHAPTER FOUR
RESULTS

In this chapter, the cooling capacity of urban area was measured. Firstly, LST distribution of İzmir urban area was analyzed to have information about existing cooling capacity. Secondly, characteristics of UCIs were explained in terms of the cooling capacity and spatial features. Thirdly, multiple linear regression results of the cooling capacity, cooling intensity and cooling extents models, were explained important parameters regarding the cooling capacity.

4.1 LST Distribution In İzmir

Lower temperature areas in İzmir were observed along the seaside due to the presumable cooling effect of the water surface but this lowest temperature did not continue to all adjacent inner sides of the city, especially Karşıyaka and Bayraklı district. Forestry areas in the urban fringe also showed lower temperatures. In addition to these areas, some urbanized areas like Evka3, Mavişehir, and Manavkuyu districts showed lower LST values. UHIs were definitively related to industrial areas of İzmir which were the north, east, and south sides of the city. Bare soil surfaces and highly urbanized areas also showed higher temperatures (Figure 12).

As for spatial autocorrelation, regarding the Anselin Local Moran I result for İzmir, there was a 3.04ºC LST difference between lower LST clusters, Low-Low, and higher LST clusters, High-High, where maximum temperature differences were 6.30 ºC and minimum one was 8.18 ºC. 26.46 % of the study area showed higher LST clusters. In relatively cooler areas, L-L clusters only consisted of 27.28% of the study area with higher standard deviation than UHIs, HH (Table 8). In the Izmir urban area, relatively cooler areas spread in the larger areas than UHIs.

Table 8. The statistics for LST distribution according to Moran Cluster Types*

Moran type	Pixel count	Land surface temperature			
		Mean	Max	Min	Std. deviation
Low-low	77005	31.61	32.73	25.08	0.77
High-High	74780	34.65	39.03	33.26	0.60

**A 30m x 30m grid database were used for this table*

Table 9 shows the results of the k-means clusters analysis which analyzed the clusters of LST values within the relatively cooler areas, L-L polygons for 7 clusters. According to descriptive statistics of LST of the k-means clusters, the mean LST of the clusters increases from 30.34 ºC to 32.23 ºC, from cluster 1 to cluster 7. There was a nearly 7 ºC difference between the minimum LST of clusters 1 and 7 while nearly 0.5 ºC maximum LST of clusters 1 and 7. The number of pixels showed increasing trend from cluster 1 to cluster 6. But the number of pixels of cluster 6 was a little bit more than the cluster 7. Clusters 1, 2, and 3 enlarged on smaller urban areas while clusters 5, 6, and 7 enlarged larger ones (Table 10). This showed that the coolest LST was areas within cluster 1,2 and 3 were limited in urban areas and the areas overlapped the lowest LST areas when observed the LST distribution. Clusters 5,6 and 7 positioned around cluster 1, 2 and 3. However, cluster 4 was like a transition cluster between these cluster groups.

Table 9. Descriptive statistics of LST of k-means clusters*

K_means cluster	LST				Pixel count	Size (ha)
	Min	Mean	Max	Std. deviation		
1	25.08	30.34	32.46	1.56	3084	277.56
2	27,96	30,56	32,33	1,11	5031	452.79
3	29,16	30,97	32,38	0,73	7584	682,56
4	30,09	31,33	32,53	0,50	10975	987.75
5	30,79	31,63	32,40	0,33	15140	136.62
6	31,38	31,93	32,56	0,20	18115	1630.35
7	31,89	32,23	32,73	0,12	17076	1536.84

**A 30m x 30m grid database were used for this table*

Table 10 shows the LST statistics RCAs and UHIs contained after converting Anselin Moran I's low-low (LL) and high-high (HH) pixels into polygons. 305 RCA polygons and 352 polygons UHI polygons were detected in İzmir. LSTs of RCAs ranged between 30.98 ºC and 32.38 ºC with a mean value of 32.00 ºC. LSTs of UHIs ranged between 33.65 ºC and 35.57 ºC with a mean value of 34.06 ºC. The size of RCAs varies between 0.27 ha and 1058.40 ha with a mean value of 22.66 ha, whereas the size of UHIs between 0.09 ha and 1570.05 ha with a mean value of 19.11 ha. Although the mean size of UHIs was smaller than RCAs, the standard

deviation of UHIs was higher due to the higher continuity of UHI pixels (Table 11, Figure 9).

Table 10. The Statistics for LST Distribution of RCAs and UHIs

Type	Polygon count	Land surface temperature				Polygon (patch) size			
		Mean	Max	Min	Std.dev.	Mean	Max	Min	Std. dev.
Relatively cooler area (RCA)	305	32.00	32.38	30.98	0.27	22.66	1058.40	0.27	998.951
Urban heat island (UHI)	352	34.06	35.57	33.65	0.40	19.11	1570.05	0.09	121649,5

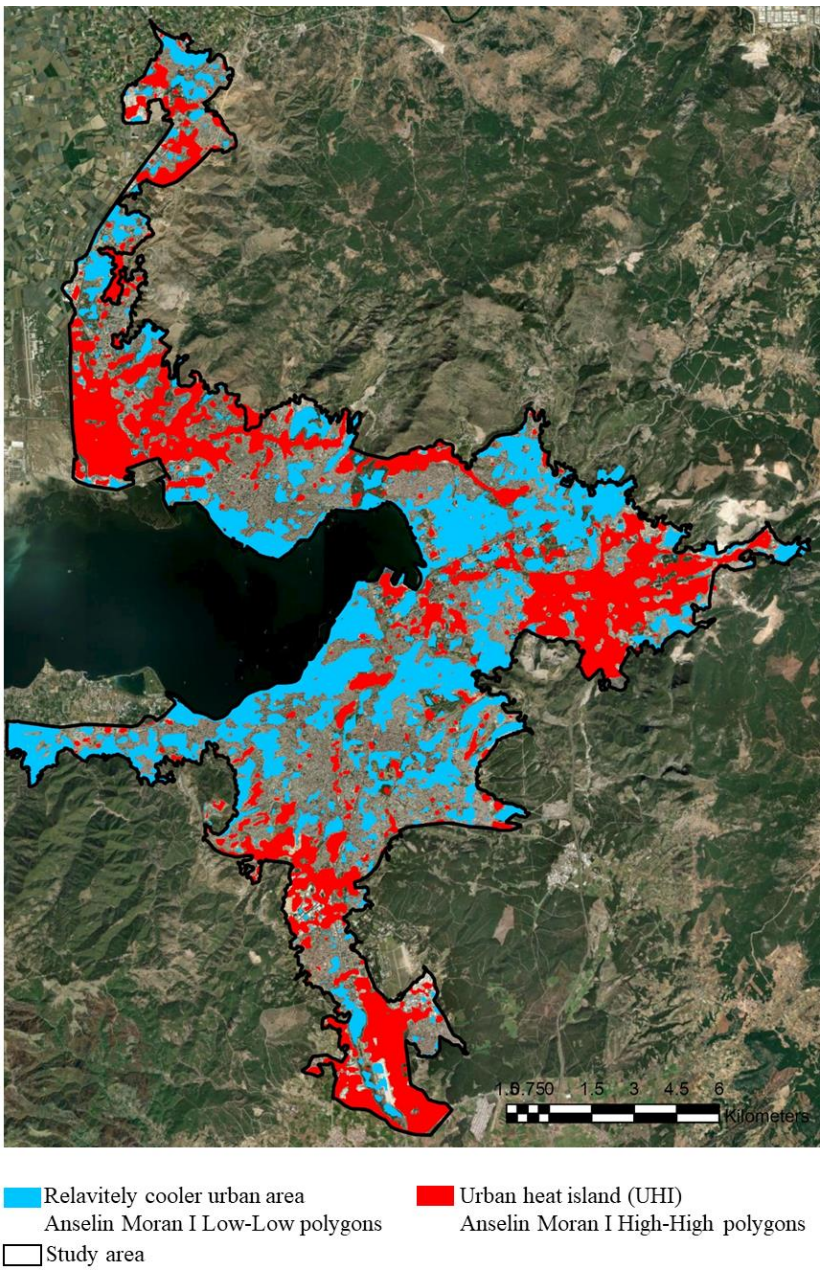


Figure 12. Anselin Local Moran I Low and High-Temperature Clusters in İzmir

The spatial distribution of k-mean clusters showed that there was a gradient pattern of LSTs. In RCA polygons, cluster numbers were decreased step by step. For instance, the boundary of Kültürpark and Hasanağa urban parks matched clusters 1, 2, and 3, and their pixels of clusters 5 and 6 were located in adjacent urban environments. Similarly, clusters 1, 2, and 3 were observed in Mavişehir residential area and along the seashore. Yet, the Manavkuyu residential area generally consisted of clusters 6 and 7 with a limited number of cluster 5 (Figure 13).

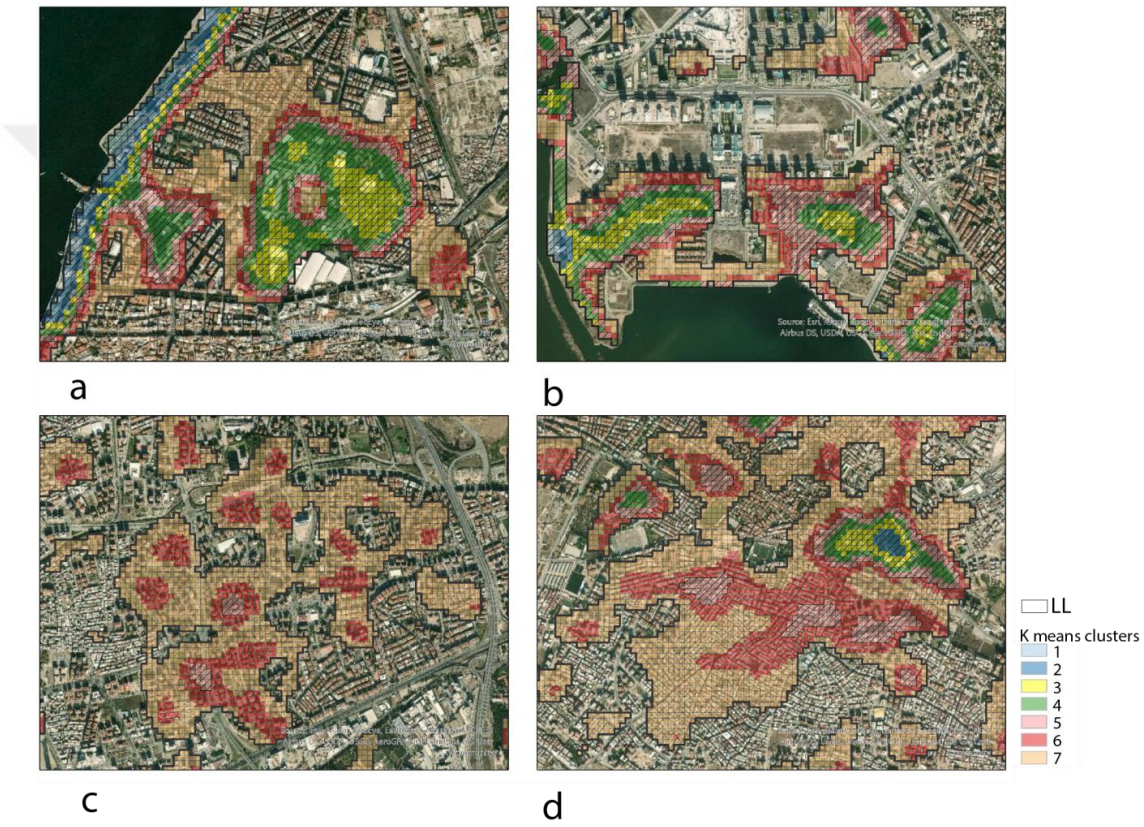


Figure 13. K means clusters of LL polygons for İzmir,(a) Kültürpark, b) Mavişehir district c) Manavkuyu district d) Buca district near Park of Hasanağa)

4.2 The Characteristics of UCIs Within The İzmir Urban Area

The LST_{mean} value for the UCIs varies between 25.558 ºC and 32.578 ºC while LST_{min} of the UCIs varies between 25.083 ºC and 32.213 ºC. Most of the UCIs show LST_{mean} values higher than 31 ºC which could not supply urban thermal comfort conditions. Similarly, LST_{min} values are mostly higher than 30 ºC. Although LST_{min}

values show a little bit lower temperatures than LST_{mean}, both of the histogram shows the same distribution shape at on the right (Figure 14).

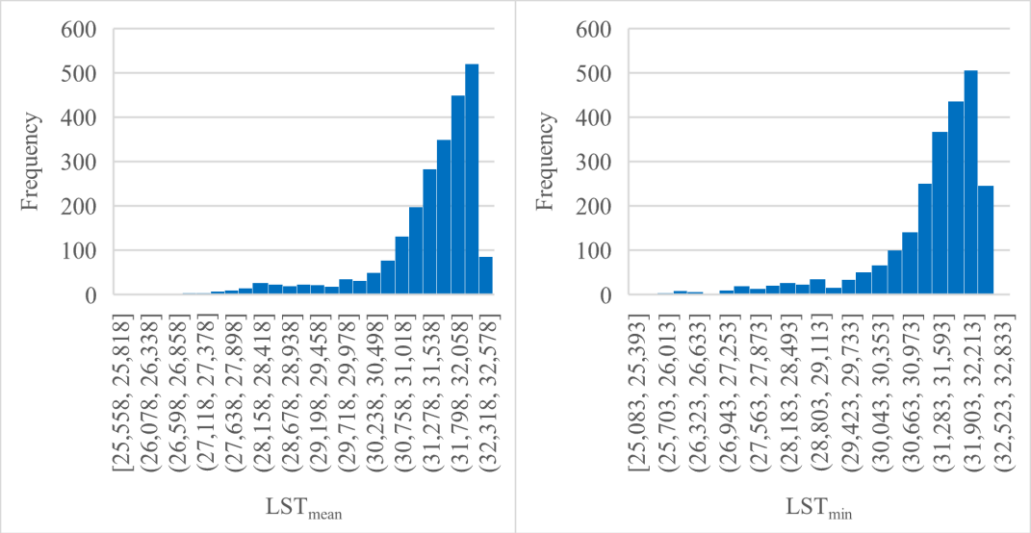


Figure 14. Histograms of LSTmean and LSTmin of UCIs

Approximately 5.7% of the Izmir urban area consists of urban cold islands with cooling capacity. On the other hand, the extented area where the cooling effect is felt covers about 21% of the study area with a total of 5290,110 ha. Kültürpark and its surroundings, Mavişehir and Atakent residential area and coastal areas, Ege University Campus, Manavkuyu and Evka 3 residential areas, Memorial Forest in Seyirtepe and the residential areas around it are among the urban relatively cool areas located. Although urban cool islands are located in different sizes and spatial configurations, they are usually concentrated in areas where green areas are clustered (Figure 15, Figure 16).

UCIs were not observed in vegetated areas. In terms of spatial magnitude, UCIs encompass various surfaces, with grass-covered covering 680.480 ha, which was approximately 47% of the total area. Tree-covered surfaces account for 456.817 ha, representing 31% of the area. Impervious surface and bare soil occupied 138.842 ha, accounting for 8%, while water bodies covered 55.057 ha, constituting %4 of the total area. Although the total grass-covered area was larger than the tree-covered area, the maximum patch size of tree-covered areas was twice as large as that of

grass. All the patch types exhibited large standard deviations, indicating fragmented patterns despite their mean patch sizes. Grass and trees were closer in size, with 0.789 ha and 0.529 ha, respectively, while nearly six times larger than bare soil and impervious patches within UCIs (Table 11).

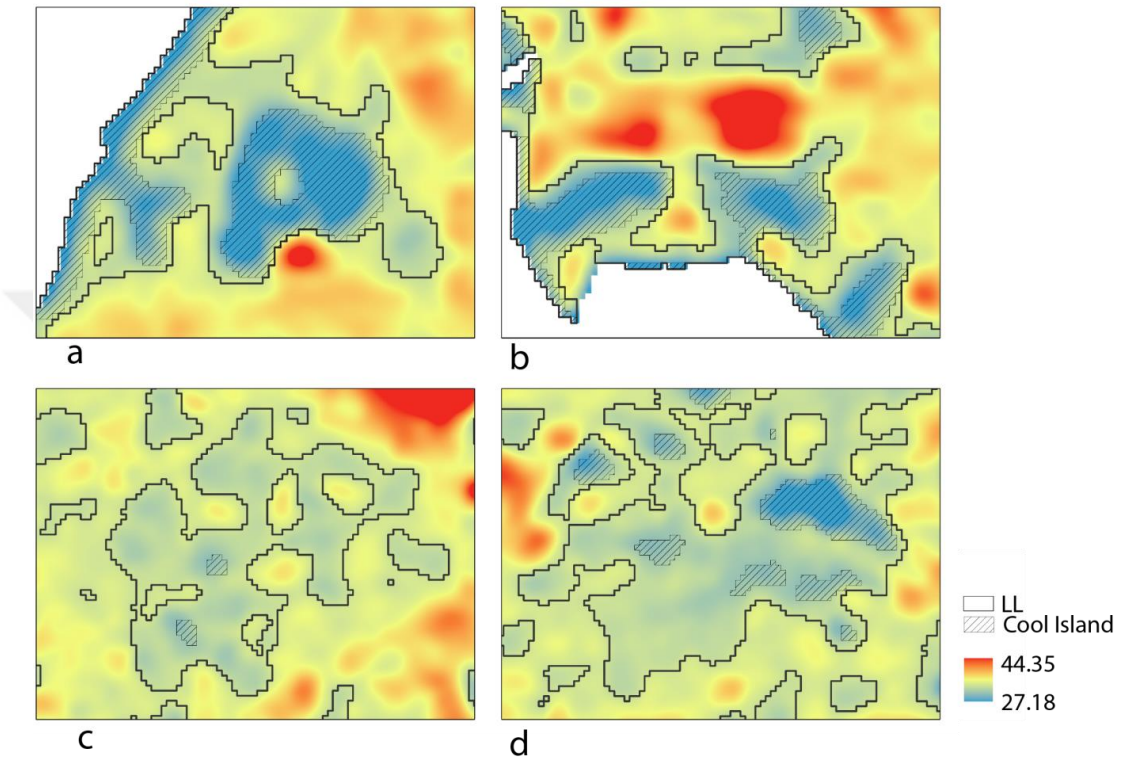


Figure 15. LST distribution of LL and UCIs polygons for İzmir(a) Kültürpark, b) Mavişehir district c) Manavkuyu district d) Buca district near Park of Hasanağa)

Table 11. Descriptive Statistics for Land Cover Surfaces within UCIs (n=862)

Land cover	Min(ha)	Max (ha)	Sum (ha)	Ratio (%)	Mean (ha)	Std. Deviation
Water	0.000	4.520	55.057	0.038	0.0638	2452.918
Grass	0.000	16.767	680.480	0.469	0.789	16002.164
Tree	0.000	33.002	456.817	0.315	0.529	20900.572
Bare soil	0.000	2.447	117.397	0.081	0.136	2338.576
Impervious	0.000	5.407	138.842	0.095	0.161	3471.608



Figure 16. Examples of UCIs of Izmir and their adjacent urban area ((a)Mavişehir ve Atakent residental district, (b) Kültürpark, (c) Press Broadcasting and Journalists Memorial Forest, (d) Air Training Command and its surroundings, (e) Aegean University Campus (f) Evka 3 residental districts)

4.3 Relationship Between the Components of Thermal Environment

The correlation analysis of the components of the cooling capacity, cooling intensity of UCIs, the cooling extents, and thermal comfort of extents showed interaction with each other. Where the cooling intensity was measured by the mean LST of UCIs, the cooling extent was measured by its size, and the thermal environment was measured by the mean LST of the extents. As seen in Table 12, all of the variables were correlated significantly at the 99% confidence level (p-statistics, α=0,01). The mean LST of UCIs and mean LST of the extents showed a positive and very strong correlation the Pearson correlation coefficient was measured as 0.787. Thus, if the cooling intensity of UCIs was decreased, thermal environment conditions would be more comfortable. Likewise, if thermal environment conditions had smaller LST values, the cooling intensity of UCIs would be stronger. The size of the cooling extent was negatively correlated with the mean LST of the extents and mean LST of UCIs. The increase of the magnitude of the cooling extents is nearly twice as effective on the cooling intensity of UCIs compared to the thermal comfort of the extents.

Table 12.Pearson correlation analysis results of the components affecting the thermal environment

Variable	Mean LST of UCIs	Size of the cooling extents	Mean LST of the extents
Mean LST of UCIs	1*	-0.406*	0.787*
Size of the cooling extents	-0.406*	1**	-0.275**
Mean LST of the extents	0.787*	-0.275**	1**

*Correlation is significant at the 0.01 confidence level (two-tailed) for n=134
**Correlation is significant at the 0.01 confidence level (two-tailed) for n=292

The scatter plot of the components showed that there is a strong linear correlation relationship between the mean LST of UCIs and the extents. When the value of the LST of UCIs under 31 ºC degrees, the LST of the extents was hotter. Above this 31 ºC, some of the extents were cooler than UCIs. However, relationships between the size of the cooling extents and both of mean LST of the extents and UCIs were not linear. The highest value of the cooling extents was nearly 31 ºC for the cooling intensity of UCIS and 31.75 ºC mean LST of the extents (Figure 17).

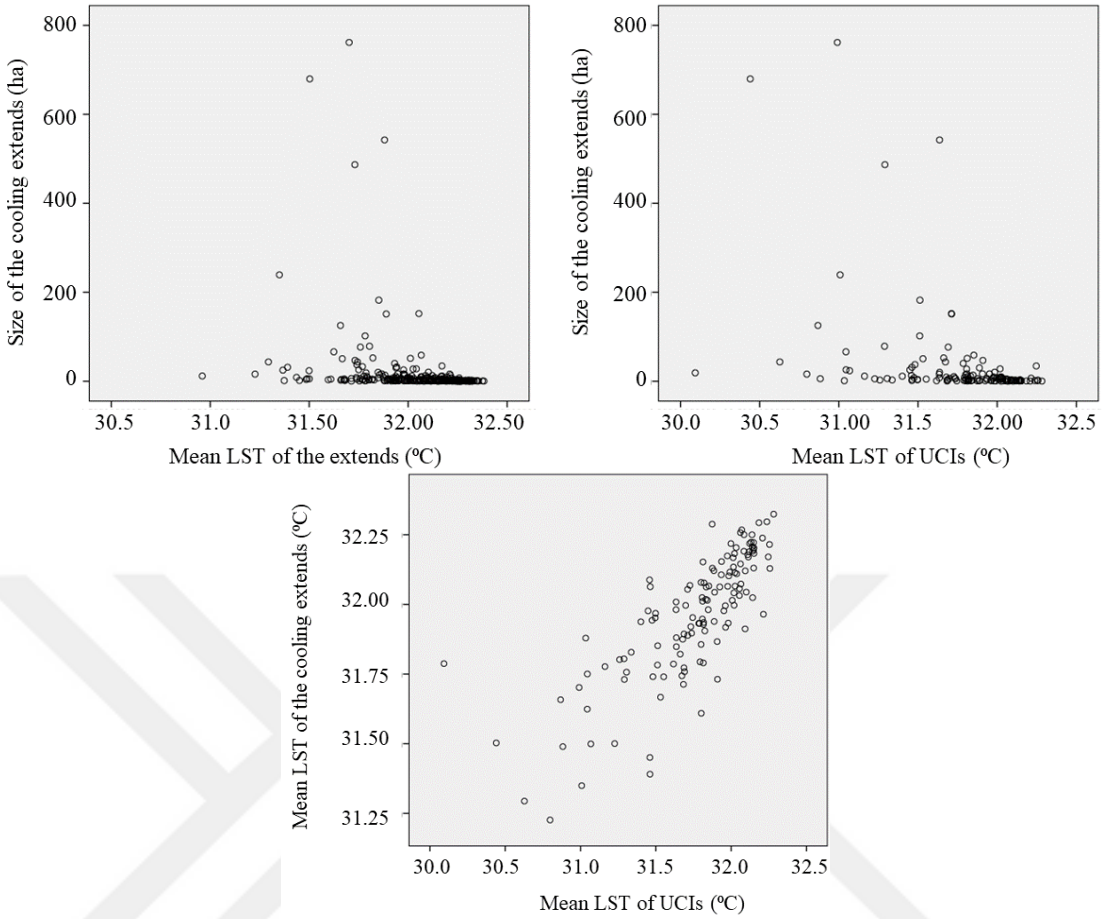


Figure 17. Scatter plots of the cooling capacity components

4.4 Relationship Between the Cooling Capacity and Important Parameters

The findings of the models aiming to analyze significant parameters in explaining the cooling capacity are presented in this section. Firstly, the LST_{mean} and LST_{min} models, related to the cooling intensity of UCIs, are explained. Secondly, the results of the Cooling Extent $Model_1$ and the Cooling Extent $Model_2$ are exhibited regarding the cooling extents. Both the LST_{mean} model and LST_{min} model are derived through multiple linear regression utilizing 862 observations. Autocorrelation seems to be not a problem in these models since the values of Dublin Watson statistics were slightly below 2.5. Additionally, the variance inflation factor (VIF) of independent variables remained below 5, indicating that multicollinearity among variables was at acceptable levels (Rogerson, 2010).

4.4.1. Results of multiple linear regression models

Table 12 shows the selected multiple linear regression model for LST_{min}. The independent variables considered in the LST_{min} model included the spatial composition of land cover, the spatial configuration of green, characteristics of UCIs, and outer thermal effects. The explanatory variables P_GR, S_UCI, D_FR, and C_UCI are all statistically significant at the α=0.05 (%95) level.

Table 13 shows the selected multiple linear regression models for the LST_{mean}. The independent variables of the LST_{mean} model, P_GR, S_UCI, D_FR, M_TR, and C_UCI, are statistically significant at the α=0.05 (%95) level, and D_SEA at α=0.10 (%90). The linear multiple regression model for the LST_{mean} explains about 57% (R^2=0.563) of the variance in the cooling capacity. Similarly, LST_{min} model explained about 61% (R^2=0.612) of the variance. When all of the variables in the models are equal to 0, the estimated LST_{min} is 32.706 ºC and the estimated LST_{mean} is 32.218 ºC (Table 13 and Table 14).

The residual analysis is depicted in Figures 18 and 19. The residual is "funnel shaped" and this finding indicates a problem.

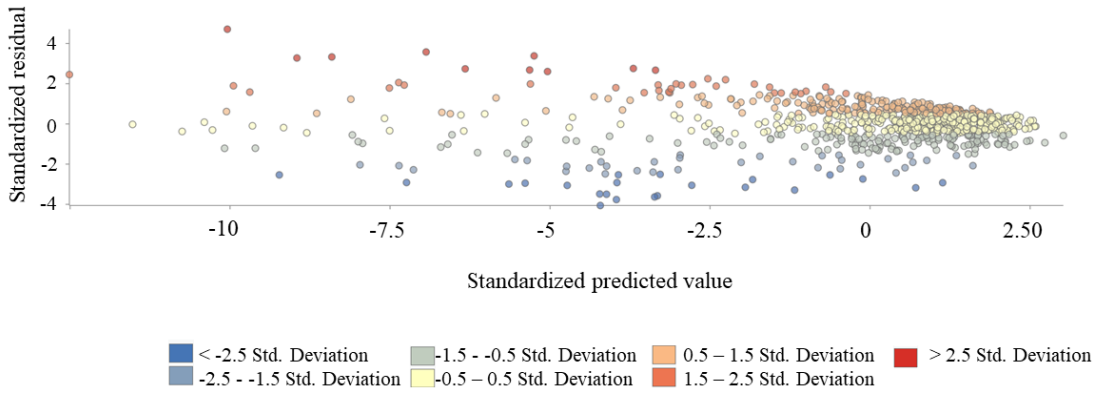


Figure 18. Scatter diagram of residual versus fit plot of LST_{min} model

Table 13. The LST_{min} Model Estimates (n=862)

Explanatory variable	Variable	Unit	Unstandardized Coefficients	Standardized Coefficients	t-statistics	Sig.	Collinearity Statistics	
				Beta			Tolerance	VIF
	(Constant)		31.829	32.706	268.668	0.000		
The proportion of tree-covered area	P_TR	%	-1.122	-0.173	-5.283	0.000	0.420	2.383
The proportion of water bodies	P_WA	%	-6.139	-0.618	-24.099	0.000	0.686	1.458
The patch density of tree-covered area	PD_TR	%	1.394	0.100	3.634	0.000	0.495	2.019
Mean patch size of tree-covered area	M_TR	ha	-0.172	-0.057	-2.249	0.025	0.699	1.431
The shape index of UCIs	LSI	km/ha	-0.010	-0.317	-14.438	0.000	0.934	1.070
Distance to the sea	D_SEA	km	0.006	0.053	2.317	0.021	0.849	1.177
Distance to the urban heat island	D_UHI	km	-0.607	-0.169	-7.701	0.000	0.938	1.066
Distance to nearest UCI	D_UCI	km	2.587	0.097	4.380	0.000	0.924	1.082

Model summary. R^2=0.612, F= 170.202 Dublin-Watson=1.965, p<0.05

Table 14. The LST_{mean} Model Estimates (n=862)

Explanatory variable	Variable	Unit	Unstandardized Coefficients	Standardized Coefficients	t-statistics	Sig.	Collinearity Statistics	
				Beta			Tolerance	VIF
	(Constant)		31.650	32.218	333.576	0.000		
The proportion of tree-covered area	P_TR	%	-0.995	-0.230	-7.756	0.000	0.579	1.729
The proportion of water bodies	P_WA	%	-5.717	-0.666	-24.492	0.000	0.686	1.458
The patch density of tree-covered area	PD_TR	%	1.534	0.110	3.565	0.000	0.531	1.884
The shape index of UCIs	LSI	km/ha	-0.003	-0.142	-6.112	0.000	0.936	1.069
Distance to the sea	D_SEA	km	0.017	0.040	1.646	0.100	0.850	1.177
Distance to the urban heat island	D_UHI	km	-0.596	-0.226	-9.732	0.000	0.939	1.065
Distance to nearest UCI	D_UCI	km	0.988	0.106	4.548	0.000	0.929	1.076

Model summary: R^2=0.563, F=185.797, Dublin-Watson=1.918, p<0.10

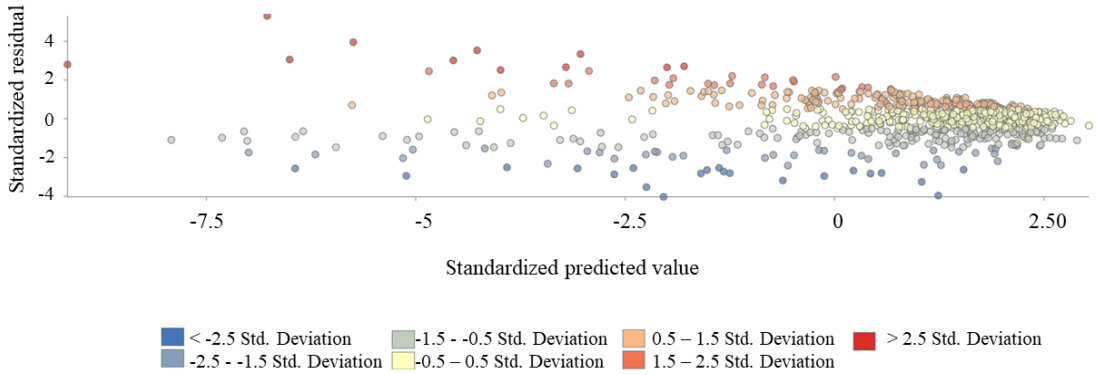


Figure 19. Scatter diagram of residual versus fit plot of LST_{mean} model

Table 15 and Table 16 show the selected multiple linear regression models for the Cooling Extent Models. Two models included the same explanatory variables except SQ_MAX_UCI and CORE_UCI. SQ_MAX_TR, CORE_TR, CORE_TR, and CORE_UCI are the most effective explanatory variables but their correlation to each other was very high. This situation is the same for SQ_MAX_UCI and SQ_MAX_TR. Therefore, these variables are included in the two models separately. The independent variables considered in the Cooling Extent Model included the spatial configuration of UCIs, tree-covered areas, and urban morphology. For the Cooling Extent $Model_1$, the statistical significances of the variables, SQ_MAX_UCI, PD_UCI, CORE_UCI, DA_UCI, DA_TR, and PD_TR are at the α=0.01 (%99) level, and the ones for E_RATIO at the α=0.05 (%95) level and SQ_B_HEIGHT at the α=0.10 (%90) level. The linear multiple regression model for the Cooling Extent $Model_1$ explains about 80% (R^2=0.801) of the variance in the cooling capacity. When all of the variables in the models are equal to 0, the estimated the extent area is 0.983 ha, nearly equal to one 30m x 30m pixel (Table 15).

Table 15 shows the selected multiple linear regression for the Cooling Extent $Model_2$. The statistical significances of these explanatory variables, PD_UCI, DA_UCI, SQ_MAX_TR, PD_TR, and CORE_TR are at the α=0.01 (%99) level. DA_TR and SQ_B_HEIGHT are statistically significant were at the α=0.05 (%95) level. This linear multiple regression model explains about 87% (R^2=0.871, $p<0.05$) of the variance in the cooling capacity. When all the explanatory variables in the models are equal to 0, the estimated extent area was 0.988 ha (Table 16).

The residual analysis is depicted in Figures 20 and 21. The plots shows the same shape, "funnel shape residual fit plot", like residual versus fit plot of LST_{min} and $LST_{mean.}$ This funnel shape in residual plots indicates a problem related to the distribution of residuals violating the linear regression assumptions.

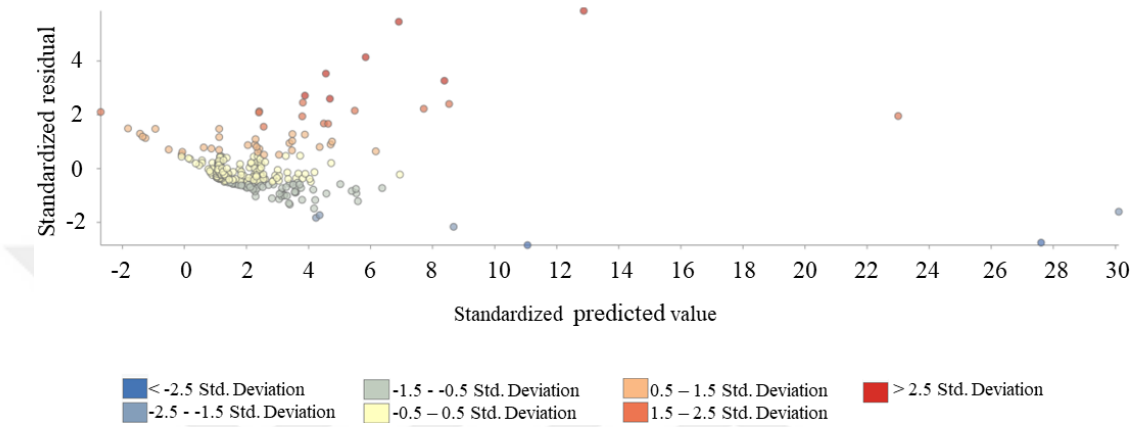


Figure 20. Scatter diagram of residual versus fit plot of $Extent_1$ model

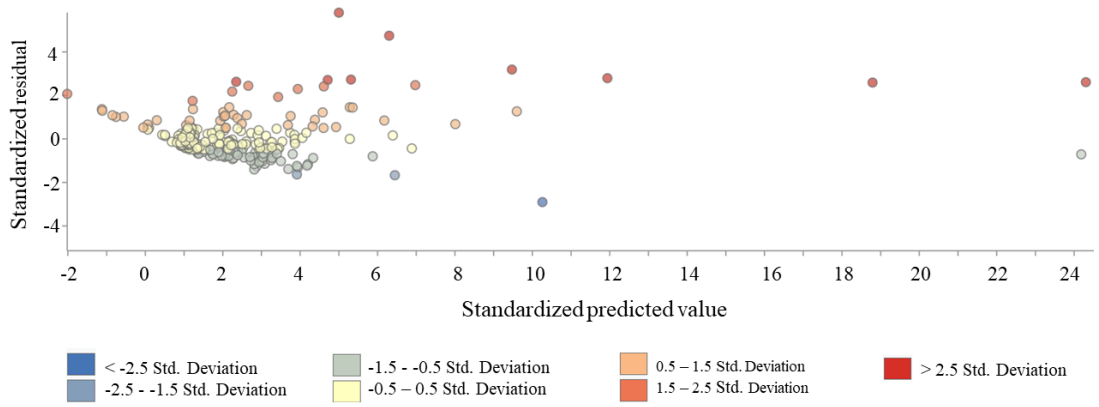


Figure 21. Scatter diagram of residual versus fit plot of $Extent_2$ model

Table 15. The Cooling Extent Model$_1$ Estimates (n=292)

Explanatory variable	Variable	Unit	Unstandardized Coefficients	Standardized Coefficients	t-statistics	Sig.	Collinearity Statistics	
				Beta			Tolerance	VIF
	(Constant)		0.983	0.983	3.422	0.001		
Square root of max patch of UCI	SQ_MAX_UCI	ha	0.413	0.139	2.774	0.006	0.279	3.583
The patch density of UCI	PD_UCI	%	-1.078	-0.192	-5.710	0.000	0.611	1.682
Core index of UCI	CORE_UCI	%	138.275	0.677	18.256	0.000	0.803	1.958
Dummy variable of UCI	DA_UCI		1.100	0.160	3.352	0.001	0.485	3.245
The patch density of tree-covered area	PD_TR	%	-0.438	-0.197	-5.891	0.000	0.653	1.216
Dummy variable of tree covered area	DA_TR		1.215	0.165	4.536	0.000	0.469	1.889
Elevation ratio	E_RATIO	%	-0.027	-0.071	-2.236	0.026	0.689	1.452
Square root of mean building height	SQ_B_HEIGHT	m	0.213	0.047	1.653	0.100	0.866	1.154

Model summary. R^2=0.801, F= 142.384, Dublin-Watson=1.249, p<0.10

Table 16. The Cooling Extent Model$_2$ Estimates (n=292)

Explanatory variable	Variable	Unit	Unstandardized Coefficients	Standardized Coefficients	t-statistics	Sig.	Collinearity Statistics	
				Beta			Tolerance	VIF
	(Constant)		0.988	0.988	4.278	0.000		
The patch density of UCI	PD_UCI	%	-0.845	-0.150	-5.509	0.000	0.611	1.636
Dummy variable of UCI	DA_UCI		1.285	0.187	6.112	0.000	0.487	2.054
Square root of max patch of tree covered area	SQ_MAX_TR	ha	2.503	0.152	4.984	0.002	0.490	2.040
The patch density of tree-covered area	PD_TR	%	-0.362	-0.163	-6.156	0.000	0.652	1.216
Core index of tree covered area	CORE_TR	%	162.140	0.737	29.384	0.000	0.722	1.385
Dummy variable of tree covered area	DA_TR		0.577	0.078	2.516	0.012	0.468	2.139
Elevation ratio	E_RATIO	%	-0.027	-0.071	-2.778	0.006	0.689	1.452
Square root of mean building height	SQ_B_HEIGHT	m	0.210	0.103	2.027	0.044	0.865	1.155

Model summary. R^2=0.871, F= 239.384, Dublin-Watson=1.356, p<0.05

4.4.2. Multiscale geographically weighted regression (MGWR) model results

In this section, Global Moran's I in ArcGIS Pro was applied to analyze the spatial autocorrelation of residuals of multi linear regression models. The results shows that Moran'I value for the regression models are spatially clustered. As the z-score of the models is a less than 1% likelihood (Table 17). Thus, Multiscale Geographically Weighted Regression (MGWR) was adopted for all the the regression models in this study.

Table 17. Spatial Autocorrelation results of the multi linear regression models

OLS model	Moran I	Z-score	P-value
LST_{min}	0.339	12.721	0.000
LST_{mean}	0.297	11.141	0.000
$Extent_1$	0.219	3.537	0.001
$Extent_2$	0.212	3.429	0.001

Table 18 shows the results of the LST_{min} MGWR model. P_TR, P_WA, PD_TR, LSI, D_UHI, D_UCI, M_TR, and D_SEA are statistically significant at the α=0.01 (%99) level whereas M_TR was not significant. In this way, M_TR was omitted from the LST_{min} MGWR model. According to the standardized estimates coefficients, the most explanatory variables follow the order of LSI, P_WA, D_UHI, P_TR, D_SEA, PD_TR and D_UCI in explaining the variance in cooling capacity. In particular, shape index (LSI) exhibits the strongest influence when compared to other variables. R^2 and Adjusted R^2 of the LST_{min} model is 0.862 and 0.823. The scatter diagram of residual versus fit plot of LST_{min} MGWR model is draw again. When compared it with the regression model as shown in Figure 15 in indicating a more random pattern (Figure 22).

Table 19 shows the results of the LST_{mean} MGWR model. P_TR, P_WA, PD_TR, LSI, D_UHI, and D_UCI are statistically significant at the α=0.01 (%99) level whereas M_TR and D_SEA is not significant. In this way, M_TR and D_SEA was omitted from the LST_{mean} MGWR model According to mean of the standardized estimates coefficients, the most, explanatory local variables follow the order of P_WA, D_UHI, P_TR, LSI, D_UCI and PD_TR in explaining the variance in

cooling capacity, which are statistically significant at the 99% (α=0,01) confidence level. In particular, the proportion of water bodies (P_WA) exhibits the strongest influence when compared to other variables. R^2 and Adjusted R^2 of the LST_{mean} model is 0.789 and 0.756 which are higher than multiple linear regression results (Adjusted R^2 =0.563). Additionally, the scatter diagram of residual versus fit plot of LST_{mean} MGWR model is draw again. When compared it with the OLS as shown in figure 16, the diagram presents a more random pattern (Figure 23).

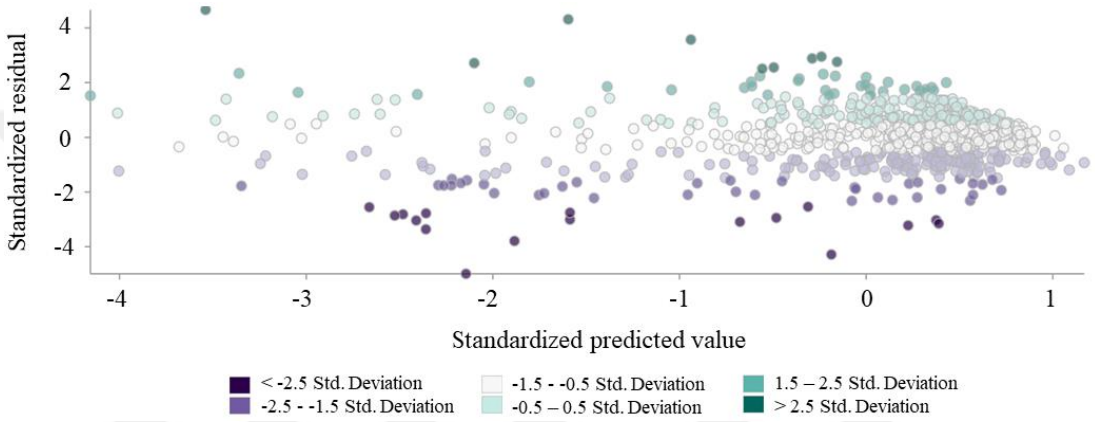


Figure 22. Scatter diagram of residual versus fit plot of LST_{min} MGWR model

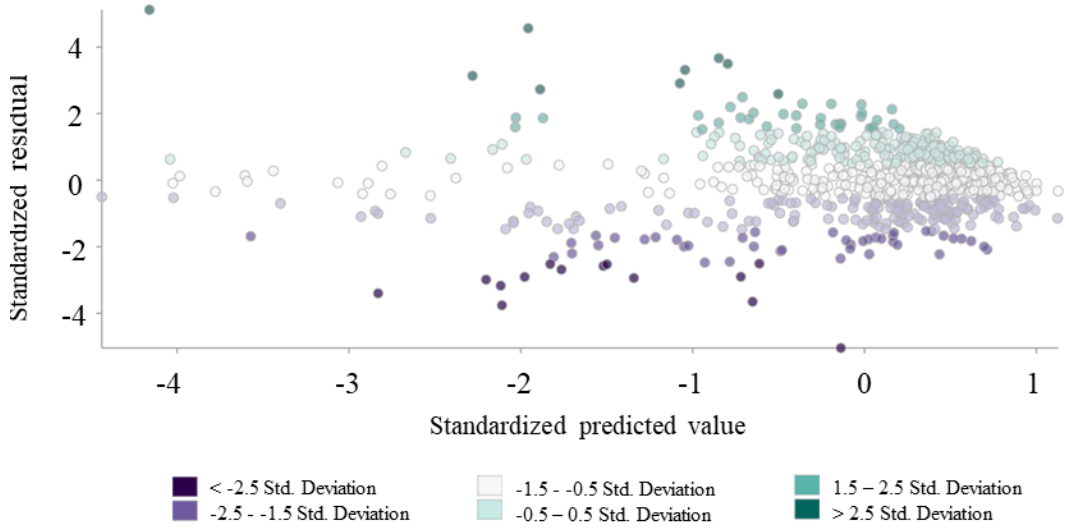


Figure 23. Scatter diagram of residual versus fit plot of LST_{mean} MGWR model

Table 18. Statistical description of LST_{min} MGWR model coefficient

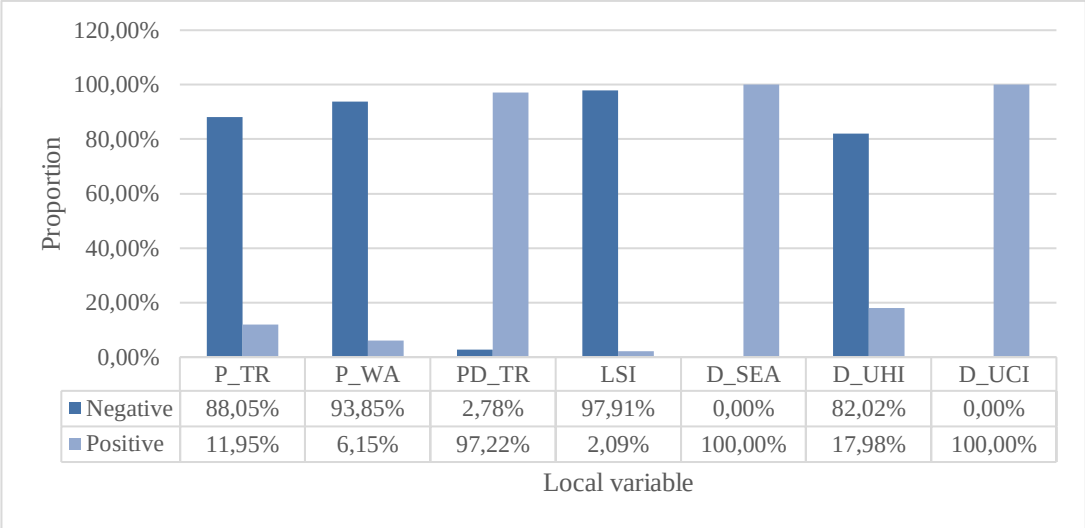
Local variable	Variable	Unit	Mean	Std. Deviation	Minimum	Median	Maximum
	Intercept		0.013	0.173	-0.371	0.479	0.303
Proportion of tree-covered area	P_TR	%	-0.196	0.192	-0.551	-0.1887	0.324
The proportion of water bodies	P_WA	%	-0.373	0.257	-0.898	-0.3163	0.178
The patch density of tree-covered area	PD_TR	%	0.108	0.072	-0.015	0.0971	0.300
The shape index of UCIs	LSI	km/ha	-0.587	0.460	-2.473	-0.4604	0.168
Distance to the sea	D_SEA	km	0.139	0.006	0.122	0.1391	0.150
Distance to the urban heat island	D_UHI	km	-0.205	0.351	-1.695	-0.1554	0.884
Distance to nearest UCI	D_UCI	km	0.085	0.026	0.025	0.0865	0.128
R^2	0.862						
Adj. R^2	0.823						
AICc	1227.441						

60

Table 19. Statistical description of LST_{mean} MGWR model coefficient

Local variable	Variable	Unit	Mean	Std.Deviation	Minimum	Median	Maximum
	Intercept		0.096	0.272	-0.702	0.192	0.635
Proportion of tree-covered area	P_TR	%	-0.190	0.162	-0.510	-0.155	0.209
The proportion of water bodies	P_WA	%	-0.406	0.319	-1.041	-0.383	0.108
The patch density of tree-covered area	PD_TR	%	0.075	0.079	-0.035	0.058	0.299
The shape index of UCIs	LSI	km/ha	-0.138	0.012	-0.161	-0.135	-0.108
Distance to the urban heat island	D_UHI	km	-0.249	0.002	-0.257	-0.248	-0.245
Distance to nearest UCI	D_UCI	km	0.090	0.042	0.0103	0.085	0.163
R^2	0.789						
Adj. R^2	0.763						
AICc	1375.2657						

Figure 24 shows proportion of negative and positive effect of the local variables of LST_{min} MWGR model. According to statistical results, PD_TR, D_SEA and D_UCI shows a positive direction relation with LST_{min} account for 97.22 %, 100 % and 100 %. These local variables mainly show positive effects of the cooling intensity. P_TR, P_WA, LSI and D_UHI shows a negative direction relation with LST_{min} account for 88.05 %, 93.85 % 97.91 and 82.02 %. When P_TR, P_WA, LSI and D_UHI decrease, the cooling intensity will be expected to decrease.



	P_TR	P_WA	PD_TR	LSI	D_SEA	D_UHI	D_UCI
Negative	88,05%	93,85%	2,78%	97,91%	0,00%	82,02%	0,00%
Positive	11,95%	6,15%	97,22%	2,09%	100,00%	17,98%	100,00%

Figure 24. Proportion of negative and positive effect of the local variables of LSTmin MWGR model

Figure 25 shows proportion of negative and positive effect of the local variables of LST_{mean} MWGR model. According to statistical results, PD_TR, D_SEA and D_UCI shows a positive direction relation with LST_{mean} account for 78,65 %, 100 % and 100 %. These local variables mainly show positive effects of the cooling intensity. P_TR, P_WA, LSI and D_UHI shows a negative direction relation with LST_{mean} account for 89,56 %, 94,08 %,100 %. and 100 %. When P_TR, P_WA, LSI and D_UHI decrease, the cooling intensity will be expected to decrease.

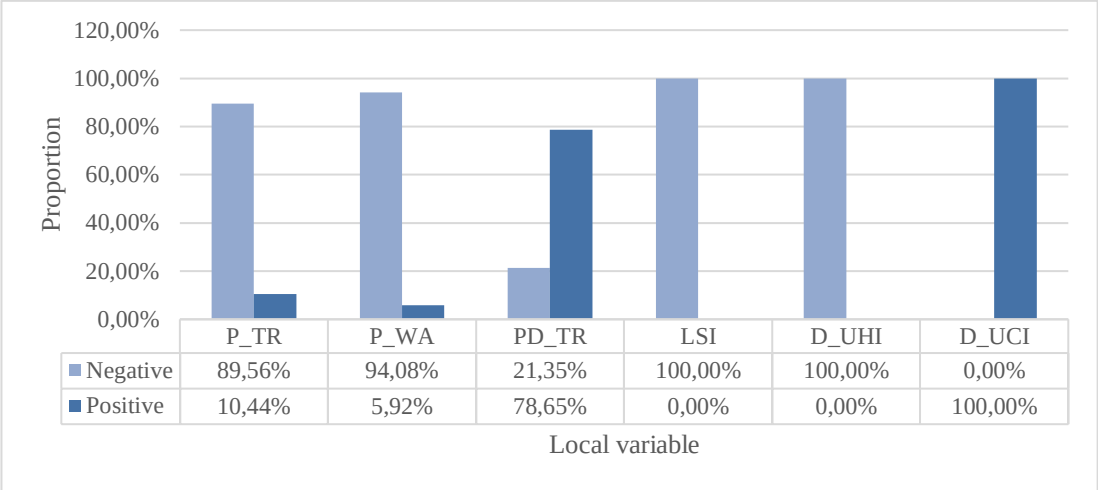


Figure 25. Proportion of negative and positive effect of the local variables of LSTmean MWGR model

Figure 26 shows the contribution proportion of dependent variables in explaining the cooling intensity according to categories. Results of the LST_{mean} and LST_{min} MGWR models show that contribution of the category was different for two models. For the LST_{mean} model the land cover composition is the most effective category while the parameters related land cover composition and UCI characteristics have nearly equal contribution for the LST_{min} model. Both models, contribution ratio of green configuration and outer thermal effect was nearly similar, and outer thermal effect has an important effect in explaining the cooling intensity of UCIs.

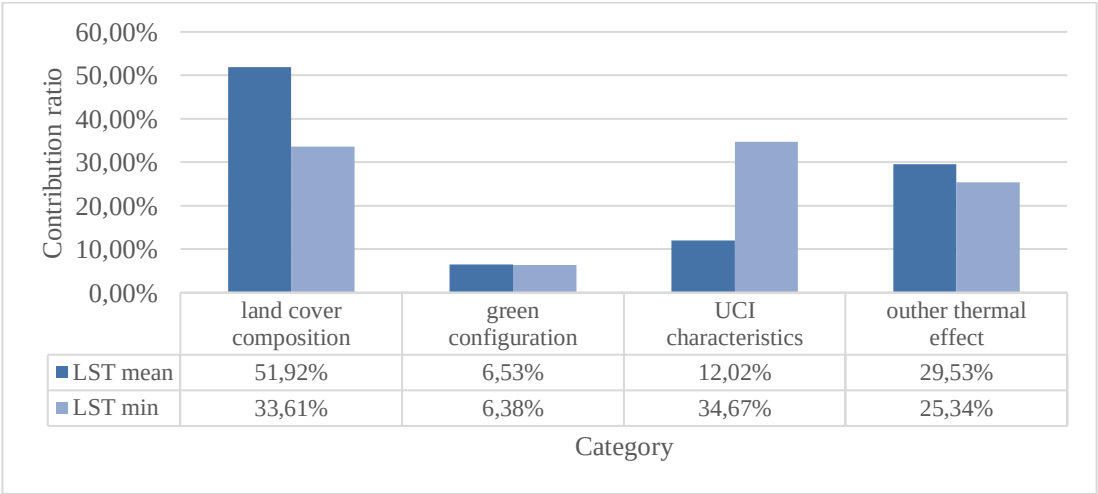


Figure 26. The contribution of the independent variables in the LST_{mean} and LST_{min} model according to category

Table 20 shows the results of the $Extend_1$ MGWR model. SQ_MAX_UCI, CORE_UCI, PD_TR, PD_UCI, DA_TR and E_RATIO is statistically significant at the α=0.01 (%99) level whereas DA_UCI and SQ_B_HEIGHT is not significant. In this way, DA_UCI and SQ_B_HEIGHT is omitted from the $Extent_1$ MGWR model. According to the standardized estimated coefficients, the most explanatory variables follow CORE_UCI, DA_TR, PD_UCI, PD_TR, PD_UCI, and E_RATIO respectively. Contribution in explaining the cooling extent, core index of UCIs (CORE_UCI) have 50% of the variance. Table 17 shows the results of the $Extend_1$ MGWR model. R^2 and Adjusted R^2 of the $Extend_1$ model was 0.918 and 0.904 which are higher than multiple linear regression results (Adjusted R^2 =0.801). Additionally, the scatter diagram of fitting value and residual of $Extend_1$ MGWR model is draw again. When compared it with the OLS as shown in Figure 17, the diagram is less scattered (Figure 27).

Table 21 shows the results of the $Extend_2$ MGWR model. PD_UCI, DA_UCI, SQ_MAX_TR, CORE_TR, PD_TR, DA_TR, SQ_B_HEIGHT and E_RATIO is statistically significant at the α=0.01 (%99) level. According to the standardized coefficient estimates, the most explanatory variables are CORE_TR, E_RATIO, PD_UCI, PD_TR, DA_TR, SQ_B_HEIGHT, DA_UCI and SQ_MAX_TR respectively in explaining the variance in the cooling extend. Table 17 shows the results of the $Extend_2$ MGWR model. R^2 and Adjusted R^2 of the $Extend_2$ model is 0.936 and 0.926 which is higher than multiple linear regression results (Adjusted R^2 =0.871). Additionally, the scatter diagram of fitting value and residual of $Extend_1$ MGWR model was draw again. When compared it with the OLS as shown in Figure 18, the diagram is less scattered (Figure 28).

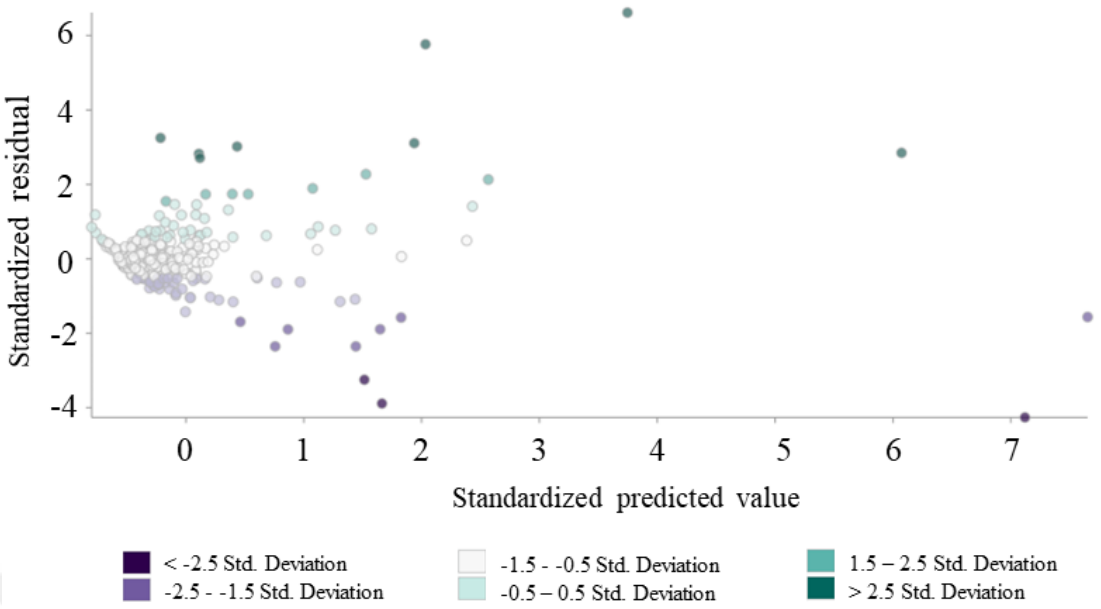


Figure 27. Scatter diagram of residual versus fit plot of $Extent_1$ MGWR model

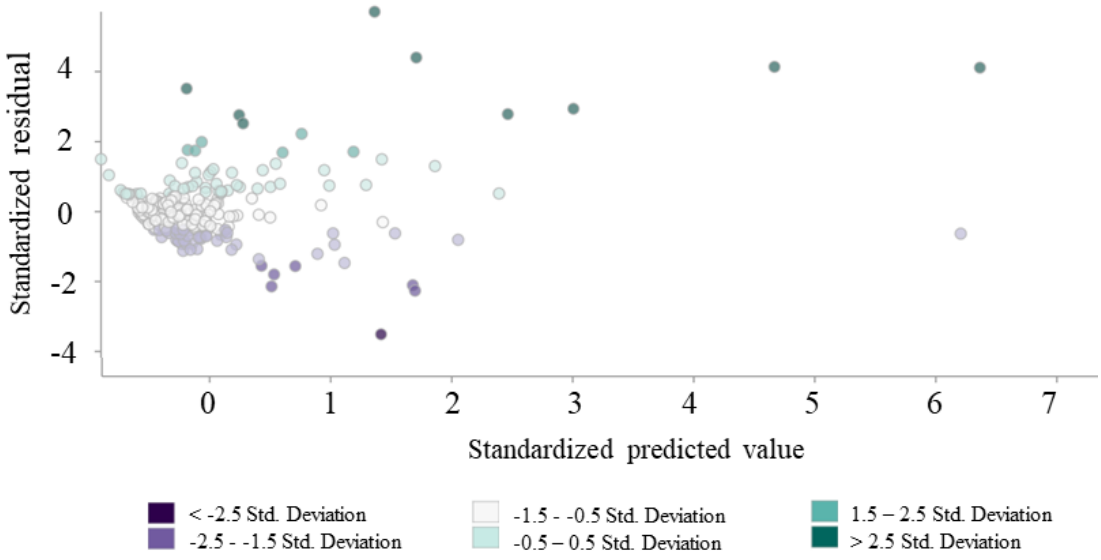


Figure 28.Scatter diagram of residual versus fit plot of $Extent_2$ MGWR model

Table 20. Statistical description of $Extent_1$ MGWR model coefficient

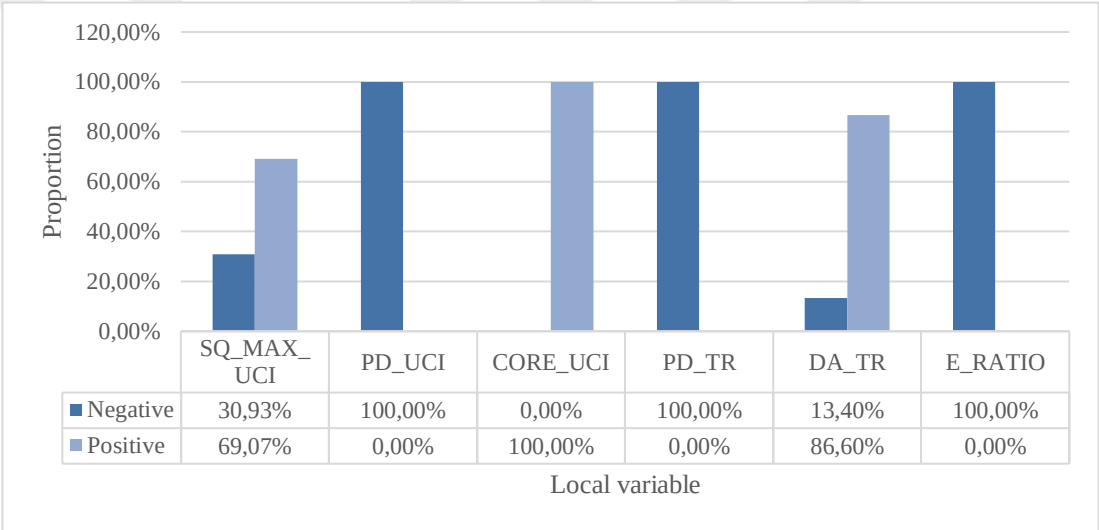
Local variable		Unit	Mean	Std. Deviation	Minimum	Median	Maximum
	Intercept		-0.038	0.132	-0.209	-0.062	0.281
Square root of max patch of UCI	SQ_MAX_UCI	ha	0.122	0.145	-0.099	0.160	0.382
The patch density of UCI	PD_UCI	%	-0.135	0.003	-0.142	-0.133	-0.133
Core index of UCI	CORE_UCI	%	0.499	0.029	0.454	0.484	0.546
The patch density of tree-covered area	PD_TR	%	-0.122	0.116	-0.492	-0.082	0.043
Dummy variable of tree covered area	DA_TR		0.183	0.337	-0.492	-0.082	-0.043
Elevation ratio	E_RATIO	%	-0.078	0.032	-0.153	-0.068	-0.039
R^2	0.918						
Adj. R^2	0.904						
AICc	205.377						

65

Table 21. Statistical description of $Extent_2$ MGWR model coefficient

Local variable		Unit	Mean	Std. Deviation	Minimum	Median	Maximum
	Intercept		0.068	0.262	-0.223	-0.009	0.939
The patch density of UCI	PD_UCI	%	-0.097	0.002	-0.098	-0.091	-0.090
Dummy variable of UCI	DA_UCI		0.045	0.112	-0.159	0.095	0.184
Square root of max patch of tree covered area	SQ_MAX_TR	ha	0.041	0.013	0.029	0.033	0.072
The patch density of tree-covered area	PD_TR	%	-0.092	0.029	-0.166	-0.084	-0.063
Core index of tree-covered area	CORE_TR	%	0.702	0.039	0.644	0.725	0.741
Dummy variable of tree covered area	DA_TR		0.052	0.004	0.046	0.051	0.063
Elevation ratio	E_RATIO	%	-0.106	0.029	-0.177	-0.092	-0.083
Square root of mean building height	SQ_B_HEIGHT	m	0.054	0.007	0.047	0.050	0.068
R^2	0.936						
Adj. R^2	0.926						
AICc	114.220						

Figure 29 shows proportion of negative and positive effect of the local variables of $Extent_1$ MWGR model. According to statistical results, SQ_MAX_UCI, CORE_UCI and DA_TR shows a positive direction relation with $Extent_1$ account for 69.07%, 100 % and 86.60%. These local variables mainly indicate positive effects of the cooling extend, PD_UCI, PD_TR and E_RATIO showed a negative direction relation with $Extent_1$ account for account for 69.07 %, 100% and 86.60%. When PD_UCI, PD_TR and E_RATIO decrease, thus, more fragmentation of UCIs and tree covered areas with denser elevation surfaces, the cooling extend will be expected to become larger.



	SQ_MAX_UCI	PD_UCI	CORE_UCI	PD_TR	DA_TR	E_RATIO
Negative	30,93%	100,00%	0,00%	100,00%	13,40%	100,00%
Positive	69,07%	0,00%	100,00%	0,00%	86,60%	0,00%

Figure 29. Proportion of negative and positive effect of the local variables of $Extent_1$ MWGR model

Figure 30 shows proportion of negative and positive effect of the local variables of $Extent_2$ MWGR model. According to statistical results, SQ_MAX_TR, CORE_TR, SQ_B_HEIGHT, DA_TR and DA_UCI shows a positive direction relation with $Extent_2$ account for 100%, 100 %, 100%, 100% and 63.57%. These local variables mainly show positive effects of the cooling extent, PD_UCI, PD_TR and E_RATIO shows a negative direction relation with $Extent_2$ account for 100%, 100% and 100 %.

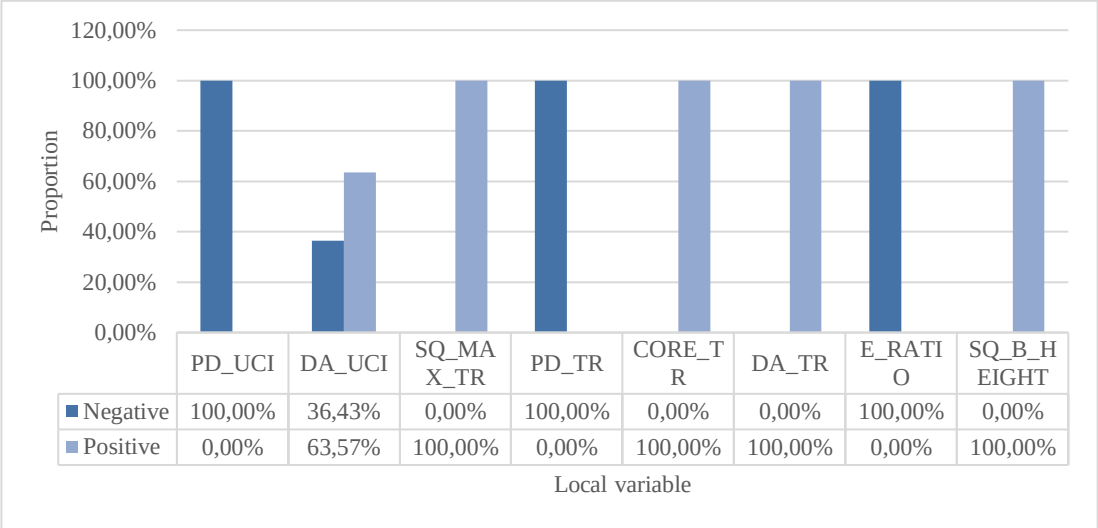


Figure 30. Proportion of negative and positive effect of the local variables of $Extent_2$ MWGR model

Figure 31 shows the contribution proportions of the explanatory variables in the Cooling Extent Models. When compared $Extent_1$ and $Extend_2$ model, the effect of the UCI configuration to the Cooling Extent $Model_1$ (66.37%) is less than the contribution of the green configuration to the Cooling Extent $Model_2$ (74.60%). Additionally, urban morphology has higher contribution ratio for Cooling Extent $Model_2$ than Cooling Extent $Model_1$.

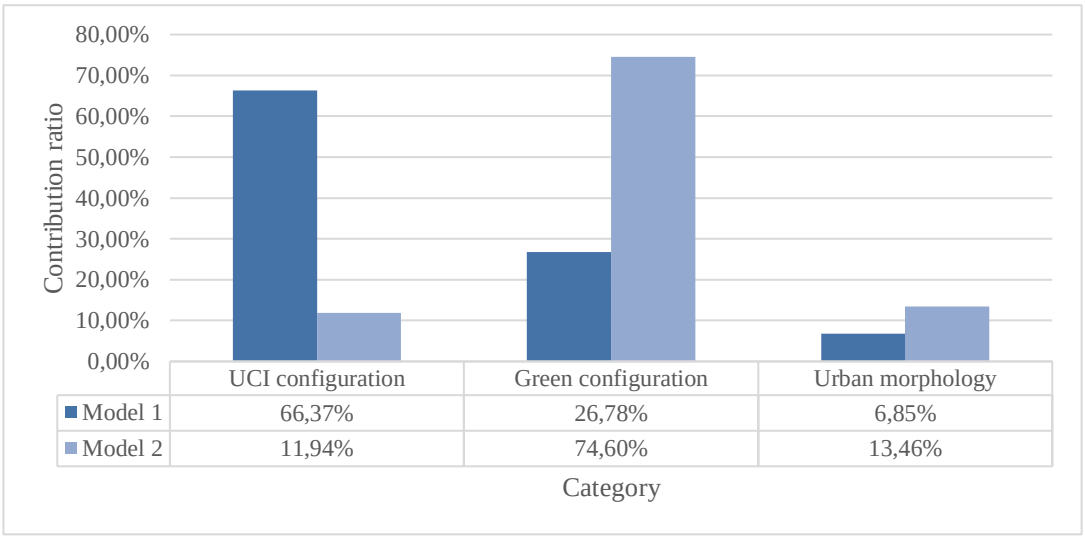


Figure 31. Contribution of categories of independent variables to the Cooling Extent Models

4.5 Using Regression Models For Policy Making

Table 22 shows alternative solutions for increasing the cooling capacity of UCIs by calculating the expected LST_{min} and LST_{mean} under different scenarios with using spatial regression models. According to scenario 1, where all explanatory variables were set to their sample existing value, the estimated LST_{min} was 30.923 ºC, between 24.430 ºC and 32.469 ºC, and LST_{mean} was 31.307 ºC, between 26.919 ºC and 32.423 ºC.

Scenario 2 represented the impact of increasing tree-covered areas and water bodies in a UCI, with the proportion of tree-covered areas set to 70% and water bodies at 30%. This intervention resulted in a temperature reduction of nearly 0,23 ºC for mean of LST_{min} compared to Scenario 1. Scenario 3 and 4 involved UCIs consisting of single tree-covered patches. In Scenario 3, assuming a 100% P_TR and the same fragmentation of tree-covered area, there was a temperature increase of approximately 0.190 ºC compared to Scenario 1. This increase is the same for the median, minimum and maximum value of LST_{min}. This means that replacement water body with tree-covered area results in increasing the temperature. In Scenario 4, assuming a 100% P_TR and very less fragmentation (PD_TR at 0.023), it is effective as Scenario 2, and a temperature decrease of 0.112 ºC compared to Scenario 1. Scenario 5 is the most effective intervention to reduce LST_{min}. Scenario 5 tests the the temperature change when increase the complexity of UCI. The mean value of LST_{min} of Scenario 5 reached to 28.250 ºC, which is equal to 2.674 ºC temperature reduction. Lastly, scenario 6 explored the doubling down distance from any UHI from UCI, resulting in a cooling increase of 0.056 °C compared to Scenario 1(Table 18).

The same predictions were occurred to estimate LST_{mean} of UCIs. The most effective Scenario is Scenario 5 that increasing the shape complexity of UCIs results in =0.871 ºC temperature reduction for LST_{mean}. The second effective is Scenario 2, 0.271 ºC temperature reduction is supplied with increasing waterbody. In contrast to LST_{min} predictions, Scenario 3, covering all surface with tree, supply 0.120 reduction for mean LST_{mean} compared to Scenario 1.

Table 22.Results of The Predictions Measuring the Cooling Intensity

S	Conditions	Estimated LST_{min} (^{o}C)				Estimated LST_{mean} (^{o}C)			
		Mean	Min	Median	Max	Mean	Min	Median	Max
1	**If all variables have their existing value**	30.923	25.430	31.352	32.469	31.307	26.919	31.591	32.423
2	**If P_WA=0.70 and P_TR=0.30**	30.693	25.314	31.092	32.095	31.036	26.746	31.305	32.094
3	**If P_TR=1**	31.114	26.159	31.495	32.637	31.187	27.192	31.436	32.306
4	**If P_TR=1, PD_TR=0.023**	30.812	25.766	31.163	32.578	31.183	27.196	31.428	32.259
5	**IF LSI 50% increases**	28.250	-32.615	30.475	31.485	30.436	-3.856	31.260	32.282
6	**IF D_UHI doubles**	30.868	25.455	31.300	32.450	31.292	26.801	31.571	32.357

Table 23 shows alternative solutions for increasing the cooling capacity of UCIs by calculating the expected Cooling Extent $Model_1$ and Cooling Extent $Model_2$ under different scenarios. According to scenario 1, where all explanatory variables were set to their sample value, the estimated $Model_1$ was 6.212 ha and $Model_2$ was 16.931 ha. According to Scenario 2, if the size of the UCI and tree-covered areas increases by 50%, the cooling extent of mean value of Extent $Model_1$, is expected to reach 6.221 ha. The increase of extent area is not high (0.009 ha) compared to Scenario 1. Scenario 2, offering larger UCI and tree-covered areas with less fragmentation, the predicted mean extent area of $Model_1$, is higher than the Scenario 1 in size by 0.830 ha. Lasty, Scenario 4 was estimated to the role of the urban morphology. SQ_B_HEIGT and E_RATIO is calculated for an urban area consisting of two stored and detached buildings with only a 15% building footprint. The increase of the are is 1.225 ha by reaching 7.437 ha. This increase shows that the most effective intervention for enlarging the cooling extent is changing urban morphology, supposed by Scenario 4.

Although estimated value of Extent $Model_2$ are higher than Extent $Model_1$, differences between Scenario 1 and other scenarios are very close to the Extent $Model_1$. These mean value differences are 0.010 ha for Scenario 2, 0.830 ha for Scenario 3 and 1.316 ha for Scenario 4 compared to Scenario 1 from bigger value to smaller ones.

Table 23. Results of The Predictions Measuring the Cooling Extent Models

S	Conditions	Estimated Extent$_1$ (ha)				Estimated Extent$_2$ (ha)			
		Mean	Min	Median	Max	Mean	Min	Median	Max
1	**If all variables have their existing value**	6.212	0.049	2.602	829.639	16.931	0.001	2.814	963.673
2	**If UCI and TR increase 50 %**	6.221	0.049	2.602	829.475	16.941	0.001	2.835	963.675
3	**If UCI and TR increase 50% with very less fragmentation**	7.074	0.017	3.173	857.872	17.761	0.037	3.303	986.470
4	**If M_B_HEIGHT=2 and E_RATIO=1,2**	7.437	0.040	3.478	857.872	18.247	0.001	3.420	1038.112

CHAPTER FİVE
DISCUSSION AND CONCLUSION

This study focused on examining the characteristics of relatively cooler areas in urban area of İzmir and determining the important parameters, related to increase the cooling capacity. In this study, the cooling capacity was measured both of cooling intensity of UCIs and the cooling extent. UCIs and their extents were identified using a spatial approach based on LST distribution. Explaining these components of the cooling capacity, multiplier linear regression models were applied. First of all, contribution of important parameters was analyzed, related to land cover composition, green configuration, UCI characteristics and outer thermal effects in enhancing the cooling intensity of UCIs. Secondly, contribution of important parameters was analyzed, related to the cooling intensity of UCIs, UCI composition and configuration, green composition and configuration and urban morphology in affecting on the cooling extents of UCIs. Lastly, parameters shaping the thermal conditions of urban environment was discussed with analyzing relationship between LST of the extent area and size of the extent. Because there was a thermal interaction between the urban environments.

5.1 Evaluation of The Results

Micro-scale studies that consider the cooling effect as an important element in reducing the UHI effect (Cheng et al., 2015; Lin et al., 2015; Wang and Zu, 2011), on the contrary, this research has developed an urban-scale approach. In the research scale approach developed in this study, a number of spatial analyses were used to identify urban cold islands with cooling capacity. Although the urban cold island boundaries obtained by this method overlap with urban green areas or water surfaces, it has excluded the built-up areas of park areas and has shown continuity with the adjacent green areas. In addition, some residential areas have also remained within the boundaries of UCIs. The direct urban green space boundary (Chang and Li, 2014; Cheng et al., 2015; Cheung and Jim, 2019; Ren et al. 2013; Vidrid and Medved, 2013) or surfaces covered with vegetation (Guo et al., 2019; Maimaitiyiming et al., 2014; Rakoto et al., 2021) has revealed a finding contrary to the studies that accept it

as an UCI (Figure 17). Based on this, a new discussion has been put forward about the investigation of the spatial distribution of temperature. It has been proved by numerical findings that the urban cold islands identified within the scope of the study are effective in regulating the local climate. The cooling extent area (Chang and Li, 2014; Cheng et al., 2015; Lin et al., 2015) describes and these emission areas combine to create a stronger cooling effect (Zhang et al., 2017). It leads to the clustering of low temperatures in the city or creating urban relatively cooler areas, which will create a multiple cooling effect of UCIs that provide thermal balance by absorbing heat. 26.7% of the urban area of Izmir was covered by urban relatively cooler areas. A similar result was measured as 29.80% for Shenzen province (Guo et al., 2019). The radial temperature pattern around the urban cold islands has been observed to show continuity in coastal areas along the Izmir Gulf. Similarly, Yüksel & Coşkun Hepcan (2023) found that low temperatures accumulated along the coastline in Karşıyaka district of Izmir to form cool islands (Figure 2). This is said to be due to the high cooling effect of the sea, which is an important cooling factor in determining the climate of Izmir. Previous studies also measured the lowest temperatures at water surfaces, such as the river and sea, which are similarly located in urban areas (Du vd., 2016; Kesgin Atak & Ersoy Tonyalıoğlu, 2020; Ünal Çiçek, 2022).

UCIs in İzmir were found to comprise 71% of total area, including green spaces. This finding showed that UCIs in İzmir were not exclusively located in green and wetland areas, but they generally overlapped with green areas. These findings aligned with the research by Peng et al. (2021), which found 64.40% overlap between urban parks and cold spot areas. UCIs in İzmir were also observed in low-density campus areas and some residential districts. According to observations, it can be supposed that the spatial distribution of UCIs in İzmir more fragmented on these areas where built environment was more open with green areas. This was specifically observed on some open mid-rise and open high-rise residential areas of İzmir. Similarly, Chen et al. (2023) discussed that UHI effect was less pronounced in more open built environment due to improved ventilation conditions, air flow and heat loss. These fragmented patterns of UCIs could have the potential to benefit a larger number of citizens by providing the cooling services in comparison to more compact

form of UCI (Zheng et al., 2023). Lee & Oh (2018) observed that mid-rise and high-rise areas with green spaces were slightly warmer than urban parks, with a temperature difference of approximately 0.3 ºC. These findings showed that local climate conditions varied within urban space. Likewise, Zheng et al. (2023) measured the lowest UHI intensities in open mid-rise and low-rise zones. In residential areas, LST distribution was influenced by both building and greenery elements, which interacted to impact the microclimate condition (Li et al., 2023).



Figure 32. Examples for a comparison of UCI and legal park boundary (UCI accurate boundary on the left, legal boundary of the parks on the right; (a) Aşık Veysel Recreation Area, (b) Kültürpark, (c) Hasanağa Park)

While the most UCIs comprised of grass and tree covered area, 22% of the total area consisted of non-vegetated area. Despite this, UCIs in İzmir showed a mean of LST_{mean} of 31.308 ºC and mean of LST_{min} of 30.924 ºC. In this study, these UCIs represented relatively the coolest urban areas, as extracted using an innovative approach based on LST distribution. Li et al. (2023) defined temperatures above 30 ºC as very hot weather conditions in the context of Hong-Kong, sup-tropical climate. The average size of the urban cold islands identified in this study is approximately 5 hectares (Figure 2). According to the assumption that greenery of more than 2 hectares has a significant cooling effect (Cao vd., 2010), the urban cold islands of Izmir have a significant influence on regulating the local climate. Previous studies have highlighted that the optimal size of the green area can vary according to climate conditions. For example, Geng vd. (2022) emphasized that the closer to the equator the greener the size of the green space.

Firstly, the study argued the components shaping the thermal environment conditions. There is a strong thermal interaction between UCIs and their extents area. If the cooling intensity of UCIs increases, thermal comfort conditions of the extent directly increases although the extents limitedly increase. This finding was close to the results of the LST models. Outer thermal effect was second effective category to explain the cooling intensity of UCIs. Reducing magnitude of UHI effect is very important to manage risk regarding human health.

Secondly, the studies developed the LST_{mean} MGWR model and LST_{min} MGWR model to explain the cooling capacity, which accounted for nearly 80% of the variation. This suggested that the presence of a complex mechanism determining LST distribution in urban areas. As emphasized by Yang et al. (2023), quantifying the impact of all parameters on urban thermal conditions proved to be challenging due to the merging of many factors. The cooling needs of urban areas were variable, requiring diverse cooling solutions (Gao et al., 2022; Peng et al., 2021; Yao et al., 2022). Additionally, the cooling efficiency of UCIs became crucial for urban spaces exposing higher UHI effects (Du et al., 2022; Yao et al., 2022).

The proportion of water bodies was the most important parameter in the LST_{mean} model to aimed at increasing the cooling capacity of UCIs, with a relative contribution of 66%. Similarly, previous studies measured that water bodies had a positive relationship with LST (Cao et al., 2010; Shi et al., 2023; Peng et al., 2021; Zho & Wu, 2022) with a relatively smaller contribution than the results of the model.

Previous studies showed that vegetation played an important role in regulating the local climate (Chen et al., 2023; Marando et al., 2019; Shi et al., 2023; Yan et al, 2021; Yao et al., 2022; Zheng et al., 2023) by providing evapotranspiration and shading (Bolund & Hunhammar, 1999) in urban areas. The findings of this study corresponded to the studies that the proportion of tree-covered areas (P_TR) has a important contribution to the cooling intensity. However, the proportion of grass-covered areas (P_GR) is not a significant variable to explain the LST of İzmir's UCIs. This finding aligns with the research conducted by Liao et al. (2023) where the effect of the land cover within urban parks on LST was analyzed.

In this study, the fragmentation in tree-covered areas within a UCI was analyzed using variables of patch density (PD_TR) and mean patch size (M_TR). The results revealed that the composition of the tree-covered areas was not only important in mitigating UHI but also green configuration, as suggested in previous studies (Estequo et al., 2017; Kong et al., 2014; Liao et al., 2023; Zhou et al., 2017; Zho & Wu, 2022). Additionally, Zhou et al. (2017) emphasized that the importance of green configuration could alter according to climate conditions.

The results of previous studies showed that UCI size was an important parameter to explain the cooling intensity (Gao et al., 2022; Peng et al., 2022; Yao et al., 2022). In contrast to these studies, some of the studies argued that greenspace size may have a limited effect on mitigating UHI (Shih, 2017) and small-scale urban parks could be effective in regulating the local climate (Oliveira et al., 2011). Additionally, Geng et al. (2022) occurred that the cooling effect related to size could indeed vary depending on climate conditions. In contrast to the size of UCIs, the shape index of the UCIs played an important role in explaining the cooling capacity for İzmir, especially for the LST_{min} of UCIs. This result was similar to previous studies (Cao et

al., 2010; Geng et al., 2022; Peng et al., 2021; Shi et al., 2023; Yao et al., 2022; Zhou et al., 2017). This result was concurred with previous studies that complex-shaped boosted heat alteration with the surroundings (Cao et al. 2010; Du et al., 2022; Shi et al., 2023; Yao et al., 2022). However, Yang et al. (2023) revealed that this could alter according to local climate.

İzmir Gulf, forest area, and UCIs were accepted as cool sources in the models, whereas UHI, the heating source. Distance to UHI (D_UHI) was more important variable than the distance to cooling sources (D_SEA, D_UCI), especially for determination of LST_{mean}. D_SEA and D_UCI was at least as much as the presence of green area to explain LST_{min} and $LST_{mean.}$ The cooling effect was affected by both internal and external factors (Du et al., 2022). One of the dominant factors regulating urban climate conditions in İzmir was the sea, particularly because UCIs located along seaside. However, D_SEA was not significant in explaining LST_{mean}. Surrounding urban development with grey abundance, less greenery, and traffic activity was significant to determine cooling capacity because of the storage of radiation (Peng et al., 2020). In addition, Yan et al. (2021) explored a strong negative correlation between LST of greenspaces and distance to nearest water and green space.

Moreover, the MGWR Models of the $Extent_1$ and $Extent_2$ were showed that UCI and tree covered areas within the extents were important elements to rise the cooling capacity. Similarly, Shih (2017) supposed that greenery of buffer area is significant like UCIs to define the cooling capacity. Higher magnitude with less fragmentation was effective to reduce urban heat island effect. Increasing total abundance of UCIs and the tree covered patches resulted in spreading the cooling effect on larger urban environment because of having higher contribution on explaining the cooling extent. Similarly, Lin vd. (2015) measured a very strong correlation between cooling spread and the size of the park's cold island, with a coefficient of 0.94. Larger urban cold islands usually do not define a larger cooling area. The average spread area identified as part of the study is about three and a half times the average size of the urban cold island. Du vd. (2022) studied parks of various sizes, from neighborhood parks to regional parks, and measured the spread of cooling to be about five times the size of

the urban cold island. The study found that cooling-effect spread areas have a fairly high standard deviation value. Similar results have been obtained in previous studies. (Cheng vd., 2015). Moreover, urban morphology had a significant relationship with the extents. For İzmir, increasing building heights and less building surfaces occurred to extent the cooling. Higher elevation ratio referred to densely building area and more impervious surfaces exposed to solar radiation. Building height generally showed significant relationship but the direction was different. For İzmir a positive relationship was measured like Sakar (2018). Sakar (2018) argued with simulating UHI intensity for different urban morphological types that UHI intensity became higher when building height increased for the same building footprint. Similarly, Li et al. (2020) supposed that slower increase in UHI intensity could be observed for the building density with high rise buildings. Similarly, according to Liao et al. (2023), an increase in impervious surfaces and a decrease in water surfaces within the buffer area resulted in a decrease in LST of urban parks.

Based on the results of this study, the following main conclusions can be made within the scope of sustainable urban planning and management in creating "Cool Cities":

- Urban relatively cooler areas where lower temperatures were clustered, could be used to understand spatial pattern of land surface temperature.
- UCIs generally overlapped urban green areas, but some residential areas also observed.
- Increasing cooling intensity of UCIs and their extents were important tools to mitigate UHI effect.
- There was a spatially significant relationship between the cooling intensity and extent and the variables studied in the study.
- The most effective categories in terms of contribution rate in explaining the LST_{mean} of UCIs are land cover configuration, outer thermal effect, UCI characteristics and configuration of green area, respectively where this importance order is UCI characteristics, land cover configuration, outer thermal effect and configuration of green area for the LST_{min} (Figure 18).

- Among the spatial intervention analyzed, increasing the proportion of water bodies within UCIs was the most effective in reducing the LST_{mean} of UCIs and second important variable for the LST_{min}.
- Composition of tree covered area was more effective than configuration of tree coverage in explaining the cooling intensity. However, increasing tree covered areas with reduced fragmentation was also identified as a crucial tool in enhancing the cooling magnitude.
- Shape compactness of UCIs exhibited a significant relationship with LST, with shape index being the most important variable in LST_{min} model. More complex shapes resulted in decreasing the LST_{min}.
- The LST models also measured efficiency of thermal interaction between heating and cooling sources in urban area of İzmir. UCIs and the sea were identified as cooling sources, UHI acted as a heating source. Heating sources were more effective in defining the cooling capacity of urban environment.
- The significant categories in terms of contribution rate in explaining the cooling extents are UCIs configuration, green configuration, and urban morphology (Figure 18).
- Increasing tree covered areas within the extents were as effective as increasing UCIs to extending cooling effect.
- Fragmentation of tree covered areas and UCIs was important to explain the cooling extent that less fragmented cooling sources resulted in increasing the cooling capacity.
- There was a mutual thermal interaction between UCIs and their adjacent.
- Decreasing building surfaces and increasing building height resulted in enlarging the size of extents.
- Increasing cooling capacity of UCIs strongly occurred to reduce LST of urban environment, while less affect to increase the cooling extents. In this way, explaining the extents was more complex than the intensity ((Figure 33).

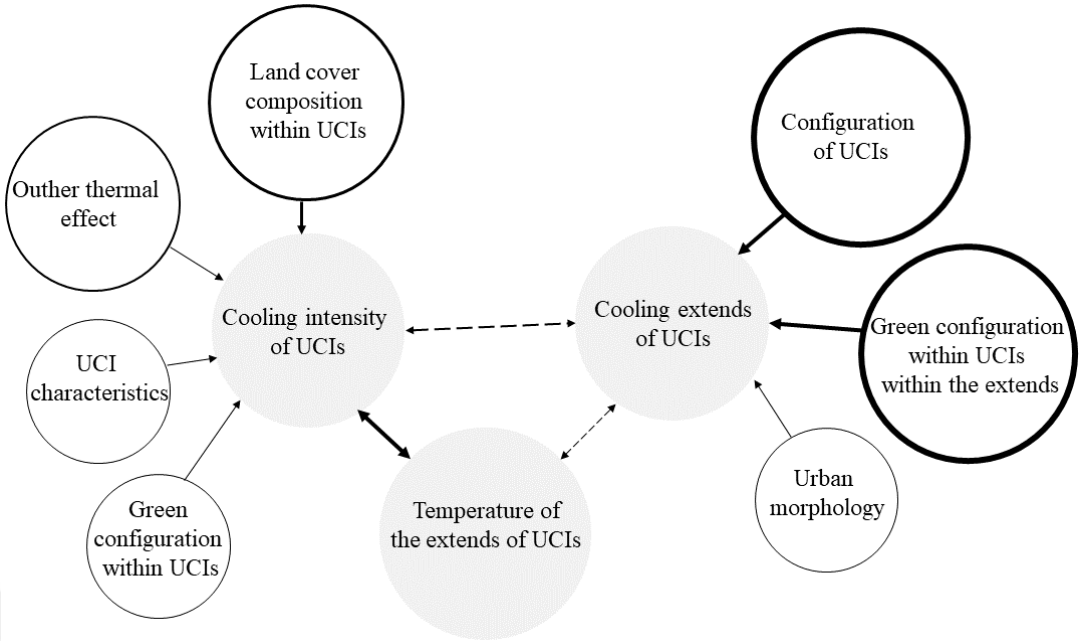


Figure 33. Relationships between important components and parameters related to the cooling capacity according to findings of the regression models

To sum up, improving the cooling capacity of urban areas is an important approach in preventing the effect of urban thermal islands. In order to optimally exploit the cooling potential, both cooling strength and cooling spread need to be increased (Gao vd., 2022). The cooling effect felt in the wider area leads to a reduction in the vulnerability of more urban residents (Shi vd., 2023) to the effect of urban thermal islands, taking advantage of the cooling effects.

5.2 Limitations of The Study

In this study, İzmir Metropolitan built-up area was selected as the study area for spatial statistical analysis to focus specifically on examining the LST distribution within urban environment. It was important to emphasize that altering the analysis area could indeed result in different outcomes regarding the identification of spatial clusters and their significant. This implies that location of UCIs would also affect by changes in the analysis area because of using method based on spatial autocorrelation method. Urban relatively cooler areas and UCIs were relatively lower temperature areas within the analysis area. If the natural areas on the city periphery were included in the study area, the urban relatively cooler area and UCIs boundaries could differ

and some UCIs were, detected by the study, could not include. Depending on UCIs locating on urban areas resulted in showing higher temperatures compared to thermal comfort conditions. Thus, the low average cooling intensity of UCIs indicates that these areas had high temperature values from the point of view of public health. This could be due to the thermal interaction of urban cold islands with their surroundings.

Moreover, previous studies argued that the important parameters related to cooling capacity of UCIs can vary across different cities, particularly under diverse climate conditions (Geng et al., 2022; Zhou et al., 2017). Therefore, in order to generalize or compare the results obtained from this study, it would be necessary to apply the same innovative analysis approach to various cities. Yet, the spatial dataset produced by this study was successfully contributed to the development of LST analysis, which can lead to spatial design and planning practices.

The study was only analyzed urban relatively cooler areas, thus, excluded urban relatively hotter areas. This resulted in more homogeneous dataset which made strong to explain dependent variables. For some independent variables especially related to urban morphology, continuous numeric values were similar. Furthermore, while developing the extent regression model, variables describing areal magnitude like green area, built up area within the extents showed positive relationship with extent size. This finding was not reliable because large extent areas had large built-up area and green areas because of locating on urban areas. In this way, these variables were not included to the extent model.

Another limitation of the study, predictions of the extents regression models were argued with acceptance of not to changing spatial pattern of LST. For example, increasing tree covered area within the extent may result in occurring an additional UCI polygon or one UCI polygon could be larger.

5.3 Contribution of The Study and Suggestions for the Future Studies

Previous studies explain that it is not known for sure how the local climate affects cooling efficiency, and it has a complex structure (Fan et al., 2019; Yu et al., 2020). To generate solutions against impact of climate change, there is need to local

findings due to generalize global ones. In this way, there is need to test the research methodology for various cases and compare the findings. This study found out quantitative results for İzmir urban area, a Mediterranean city and the findings were compared to previous findings. The spatial dataset produced by this study was successfully contributed to the development of LST analysis, which can lead to spatial design and planning practices. this study served as a valuable reference for optimizing the design of urban thermal environments and developing strategies to mitigate UHI effects. But there is need to apply to methodology other cities to define similarity and differences of important variables and LST pattern.

In Turkish literature, the studies usually analyzed the relationship between LST distribution and land cover change or vegetation abundance (Kesgin Atak, 2020; Atak & Tonyalıoğlu, 2020; Şimşek & Şengezer, 2012). Analyzing methodology of the study presented contribution to another innovative research (Şentürk & Çubukçu, 2023; Yüksel & Coşkun Hepcan, 2023).

This study used spatial autocorrelation methods to detect relatively cooler and coolest areas and finding of the regression model showed that thermal interaction between urban areas was very effective to explain the cooling. However, this study did not simulate the LST distribution after application of spatial interventions. Further studies can analyze how the spatial pattern of LST change rather than estimating size of extent and LST of UCIs. This approach can give more information about thermal interactions between urban areas.

The regression models of the study were successful to explain the cooling capacity. The study emphasized the importance of considering the specific characteristics of UCIs in different density built-up environments with varying thermal effects for sustainable urban planning (Peng et al., 2020). Explaining the cooling extent was more complex, so this study highlights the need for multi-scale perspective in researching urban microclimate, as emphasized in the literature by Yang et al. (2023). Especially, there was need to analysis relationship between urban morphology and the extent. In this study, only two variables were included in the extents models due to high correlation between variables.

As a result, the findings of the study will not only guide in understanding the importance of UCIs and urban relatively cooler areas in regulating local climate; it will also give information about urban policies. Finding of the study supply information for multi-scale spatial cooling interventions, for urban design and city planning. Considering that the atmospheric temperature tends to increase due to climate change in cities with a Mediterranean climate, increasing the cooling capacity is even more important for Izmir province. In summary, spatial decisions should be in a direction that will increase the thermal comfort of the built environment. The methods and quantitative results revealed by the study are important in terms of contributing to urban planning practice and guiding planning decisions to be made in the future.

REFERENCES

Abougendia, S. M., Ayad, H. M. ve El-Sayad, Z. T. (2020). "Classification Framework of Local Climate Zones Using World Urban Database and Access Portal Tools: Case Study of Alexandria City, Egypt". WIT Transactions on Ecology and the Environment, 241, 309-322. doi:10.2495/SDP200251

Amiri, R., Weng, Q., Alimohammadi, A. ve Alavipanah, S. K. (2009). Spatial–temporal dynamics of land surface temperature in relation to fractional vegetation cover and land use/cover in the Tabriz urban area, Iran. *Remote Sensing of Environment*, 113, 2606–2617.

Aram, F., Solgi, E., Garcia, E. H., Mosavi, A. & Varkonyi-Koczy, A. R. (2019). The Cooling Effect of Large-Scale Urban Parks on Surrounding Area Thermal Comfort. *Energies*,12, 3904-3925**.** doi:10.3390/en12203904

Asgarian, A., Amiri, B. J. & Sakieh, Y. (2015). Assessing the effect of green cover spatial patterns on urban land surface temperature using landscape metrics approach. *Urban Ecosyst*, 18, 209-222. doi: 10.1007/s11252-014-0387-7.

Breiman, L. (2001). Random forests. *Machine Learning*, 45, 5–32.

Bolund P., Hunhammer S. (1999). Ecosystem services in urban areas. *Ecological Economics*, 29, 293-301.

Cao, X., Onishi, A., Chen, J. & Imura, H. (2010). Quantifying the cool island intensity of urban parks using ASTER and IKONOS data. *Landscape and Urban Planning*, 96, 224-231.

Carlson, T. & Arthur, S. T. (2000). The impact of land use - Land cover changes due to urbanization on surface microclimate and hydrology: A satellite perspective. *Global and Planetary Change*,25(1), 49-65. doi:10.1016/S0921-8181(00)00021-7

C40 Cities (2020). A global opportunity for cities to lead.

Chen, X., Su, Y., Dan, L., Huang, G., Chen, W. & Chen, S. (2012). Study on the cooling effects of urban parks on surrounding environments using LandsatTM data: a case study in Guangzhou, southern China, *International Journal of Remote Sensing*,33 (18), 5889-5914. Doi: 10.1080/01431161.2012.676743

Chen, G., Chen Chen, G., He, H., Wang, J., Zhao, L. And Cai, Y. (2023). Assessing the synergies between heat waves and urban heat islands of different local climate zones in Guangzhou, China. *Building and Environment*, 240,110434.

Cheng, X., Wei, B., Chen, G., Li, J. & Song, C. (2015). Influence of Park Size and Its Surrounding Urban Landscape Patterns on the Park Cooling Effect. *J. Urban Plann. Dev.*, 141(3), A4014002 1-10 doi: 10.1061/(ASCE)UP.1943-5444.0000256.

Cheung, P. K. & Jim, C. Y. (2019). Differential cooling effects of landscape parameters in humid-subtropical urban parks. *Landscape and Urban Planning*, 192, 103- 651.

Chang, C. R. & Li, M. H. (2014). Effects of urban parks on the local urban thermal environment. *Urban Forestry & Urban Greening*, 13, 672-681.

Chun, B. and Guldmann, J-M. (2014). "Spatial statistical analysis and simulation of the urban heat island in high-density central cities". *Landscape and Urban Planning*, 125, 76-88.

Congedo, L. & Munafo,M. (2014). Urban Sprawl as a Factor of Vulnerability to Climate Change: Monitoring Land Cover Change in Dar es Salaam. Macchi, S. & Tiepolo, M. (Eds) inside *Climate Change Vulnerability in Southern African Cities*, London, 73-88, Springer.doi: 10.1007/978-3-319-00672-7

Çubukçu, K. M. (2015). *Basic Statistics and Spatial Statistics in Planning and Geography* (1). Ankara: Nobel Academic Publications.

Dai, X., Guo, Z. ve Zhang, L. (2010). Spatio-temporal exploratory analysis of urban surface temperature field in Shanghai, China. *Stoch Environment Res Risk Assess*, 24, 247-257

Dimoudi, A., Kantzioura, A., Zoras, S., Pallas, C. and Kosmopoulos, P. (2013) "Investigation of urban microclimate parameters in an urban center". *Energy and Buildings*, 64,1-9.

Du, S., Xiong, Z., Wang, Y. & Guo, L. (2016). Quantifying the multilevel effects of landscape composition and configuration on land surface temperature. *Remote Sensing of Environment*, 178, 84-92.

Du, C., Jia, W., Chen, M., Yan, L. & W. K. (2022). How can urban parks be planned to maximize cooling effect in hot extremes? Linking maximum and accumulative perspectives. *Journal of Environment Management*, 317, 115346. doi: 10.1016/j.jenvman.2022.115346

Edussuriya, P., Chan, X. ve Ye, A. (2011). "Urban morphology and air quality in dense residential environments in Hong Kong. Part I: District-level analysis". *Atmospheric Environment,* 45,4789-4803.

Esche, H. A., Franklin, S. E., & Wulder, M. A. (2002). Assessing cloud contamination effects on K-means unsupervised classifications of Landsat data. Geoscience and Remote Sensing Symposium, IGARSS'02. *IEEE International*, 6(C), 3387–3389. doi: 10.1109/IGARSS.2002.1027191.

Estequo, R. C., Murayama, Y. & Myint, S. W. (2017). Effects of landscape composition and pattern on land surface temperature: An urban heat island study in the megacities of Southeast Asia. *Science of the Total Environment*, 577, 349-359.

İzmir Büyükşehir Belediyesi (İBB) (2019) 2015-2019 Stratejik Planı (İzmir)

İzmir Metropolitan Municipality (IMM) & Landscape Research Society (2019). A Framework for Resilient Cities to Climate Change: A Green Revision Guidebook, Pardus Publications.

İzmir Metropolitan Municipality (IMM) (2020). Green City Action Plan.

Kong, F., Yin, H., Wang, C., Cavan, G. ve James, P. (2014). A satellite image-based analysis of factors contributing to the green-space cool island intensity on a city scale. *Urban Forestry and Urban Greening*, 13, 2014, 846-853.

Kuba, E. B., Acar Deniz, Z. & Öztürk, B. (2016). Climatological and meteorological analysis of heat wave over the Turkey in the 1960-2010 period. TÜCAUM International Geography Symposium, 13-14 October 2016, Ankara.

Hamada, S., Tanaka, T. & Ohta, T. (2013) Impacts of land use and topography on the cooling effect of green areas on surrounding urban areas. *Urban Forestry & Urban Greening,* 12,426–434.

Hardin, P. J. & Jensen, R. R. (2007). The effect of urban leaf area on summertime urban surface kinetic temperatures: A Terre Haute case study. *Urban Forestry & Urban Greening*, 6(2),63-72.

Hathway, E.A., Sharples, S. (2012). "The interaction of rivers and urban form in mitigating the Urban Heat Island effect: A UK case study". *Building and Environment, 58,* 14-22.

Hung, T., Uchihama, Ochi, S. ve Yasuoka, Y. (2006). Assessment with satellite data of the urban heat island effects in Asian mega cities, *International Journal of Applied Earth Observation and Geoinformation*,8 (1):, 2006:, 34-48.

Fan, H., Yu, Z., Yang, G., Liu, T., Liu, T., Hung, C. & Vejre, H. (2019). How to cool hot-humid (Asian) cities with urban trees? An optimal landscape size perspective. *Agricultural and Forest Meteorology*, 265, 338–348.

Fintikakis, N., Gaitani, N., Santamouris, M., Assimakopoulos, M., Assimakopoulos, D. N., Fintikaki, M., Albanis, G., Papadimitriou, K., Chryssochoides, E., Katopodi, K. and Doumas, P. (2011) "Bioclimatic design of open public spaces in the historic centre of Tirana, Albania". *Sustainable Cities and Society*, 1, 54-62.

Geng, X., Yu, Z., Zhang, D., Li, C., Yuan (2022) The influence of local background climate on the dominant factors and threshold-size of the cooling effect of urban parks. *Science of the Total Environment*, 823, 153806-153816. doi: 10.1016/j.scitotenv.2022.153806

General Directorate of Meteorology (April 2022). *Resmi İstatistikler.* Taken from https://www.mgm.gov.tr/veridegerlendirme/il-ve-ilceler-istatistik.aspx?m=İZMİR at 20 April 2023.

Groot, R. S., Wilson, M. A. & Boumans, R. M. J. (2002). A typology for the classification, description and valuation of ecosystem functions, goods, and services. *Ecological Economics,* 41, 393-408.

Gao, Z., Zaitchik, B., Hou, Y. & Chen, W. (2022). Toward park design optimization to mitigate the urban heat Island: Assessment of the cooling effect in five U.S. cities. *Sustainable Cities and Society*, 81, 103870.

Guo, G., Wu,Z., Xiao, R., Chen,Y., Liu, X. & Zhang, X. (2015). Impacts of urban biophysical composition on land surface temperature in urban heat island clusters. *Landscape and Urban Planning*, 135,1-10.

Guo, G., Wu, Z. & Chen, Y. (2019). Complex mechanisms linking land surface temperature to greenspace spatial patterns: Evidence from four southeastern Chinese cities. *Science of Total Environment*, 674, 77-87.

Kesgin Atak, B. (2020). Analysing the relationships between land use/land cover and urban land surface temperature using regression tree in İzmir. *International Journal of Geography and Geography Education (IGGE),* 41, 280-291.

Kesgin Atak, B. & Ersoy Tonyalıoğlu, E. (2020). Alan kullanım/arazi örtüsü ve bitki örtüsündeki değişimin arazi yüzey sıcaklığına etkisinin değerlendirilmesi: Aydın ili örneği. *Türkiye Ormancılık Dergisi,* 21 (4), 489-497.

Kong, F., Yin, H., Wang, C., Cavan, G. ve James, P. (2014). A satellite image-based analysis of factors contributing to the green-space cool island intensity on a city scale. *Urban Forestry and Urban Greening*, 13, 2014, 846-853.

Kwak, Y., Park, C. & Deal, B. (2020). Discerning the success of sustainable planning: A comparative analysis of urban heat island dynamics in Korean new towns. *Sustainable Cities and Society*, 61, 102341- 102354. doi: 10.1016/j.scs.2020.102341

Leconte, P., Bouyer, J. Claverie., R. & Petrissans, M. (2015). Using Local Climate Zone scheme for UHI assessment: Evaluation of the method using mobile measurements. *Building and Environment*, 83, 39-49.

Lee, D. & Oh, K. (2018). Classifying urban climate zones (UCZs) based on statistical analysis. *Urban Climate*, 24, 503-516. doi: 10.1016/j.uclim.2017.06.005

Li, J. J., Wang, X., Wang, X, Ma, W., Zhang, H. (2009). "Remote sensing evaluation of urban heat islve ve its spatial pattern of the Shanghai metropolitan area, China". *Ecological Complexity*, 6, 413-420.

Li, X., Zhou, W., Quyang, Z., Xu, W., Zheng, H. (2012). "Spatial pattern of greenspace affects land surface temperature: evidence from the heavily urbanized Beijing metropolitan area, China". *Lanscape Ecology,* 27, 887-898.

Li, W., Cao, Q., Lang, K., Wu, J. (2017). Linking potential heat source and sink to urban heat island: Heterogeneous effects of landscape pattern on land surface temperature. *Science of the Total Environment*, 586, 457–465.

Li, Y., Schubert, S., Kropp, J. P. & Rybski, D. (2020). On the influence of density and morphology on the Urban Heat Island intensity. *Nature Communications*, 11, 2647.

Li, Y., Quyang, W., Yin, S., tan, Z. & Ren, C. (2023). Microclimate and its influencing factors in residential public spaces during heat waves: An empirical study in Hong Kong Building and Environment, 236, 110225. doi: 10.1016/j.buildenv.2023.110225

Liao, W., Guldmann, J-G, Hu, L., Cao, Q, Gan, D. & Li, X. (2023). Linking urban park cool island effects to the landscape patterns inside and outside the park: A simultaneous equation modeling approach. *Landscape and Urban Planning*, 232, 104681.

Lin, W., Yuc,T., Changa,X., Wua, W. & Zhanga, Y. (2015). Calculating cooling extents of green parks using remote sensing: Method and test. *Landscape and Urban Planning*, 134, 66–75.

Liu,L., Lin, Y., Wang, L., Cao, J., Wang, D.,Xue, P. & Liu, J. (2017). An integrated local climatic evaluation system for green sustainable eco-city construction: A case study in Shenzhen, China. *Building and Environment*, 114, 82-95.

Luo, Y., Shizhang, P., Jiang, Y., Yuehua, F., Khan, S. & Han, B. (2010). Analysis of urban heat island effect using k-means clustering. The 2nd International Conference on Information Science and Engineering, 4-6 December 2010, IEEE Press. doi: 10.1109/ICISE.2010.5691908

Mackey, C. W., Lee, X. ve Smith, R. B. (2012). Remotely sensing the cooling effects of city scale efforts to reduce urban heat island. *Building and Environment*, 49, 348-358.

Maimaitiyiming, M., Ghulam, A.; Tiyip, T., Pla, F, Carmona, P., Halik. Ü., Sawut, M. & Caetano, M. (2014). Effects of green Space Spatial Pattern On Land Surface Temperature: Implications for sustaniable Urban Planning and Climate Change Adaptation. *ISPRS Journal of Photogrammetry and Remote Sensing*, 89, 59-66.

Marando, F., Salvatori, E., Sebastiani, Fusaro, L. ve Manes, F. (2019). Regulating Ecosystem Services and Green Infrastructure: assessment of Urban Heat Island effect mitigation in the municipality of Rome, Italy *Ecological Modelling,* 392, 92–102.

MetLink, Royal Meteorological Society (2023, 25 October*). Urban Heat Island Information*. https://www.metlink.org/fieldwork-resource/urban-heat-island-introduction/

Middel, A., Hab, K., Brazel, A. J., Martin, C. A., Guhathakurta, S. (2014). "Impact of urban form and design on mid-afternoon microclimate in Phoenix Local Climate Zones". *Landscape and Urban Planning,* 122, 16-28.

Monteiro, M. V., Doick, K. J., Handley, P. ve Peace, A. (2016). The impact of greenspace size on the extent of local nocturnal airtemperature cooling in London. *Urban Forestry ve Urban Greening*, 16, 2016, 160–169.

Mirzaei, P. A. ve Haghighat, F. (2010). Approaches to study Urban Heat Island – Abilities and limitations. *Building and Environment*, 45(10), 192-220.

Myint, S. W., Zheng, B., Talen, E., Fan, C., Kaplan, S., Middel, A., Smith, M., Huang, H. & Brazel, A. (2017) Does the spatial arrangement of urban landscape matter? examples of urban warming and cooling in phoenix and las vegas. *Ecosystem Health and Sustainability*, 1 (4), 1-15. doi: 10.1890/EHS14-0028.1

Ng, E., Chen, L., Wang, Y. ve Yuan,C. (2012) "A study on the cooling effects of greening in a high-density city: An experience from Hong Kong". *Building and Environment,* 47, 256-271.

Oliveira, S., Andrade, H. & Vaz, T. (2011). The cooling effect of green spaces as a contribution to the mitigation of urban heat: A case study in Lisbon. *Building and Environment,* 46, 2186-2194.

Pan, J. (2016). Area Delineation and Spatial-Temporal Dynamics of Urban Heat Island in Lanzhou City, China Using Remote Sensing Imagery. *J Indian Soc Remote Sensing*, 44, 111-127.

Park, C., Ha, J & Lee, S. (2017). Association between Three-Dimensional Built Environment and Urban Air Temperature: Seasonal and Temporal Differences. Sustainability, 9, 1338. doi:10.3390/su9081338

Peng, F., Wong, M. S., Ho, H. C., Nichol, J. & Chan, P.W. (2017). Reconstruction of historical datasets for analyzing spatiotemporal influence of built environment on urban microclimates across a compact city. *Building and Environment,* 123, 649-660.

Peng,J., Jia, J., Liu, Y., Li, H. & Wu, J. (2018) Seasonal contrast of the dominant factors for spatial distribution of land surface temperature in urban areas. *Remote Sensing of Environment*, 215, 255–267.

Peng, J., Liu, Q., Xu, Z., Lyu, D., Du, Y., Qiao & Wu, J., (2020). How to effectively mitigate urban heat island effect? A perspective of waterbody patch size threshold. *Landscape and Urban Planning*, 202, 103873-103883. doi: 10.1016/j.landurbplan.2020.103873

Peng, J., Dan, Y., Qiao, R., Liu, Y., Dong, J. & Wu, J. (2021). How to quantify the cooling effect of urban parks? Linking maximum and accumulation perspectives. *Remote Sensing of Environment,* 252, 112135. doi: 10.1016/j.rse.2020.112135

Priya, U. K. & Senthil, R. (2021). A review of the impact of the green landscape interventions on the urban microclimate of tropical areas. *Building and Environment,* 205, 108190.

Ren, Z., He, X., Zheng, H., Zhang, D., Yu, X., Shen, G. & Guo, R. (2013). Estimation of the Relationship between Urban Park Characteristics and Park Cool Island Intensity by Remote Sensing Data and Field Measurement. *Forests.* 4, 868-886.

Rakoto P. Y., Deilami, K., Hurley, J., Amati, J. & Sun, Q. (2021) Revisiting the cooling effects of urban greening: Planning implications of vegetation types and spatial configuration. *Urban Forestry & Urban Greening*, 64, 127-266.

Rizwan, A. M., Dennis Y.C. L & Chunho, L. (2008). A review on the generation, determination and mitigation of Urban Heat Island. *Journal of Environmental Sciences,* 20, 120–128.

Rogerson, P. A. (2010). *Statistical methods for geography: A student's guide*. (4th Edition ed.). Sage Publications.

Romero-Lankao, P., Quin, H. and Dickinson, K. (2012). "Urban vulnerability to temperature-related hazards: A meta-analysis and meta-knowledge approach". *Global Environmental Change*, 22, 670-683.

Qaid, A., Lamit, H. B., Ossen, D. R. & Shahminan, R. N. R. (2016). "Urban heat island and thermal comfort conditions at micro-climate scale in a tropical planned city". *Energy and Buildings, 133,* 577-595.

Quin Z., Zhang M., Amon K. & Pedro B. (2001). Mono-window algorithm for retrieving land surface temperature from Landsat TM 6 data. *Acta Geogr. Sin., 56,* 456--466.

Sakar, B. (2018). P*arametric Modelling For the Mitigation of Urban Heat Island Efffect: A Model Proposal.* Master Thesis, The Graduate School of Natural and Applied Sciences, Middle East Technical University, Ankara, Turkey.

Shahidan, M. F., Jones, P. J., Gwilliam, J. & Salleh, E. (2012). An evaluation of outdoor and building environment cooling achieved through combination modification of trees with ground materials. *Building and Environment*, 58, 245-257.

Shashau-Bar, L. & Hoffman, M.E. (2010). Vegetation as a climatic component in the design of an urban street: An empirical model for predicting the cooling effect of urban green areas wth trees. *Energy and Buildings*, 31, 221-235.

Shi, M., Chen, M., Jia, W., Du, C. & Wang, Y. (2023). Cooling effect and cooling accessibility of urban parks during hot summers in China's largest sustainability experiment. *Sustainable Cities and Society*, 93, 104519. doi: 10.1016/j.scs.2023.104519

Shih, W. (2017). Greenspace patterns and the mitigation of land surface temperature in Taipei metropolis. *Habitat International,* 60, 69- 80.

Silva, I., Santos, R., Lopes, A. & Araujo, V. (2018). Morphological Indices as Urban Planning Tools in Northeastern Brazil. *Sustainability*, 10, 4358; doi:10.3390.

Sun, X., Tan, X., Chen, K., Song, S., Zhu, X. & Hou, D. (2020). Quantifying landscape-metrics impacts on urban greenspaces and waterbodies cooling effect: The study of Nanjing, China. *Urban Forestry & Urban Greening,* 55, 126838-126849. doi: 10.1016/j.ufug.2020.126838

Şimşek, Ç. & Şengezer, B. (2012). The Importance of Green Spaces in Minimizing Urban Heat in the Istanbul Metropolitan Area. *Megaron,* 7(2), 112-128.

Şentürk, Y. & Çubukçu, K. M. (2023). Impacts of urban green area on local climate: Suggestions for spatial planning. Saygın, H, Balyemez, S. &Oral, H.V. (Eds) inside *Sürdürülebilir Kent Planlama Ekseninde Enerji Verimliliği ve Ekoloji* (p. 103-130). Nobel Academic Publications.

Tan, P. N., Steinbach, M. & Kumar. V. (2005). Introduction to Data Mining. (1st Edition ed.). Addison Wesley.

Tiangco, M., Lagmay, A. M. ve Argete, J. (2008) ASTER-based study of the night-time urban heat island effect in Metro Manila. *International Journal of Remote Sensing,* 29(10), 2799-2818. DOI:10.1080/01431160701408360

Unger, J. (2004) "Intra-urban relationship between surface geometry and urban heat island: review and new approach". *Climate Research,* 27, 253-264.

Unger, J. (2006) "Modelling of the annual mean maximum urban heat island using 2D and 3D surface parameters". *Climate Research,* 30, 215-226.

Vidrih, B. & Medved, S. (2013). Multiparametric model of urban park cooling island. *Urban Forestry & Urban Greening*, 12 (2013) 220– 229.

Voogt, J. A. ve Oke, T. R. (2003). Thermal remote sensing of urban climate. *Remote Sensing of Environment*, 86, 370-384.

Yan, H., Fan, S., Guo, C., Wu, F., Zhang, N. & Dong, L. (2014). Assessing the effects of landscape design parameters on intra-urban air temperature variability: The case of Beijing, China. *Building and Environment,* 76, 44-53.

Yan, L., Jia, W. & Zhao, S. (2021). The Cooling Effect of Urban Green Spaces in Metacities: A Case Study of Beijing, China's Capital. Remote Sens. 2021, 13, 4601. https://doi.org/10.3390/rs13224601

Yang, S., Wang, L., Stathopoulos, T. & Marey, A., M. (2023). Urban microclimate and its impact on built environment − A review. *Building and Environment*, 238, 110-334.

Yao, X., Yu, K., Zeng, X., Lin, Y., Ye, B., Shen, X., et al. (2022). How can urban parks be planned to mitigate urban heat island effect in "Furnace cities". An accumulation perspective. *Journal of Cleaner Production,* 330-334.

Yin, C., Yuan, M., Lu, Y., Huang, Y. & Liu, Y. (2018). Effects of urban form on the urban heat island effect based on spatial regression model. *Science of the Total Environment,* 634, 696-704.

Yu, Z., Xu, S., Zhang, Y., Jorgensen, G., Vejre, H. (2018). Strong contributions of local background climate to the cooling effect of urban green vegetation. *Sci. Rep.* 8 (1), 6798. doi: 10.1016/j.landurbplan.2017.04.009

Yu, Z., Yang, G., Zuo, S., Jørgensen, G., Koga, M., Vejre, H. (2020). Critical review on the cooling effect of urban blue-green space: a threshold-size perspective. *Urban For. Urban Green.* 49, 1–11.

Yüksel, A. & Coşkun Hepcan, Ç. (2023). The Relationship Land Surface Temperature and Blue-Green Infrastructure: The Case of Karsiyaka. *Adnan Menderes Üniversitesi Ziraat Fakültesi Dergisi,* 20(1), 91-98. doi: 10.25308/aduziraat.1214763

Walawender, J. P., Szymanowski, M., Hajto, M. J. ve Bokwa, A. (2014). Land Surface Temperature Patterns in the Urban Agglomeration of Krakow (Poland) Derived from Landsat-7/ETM+ Data. *Pure and Applied Geophysics*, 171, 913-940.

Wang, C. & Zhu, W. (2011). Analysis of the Impact of Urban Wetland on Urban Temperature Based on Remote Sensing Technology. *Procedia Environmental Sciences, 10,*1546-1552

Weng, Q., ve Lu, D. (2008). A sub-pixel analysis of urbanization effect on lve surface temperature ve its interplay with impervious surface ve vegetation coverage in Indianapolis. *United States,* 10, 68–83.

Wheeler, S. M., Abunnasr, Y., Dialesandro, J., Assaf, E., Agopian, S. and Gamberini, V. C. (2019) "Mitigating Urban Heating in Dryland Cities: A Literature Review". *Journal of Planning Literature,* 34 (4), 434-446

Wong, N. H. ve Yu, C. (2005). Study of green areas ve urban heat islve in a tropical city. *Habitat International,* 29, 547–558.

Yin, C., Yan, M., Lu, Y., Huang, Y. & Liu, Y. (2018). Effects of urban form on the urban heat island effect based on spatial regression model. *Science of the Total Environment,* 634, 696-704.

Yuan, F. ve Bauer, M.E. (2007). Comparison of Impervious Surface Area and Normalized Difference Vegetation Index as Indicators of Surface Urban Heat Island Effects in Landsat Imagery. *Remote Sensing of Environment,* 106, 375-386.

Zardo, L., Geneletti, D., Perez-Soba, M. ve Van Eupen, M. (2017). Estimating the cooling capacity of green infrastructures to support urban planning. *Ecosystem Services*, 26, 2017, 225-235.

Zhang, W., Zhu, Y. ve Jiang, J. (2016). Effect of the Urbanization of Wetlands on Microclimate: A Case Study of Xixi Wetland, Hangzhou, China, *Sustainability*, 8(9), 2016, 885.

Zhang Y., Murray, A. T. & Turner, B. I. (2017). Optimizing green space locations to reduce daytime and nighttime urban heat island effects in Phoenix, Arizona. *Landscape and Urban Planning,* 165, 162-171.

Zhou, W., Wang, J. & Cadenasso, M. (2017). Effects of the spatial configuration of trees on urban heat mitigation: A comparative study. *Remote Sensing of Environment,* 195, 1-12.

Zhou, W., Yu, W. & Wu, T. (2022). An alternative method of developing landscape strategies for urban cooling: A threshold-based perspective. *Landscape and Urban Planning*, 225. 104449. Doi: 10.1016/j.landurbplan.2022.104449

Zhang, W., Zhu, Y. ve Jiang, J. (2016). Effect of the Urbanization of Wetlands on Microclimate: A Case Study of Xixi Wetland, Hangzhou, China, *Sustainability*, 8(9), 885.

Zhang, Y., Jiang, P., Zhang, H. & Cheng, P. (2018). Study on Urban Heat Island Intensity Level Identification Based on an Improved Restricted Boltzmann Machine. *International journal of Environmental Research and Public Health*, 15, 186-202. doi: 10.3390/ijerph15020186

Zheng, Y., Ren, C., Shi, Y., Yim, S., Lai, D., Xu, Y., Fang, C & Li, w. (2023). Mapping the spatial distribution of nocturnal urban heat island based on Local Climate Zone framework. *Building and Environment*, 234, 110197.

Zhao, C., Fu, G., Liu, X. & Fu, F. (2011). Urban planning indicators, morphology and climate indicators: A case study for a north-south transect of Beijing, China. *Building and Environment*, 46, 1174-1183. doi: 10.1016/j.buildenv.2010.12.009